

Global ecological drivers of transpiration regulation in woody plants

DOCTORADO EN ECOLOGIA TERRESTRE

Centre de Recerca Ecològica i Aplicacions Forestals

Autonomous University of Barcelona

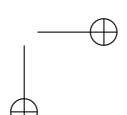
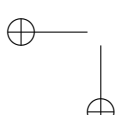
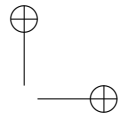
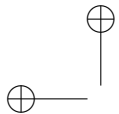
Author:

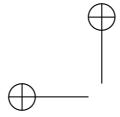
Víctor Flo Sierra

Advisors:

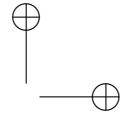
Rafael Poyatos López
Jordi Martínez Vilalta

Dec 2020



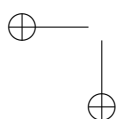


“thesis” — 2020/11/3 + 9:01 — page 2 — #2

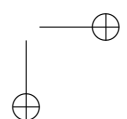


—

—



|



Acknowledgements

Mucha gente es co-responsable de este trabajo, de haberme empujado y acompañado hasta aquí. Me gustaría empezar agradeciendo a mis directores de tesis, Rafa y Jordi, sin los que esta tesis no hubiera sido posible, gracias por la oportunidad de trabajar con vosotros. He sido muy afortunado de haber contado con dos mentores excelentes en lo profesional y en lo personal. Rafa, tu dedicación es envidiable, gracias por todas las buenas ideas, los comentarios y críticas, las correcciones perfectas, por los viajes a congresos y por sufrir de mi insomnio y jet-lag. Jordi, ha sido un privilegio tenerte como tutor, por tu conocimiento transversal y profundo, por tu capacidad inata e inmediata de entenderlo todo, por mejorar siempre todas las ideas y textos, y por tu calidad humana.

Esta tesis tampoco hubiera sido igual sin haber compartido estos cuatro años con tantos buenos compañeros. Gracias a los compañeros de despacho, a Anna, Javi, Judit, Carlos, Manu, Aina, Marta, Pere y Pol. Creo que habéis sido los mejores compañeros posibles y que tuve mucha suerte de acabar en el -150. Sé que me llevo grandes amistades para toda la vida. No quiero olvidarme tampoco de muchos otros compañeros como Jordi, Sara, Kevin, Xavi, Vicenç, Joan, Marina, con los que hemos compartido café, discusiones y charlas. Gracias también a Luciana por acompañarnos en ese genial viaje relámpago por el desierto americano.

Gracias también en especial a los compañeros que estan o han pasado por el grupo. Maurizio, Tere, Miquel, Lucia, Víctor, Raul, Rosella, Pipo, Mireia, Lies, David, Jacob, Aude, Antonine, Pablo, Luca y Brenda, sin duda un grupo envidiable. Gracias por tantos buenos momentos, por la vertiente

académica, pero especialmente por las salidas de grupo, por las barbacoas, cenas y cervezas. Me gustaría agradecer especialmente a Víctor Granda, por su excelente trabajo, sin el que hubiera sido imposible enfrentarnos a la difícil tarea de llevar adelante SAPFLUXNET. Gracias por enseñarme a querer R, pero sobre todo por las risas y los enfados jugando a basquet.

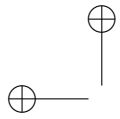
Durante estos años he tenido la suerte de vivir y conocer a mucha gente lejos de casa. Muchas personas que me han enseñado otras maneras de ver el mundo. Me gustaría mencionar especialmente a Martin y a Elena, gracias por acogerme y hacerme sentir como en casa en Salt Lake City. Gracias por darnos cobijo cuando nos quedamos en la calle por unos días, dejarme vuetro coche, y gracias por un viaje inolmidable a Glacier. No os lo podré agradecer suficiente. Gracias a Bill Anderegg por acogerme en su laboratorio donde he tenido la suerte de conocer a gente genial como Kelly, Nicole, Jaycee. Me gustaría agradecer también a Kathy Steppe por darme la oportunidad de visitar su laboratorio en Ghent y por sus buenos consejos. A Roberto por enseñarme a intalar la mi primera sonda de flujo de sabia. Gracias también a los que llevan tiempo compartiendo su camino conmigo o han caminado alguna etapa, me han marcado y ayudado, a los amigos de toda la vida y a mis compañeros de andanzas musicales. Gracias Pablo, Marc, Laura, Oscar, Carles, Jordi, Larry, Cristian, Pol, Kuni, Julio, Lorenzo, Barbara, Edgar, Jan, Arnau. También a Marta, Rosa, Florian, Daniel Lola, Magdalena y Esther, por haber creído tanto en mi y haber sido parte de mi vida durante muchos años.

Quiero agradecer también a mi familia. A mis abuelos, a mis tíos y primos, por haber sido una referencia.

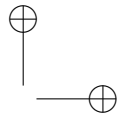
Gracias sobre todo a quien desde hace cuatro años es mi compañera de viaje. Gracias Mari Angeles por tu sonrisa, tu apoyo incondicional y tu amor. Esta tesis no hubiera sido sin ti. Gracias por ser brillante, por que es un placer escucharte y por intentar “salvar al mundo”. Gracias por dejarme formar parte de tu familia murciana.

Gracias finalmente a mis padres, por dejarme decidir mi camino, por apoyarme en cada decisión que he tomado. Me habeis hecho libre y feliz. Mil

gracias Ana por haber creido en mi, por ser un ejemplo desde que eramos pequeños, por ser tan buena y trabajadora. Si alguien es responsable directo de que me lanzara ha recorrer este camino esa eres tu. Gracias Clara por ser la alegría de nuestra casa y ser una hermana maravillosa. Gracias Marc y Jose por formar parte de nuestra vida y por esas charlas sobre tecnologia y negocios. Para acabar, gracias Arnau, el último fichaje de la familia. ¡Os quiero!

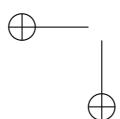


“thesis” — 2020/11/3 — 9:01 — page iv — #6



—

—



|

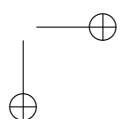


Table of Contents

1: Bias and uncertainty in sap flow methods	1
1.1 Introduction	3
1.2 Material and methods	7
1.2.1 Sap flow calibration datasets	7
1.2.2 Calibration assessment	9
1.2.3 Statistical analyses	13
1.3 Results	14
1.3.1 Calibration performance compared among methods and families of methods	14
1.3.2 Influence of wood traits	18
1.4 Discussion	19
1.4.1 Sap flow measurement errors across methods and methodological families	21
1.4.2 The performance of sap flow calibrations is largely unrelated to species wood traits	26
1.4.3 Implications and recommendations	29
1.5 Conclusions	30
2: The SAPFLUXNET database	33
2.1 Introduction	35
2.2 The SAPFLUXNET data workflow	38
2.2.1 An overview of sap flow measurements	38
2.2.2 Data compilation	40
2.2.3 Data harmonisation and quality control: QC1	41

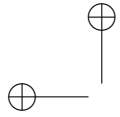
2.2.4	Data harmonisation and quality control: QC2	43
2.2.5	Data structure	44
2.3	The SAPFLUXNET database	44
2.3.1	Data coverage	44
2.3.2	Methodological aspects	48
2.3.3	Plant characteristics	49
2.3.4	Stand characteristics	53
2.3.5	Temporal characteristics	54
2.3.6	Availability of environmental data	56
2.4	Potential applications	56
2.4.1	Applications in plant ecophysiology and functional ecology	56
2.4.2	Applications in ecosystem ecology and ecohydrology . .	61
2.5	Limitations and future developments	65
2.5.1	Limitations	65
2.5.2	Outlook	67
2.6	Data availability, access and feedback	68
2.7	Conclusion	69
3:	Climate and functional traits jointly mediate tree water use strategies	71
3.1	Introduction	73
3.2	Material and methods	76
3.2.1	Sap flow data	77
3.2.2	Evaporative demand and soil water availability data .	78
3.2.3	Data filtering	79
3.2.4	Whole-tree canopy conductance calculation	80
3.2.5	Traits and climatic data	81
3.2.6	G_{Asw} sensitivity to soil water availability and water demand	82
3.2.7	Statistical analyses	82
3.3	Results	85

3.3.1	Water use parameters and differences between angiosperms and gymnosperms	85
3.3.2	Coordination with hydraulic and allocation traits	86
3.4	Discussion	92
3.4.1	Climate influence on water use strategies across species	93
3.4.2	Water use parameters	93
3.4.3	Coordination between water use parameters and water relations traits	94
3.4.4	Conclusions	97
References		99

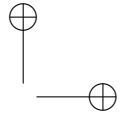
“thesis” — 2020/11/3 — | 9:01 — page viii — #10

List of Tables

1.1	Analysis summary for the different methods and families.	15
1.2	Error analysis of different sap flow methods.	19
1.3	Least-squares means and 95% CI calculated from the LMM models testing the effect of different wood porosity types	21
1.4	Synthesis of the potential sources of error and use adequacy for each method.	23
—	—	—
2.1	Number of sap flow times series in SAPFLUXNET depend- ing on whether they were calibrated for the different sap flow methods.	50
2.2	Number of plants in the SAPFLUXNET database using differ- ent radial and azimuthal integration.	51
2.3	Number of datasets, plants and species by stand-level treat- ment in the SAPFLUXNET database.	60
3.1	Description of variables and units in this study.	77
3.2	Results of the bi-variate linear models relating water use pa- rameters and water relations traits	87
3.3	Results of the bi-variate linear models relating water use pa- rameters, water relations traits, climate and tree height.	90

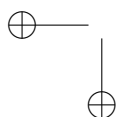


“thesis” — 2020/11/3 — 9:01 — page x — #12

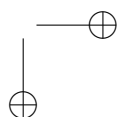


—

—



|



List of Figures

1.1	Graphical representation of the calibration performance metrics.	12
1.2	Distribution of the calibration performance metrics for each method.	16
1.3	Predictions of the LMM models of the four calibration metrics.	17
1.4	Relationship between the four calibration performance and wood density, for different sap flow methods.	20
1.5	Relationship between measured and reference sap-flux density (SFD) for different sap flow methods, studies and calibrations.	25
1.6	Relationship between measured and reference sap flow (SF) for different sap flow methods, studies and calibrations.	27
2.1	Overview of the SAPFLUXNET data workflow.	42
2.2	Geographic, bioclimatic and vegetation type distribution of SAPFLUXNET datasets.	46
2.3	Taxonomic distribution of genera and species in SAPFLUXNET.	47
2.4	Distribution of plants according to major taxonomic group and sap flow method.	49
2.5	Characteristics of trees and stands in the SAPFLUXNET database.	52
2.6	Duration and number of plants measured in each dataset.	55
2.7	Fingerprint plots showing hourly sap flow per unit sapwood area.	57
2.8	Summary of the availability of different environmental variables in SAPFLUXNET datasets.	58
2.9	Potential for upscaling species-specific plant sap flow to stand-level.	63

3.1	Distribution of the plots from the SAPFLUXNET database included in this study.	78
3.2	Boxplots of water use parameters for both Angiosperms and Gymnosperms.	84
3.3	Bi-variate relationships between G_{REF} water relations traits.	86
3.4	Bi-variate relationships between β_{VPD} water relations traits.	88
3.5	Bi-variate relationships between β_{SWC} water relations traits.	89
3.6	Path analyses of species-specific water use parameters.	92

Abstract

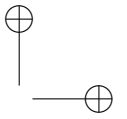
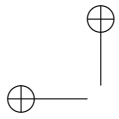
Understanding how climate affects species' distribution and performance is a central issue in ecology since its origins. In last decades, however, the interest in this question has been reactivated by the current context of climate change. Species Niche Modelling has been widely used to assess shifts in species distribution and to test the relationship between species' climatic niche and species physiological and demographic performance, implicitly assuming that species occurrence portrays the environmental and biotic species' suitable conditions. Nevertheless it is still largely undetermined whether these models can portray population and community responses, particularly in relation to extreme climatic episodes.

In this thesis I aim at exploring the capacity of niche modelling to predict species decay under extreme climatic conditions, particularly droughts, addressing some constraints of this approach and proposing possible solutions. To achieve this goal, I counted with 3 vegetation decay datasets measured in the Spanish SE after the extreme drought year 2013-2014. Two of these datasets were based on defoliation sampling of individual plants belonging to more than 40 semiarid shrubland species (chapters 2, 4 and 5), while the other one was based on regional compiled data of *Pinus halepensis* L. affection in plots of 1km^2 (chapter 3). In second chapter I used different Species Distribution Model (SDMs) algorithms to estimate species' climatic suitability before (1950-2000) and during the extreme drought, in order to test the possible correlation between suitability and decay, and whether the existence of this relationship depended on the applied SDM algorithm. I consistently found a

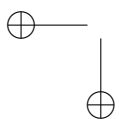
positive correlation between remaining green canopy and species' climatic suitability before the event, suggesting that populations historically living closer to their species' tolerance limits are more vulnerable to drought. Contrastingly, decreased climatic suitability during the drought period did not correlate with remaining green canopy, likely because of extremely low climatic suitability values achieved during the exceptional climatic episode. In order to test whether this extremely low suitability values could derive as a consequence of only considering climatic averages when calibrating SDMs, in the third chapter I developed a method to include inter-annual climatic variability into niche characterization. I then compared the respective capacities of climatic suitabilities obtained from averaged-based and from inter-annual variability-based niches to explain demographic responses to extreme climatic events. I found that climatic suitability obtained from both niches quantifications significantly explained species demographic responses. However, climatic suitability from inter-annual variability-based niches showed higher explanatory capacity, especially for populations that tend to be more geographically marginal. In the fourth chapter I tried to overcome the inability of the SDMs to predict populations decay during extreme conditions, as observed in the second chapter, by using Euclidean distances to species' niche in the environmental space. I compared the capacities of both population distances in the climatic environmental space and population climatic suitability derived from SDMs to explain population observed physiological and demographic responses to an extreme event. Additionally, I tested such relationship in populations located in three different bedrock sites, corresponding to a gradient of water availability. I found that SDMs-derived suitability failed to explain population decay while distances to the niche centroid and limit significantly explained population die-off, highlighting that population displaced farther from species' niche during the extreme episode showed higher vulnerability to drought. The results also suggested a relevant role of some bedrocks buffering species decay responses to extreme drought events mainly according to soil water holding capacity. Finally, in the fifth chapter, I used species niche characterizations in the environmental space and demographic data to address the impact of extreme events

at community level. Particularly, I estimated the community climatic disequilibrium before and after a drought episode along a gradient of water availability in three bedrock types. Disequilibrium was computed as the difference between observed climate and community-inferred climate, which was calculated as the mean of species' climatic optimum weighted by species abundance collected in field surveys. I found that extreme drought nested within a decadal trend of increasingly aridity led to a reduction in community climatic disequilibrium, particularly when combined with low water-retention bedrocks. In addition, community climatic disequilibrium also varied before the extreme event across bedrock types, according to soils water-retention capacity. In conclusion, by developing different techniques, derived from species distribution, that characterize climatic accuracy at population and community level, this work reveals the capacity of species climatic niche to explain demographic responses under climate change-induced episodes of extreme drought.

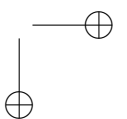
“thesis” — 2020/11/3 — | 9:01 — page xvi — #18



— —



|



— “*No one will protect what they don’t care about;
and no one will care about what they have never experienced*” —

David Attenborough

“thesis” — 2020/11/3 — 9:01 — page xviii — #20

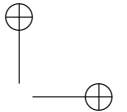
1

A synthesis of bias and uncertainty in sap flow methods

Victor Flo, Jordi Martínez-Vilalta, Kathy Steppe, Bernhard Schuldt, Rafael Poyatos

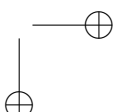
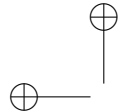
Abstract

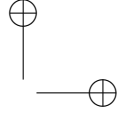
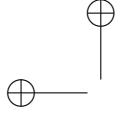
Sap flow measurements with thermometric methods are widely used to measure transpiration in plants. Different method families exist depending on how they apply heat and track sapwood temperature (heat pulse, heat dissipation, heat field deformation or heat balance). These methods have been calibrated for many species, but a global assessment of their uncertainty and reliability has not yet been conducted. Here we perform a meta-analysis of 290 individual calibration experiments assembled from the literature to assess calibration performance and how this varies across methods, experimental conditions and wood properties (density and porosity types). We used different metrics to characterize mean accuracy (closeness of the measurements to the true, reference value), proportional bias (resulting from an effect of measured flow on the magnitude of the error), linearity in the relationship between measurements and reference values, and precision (reproducibility and repeatability). We found a large intra- and inter-method variability in calibration performance, with a low proportion of this variability explained by species. Calibration performance was best when using stem segments. We did not find evidence of strong effects of wood density or porosity type in calibration performance. Dissipation methods showed lower accuracy and higher proportional bias than the other methods but they showed relatively high linearity and precision. Pulse methods also showed significant proportional bias, driven by their overestimation of low flows. These results suggest that Dissipation methods may be more appropriate to assess relative sap flow (e.g., treatment effects within a study) and Pulse methods may be more suitable to quantify absolute flows. Nevertheless, all sap flow methods showed high precision, allowing potential correction of the measurements when a study-specific calibration is performed. Our understanding of how sap flow methods perform across species would be greatly improved if experimental conditions and wood properties, including changes in wood moisture, were better reported.



1.1 Introduction

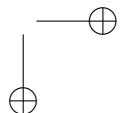
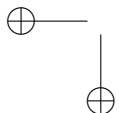
Quantifying transpiration of vegetation is of major importance for hydrological, ecological, and agricultural sciences, since it represents 60-80% of the water that returns from the land surface to the atmosphere (Jasechko et al. (2013); Schlesinger & Jasechko (2014); Wei et al. (2017)). The study of transpiration and its environmental sensitivity is essential to understand vegetation water cycling (D. C. Frank et al. (2015); Konings, Williams, & Gentine (2017); Novick et al. (2016)) and to forecast changes in vegetation functioning and composition under climate change (C. D. Allen, Breshears, & McDowell (2015)). Addressing these questions requires non-destructive measurements of whole-plant transpiration at multiple timescales (S. D. Wullschleger, Meinzer, & Vertessy (1998)). Thermal methods of sap flow measurement show a number of advantages over other methods such as those based on isotopes tracing or leaf gas exchange (D. M. Smith (1995)), and have become the most widely used approach to estimate tree-level transpiration (Poyatos et al. (2016)) (Fig. A1). When compared against independent estimates of evapotranspiration components, sap flow methods have provided reasonable qualitative and quantitative results (Diawara, Loustau, & Berbigier (1991), Hogg et al. (1997), Kool et al. (2014), Schlesinger & Jasechko (2014), Zhang, Manzoni, Katul, Porporato, & Yang (2014), but see K. B. Wilson, Hanson, Mulholland, Baldocchi, & Wullschleger (2001), A. C. Oishi, Oren, & Stoy (2008), T. Shimizu et al. (2015)). However, sap flow measurements may be subject to various potential sources of error. Some of these errors are related to scaling sap flow variability both within trees and from tree to stand level (T. J. Hatton, Moore, & Reece (1995); Hernandez-Santana, Hernandez-Hernandez, Vadeboncoeur, & Asbjornsen (2015); Mitchell, Irwin, Flanagan, & Karron (2009)), while others are related to intrinsic limitations of the methods or to how these methods are applied (see Vandegehuchte & Steppe (2013)). Although these biases have been studied, they have not yet been quantified globally and there is no conclusive assessment of how they differ across methods or species characteristics, including wood properties (Poyatos et al. (2016)).





Sap flow methods (Vandegehuchte & Steppe (2013)) can measure sap flow rate (SF, g h⁻¹ or equivalent units) or sap flux density (i.e., sap flow rate per unit sapwood area, SFD, cm³ cm⁻² h⁻¹ or equivalent units) in a plant’s conductive tissue and can be classified in four families depending on how they heat the sapwood and how they measure sapwood temperatures: (1) the Dissipation family, including thermal dissipation (TD; Granier & Une (1985)) and transient thermal dissipation (Do & Rocheteau (2002), TTD (????)) methods, which measure the dissipation of heat from a heated probe inserted in the sapwood with reference to a reference, non-heated probe; (2) the Pulse family, including the compensation heat pulse (CHP; Swanson & Whitfield (1981)), heat ratio (HR; S. S. Burgess et al. (2001)), T-max (Y. Cohen, Fuchs, & Green (1981)), calibrated average gradient (CAG; Testi & Villalobos (2009)), sapflow+ (SF+; Vandegehuchte & Steppe (2012b), Vandegehuchte, Steppe, & Phillips (2012)), single probe heat pulse (SPHP; (????)) and dual heat pulse methods (Dual; Pearsall, Williams, Castorani, Bleby, & McElrone (2014)), which all apply heat in pulses and track sapwood temperature changes caused by thermal convection and conduction; (3) the Field family, including the heat field deformation (HFD; N. Nadezhina (2018); N. Nadezhina, Cermák, & Nadezhdin (1998)) and its derivatives, which measure the shape changes of a continuous heat field in the sapwood, using axial and tangential probes; and (4) the Balance family, represented by stem heat balance (SHB; (????); Sakuratani (1981); (????)) and trunk heat balance (THB; Čermák, Kučera, & Nadezhdina (2004); Čermák 1973) methods, which measure the energy balance across a heated wood section. This latter family is the only one directly measuring sap flow rate, while all the others measure sap flux density.

Methodological errors in sap flux density measurements may be caused by wounding following probe insertion into the sapwood (except for the miniaturized non-invasive ones; see (Michael J. Clearwater, Luo, Mazzeo, & Dichio (2009); Hanssens, De Swaef, Nadezhdina, & Steppe (2013); Schreel & Steppe (2018)), biological variation in wood parameters and diverse raw data processing approaches (A. C. Oishi, Hawthorne, & Oren (2016); Peters et al. (2018); Vergeynst, Vandegehuchte, McGuire, Teskey, & Steppe (2014)). Wounding



1.1. Introduction

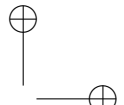
5

affects heat and water transport and thus may disrupt sap flow measurements (Barrett, Hatton, Ash, & Ball (1995); S. S. Burgess et al. (2001); S. Green, Clothier, & Perie (2009); Steve Green, Clothier, & Jardine (2003); S. R. Green & Clothier (1988); Steppe, Vandegheuchte, Tognetti, & Mencuccini (2015)), especially during long-term installations (S. Marañón-Jiménez et al. (2018); A Wiedemann, Jiménez, Rebman, Cuntz, & Herbst (2013)). While wound corrections have been available for a long time for some Pulse family methods (Steve Green et al. (2003); Swanson & Whitfield (1981)), they have only become recently available for other methods such as TD (Andreas Wiedemann et al. (2016)). Sap flux density methods are also affected by changes in radial patterns, which are not constant over time, so these methods have to measure the entire sapwood depth by sufficiently large probes, or by individual measurement points at different depths (T. Hatton (1990)). Although some methods have a more solid theoretical background based on the physics of thermal transport (Pulse and Balance methods), all of them rely on a certain degree of empiricism, which may introduce errors caused by biological variability and/or variation in signal processing approaches: species-specific empirical calibrations in Dissipation methods (S. Fuchs, Leuschner, Link, Coners, & Schuldt (2017)), zero-flow determination or baselining (Ping Lu, Urban, & Zhao (2004); Peters et al. (2018)), and different parameterization of thermal sapwood properties in Pulse and Field methods (Chen, Miller, Rubin, & Baldocchi (2012)). These thermal sapwood parameters could change over time, introducing further errors in the measurements (e.g. changes in stem water content; Vergeynst et al. (2014)). Within the Balance family, those using external heating do not suffer from potential errors due to wounding, but they all require zero-flow determination (D. Smith & Allen (1996)). Balance methods have often been considered to better integrate spatial variability in sap flow (Čermák et al. (2004)), but whether they perform generally better than sap flux density methods remains unknown.

Other errors in sap flow measurement may result from not accounting properly for method-specific assumptions. For many sap flow methods, natural temperature gradients (NTG) need to be minimized and/or accounted

for to obtain unbiased estimates of sap flow (Reyes-Acosta, Vandegehuchte, Steppe, & Lubczynski (2012); Vandegehuchte, Burgess, Downey, & Steppe (2015)). Incorrect sensor geometry (misalignment) affects the accuracy of the measurements (S. S. Burgess et al. (2001); Cabibel & F (1991); Ren et al. (2017); Swanson (1983); Swanson & Whitfield (1981)). Other application errors, such as those arising from the incomplete contact of TD probes with the sapwood (Michael J Clearwater, Meinzer, Andrade, Goldstein, & Holbrook (1999)) are difficult to prevent, though they can be reasonably corrected a posteriori (e.g. Clearwater correction, K. R. Hultine et al. (2010); Paudel, Kanety, & Cohen (2013)). Despite that these application errors have been well described in individual studies, a general quantification of these errors for the most employed sap flow methods is currently lacking.

Comparisons of sap flow measurements with respect to a reference method (hereafter, for simplicity, ‘sap flow calibrations’) are usually aimed at obtaining species-specific calibrations (Vandegehuchte & Steppe (2013)) to assess different parameterizations of wood thermal properties (Vandegehuchte & Steppe (2012a)) or to validate empirical corrections (e.g., wounding, NTG, changes in water content, misalignment; S. S. Burgess et al. (2001); Vergeynst et al. (2014)). Although few studies calibrate multiple sap flow methods for different species (S. Fuchs et al. (2017)), collectively these calibration studies have shown the inherent limitations of different sap flow methods to deal with low (Steve Green et al. (2003)) or high flows (S. Green et al. (2009)). Variability and quality in calibration performance may also be related to specific wood properties such as wood density (Suleiman, Larfeldt, Leckner, & Gustavsson (1999); Wullschleger, Childs, King, & Hanson (2011)), especially given the fact that wood density enters the calculation of sap flux density for some methods (Vandegehuchte & Steppe (2012a)) and co-varies with wood moisture content (Looker, Martin, Jencso, & Hu (2016)). Because thermal properties of wood are dependent on both, i.e. wood density and moisture content (MacLean (1941)), they might additionally be influenced by wood anatomical traits such as wood porosity type, i.e. coniferous, diffuse-porous or ring-porous wood. In conifers, however, no clear effects of wood density



1.2. Material and methods

7

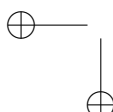
on calibration variability have been reported (Peters et al. (2018)). Therefore, a quantitative synthesis of sap flow calibrations, accounting for variation caused by different flow ranges and wood properties is needed to generalize and understand the patterns observed in individual calibration studies.

Here, we compile a global database of published sap flow calibrations to quantify the measurement errors associated with different sap flow methods and to assess the factors underlying variability across methods. In assessing calibrations, we distinguished between mean systematic bias (accuracy), a measure of the average degree of closeness of the measurements to the value obtained with a reference method; proportional bias, which occurs when the magnitude of the error is a function of the flow; linearity in the relationship between measurements and values obtained with a reference method; and precision, a measure of reproducibility and repeatability. Our main objective is to assess the differences in accuracy, proportional bias, linearity and precision among methodological families and individual sap flow methods; in addition, we will determine whether calibration performance across methods is associated with species wood traits (wood density and porosity type).

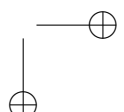
1.2 Material and methods

1.2.1 Sap flow calibration datasets

We retrieved sap flow calibration studies of the seven most common methods (CHP, T-max, HR, HFD, SHB, TD, TTD) applied on trees, palms or lianas, using standard database searching tools (i.e. Scopus, Web of Science and Google Scholar). The search was conducted in June 2017 applying the following keywords: sap fl*, sap flux density, calibration, potomet*, gravimet*, thermal dissipation, heat pulse, heat balance, heat field deformation, compensation heat pulse, T-max, and their combinations. Other sources of data were obtained from the references of previously collected studies. For each calibration experiment, we obtained paired observations of sap flow, measured with a thermal method and with an independent reference method (typically gravimetric or volumetric). Data was digitized from published figures (using



|

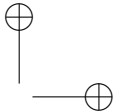


GetData Graph Digitalizer version 2.26.0.20). We asked the authors to supply the raw data when these were unavailable from the original publication. We obtained data from 60 studies (see Table A1) reporting 374 individual calibration experiments performed on 81 different shrub and trees species (10,186 data points in total). In the analysis, we only used calibrations that were properly applied according to our definition below (i.e. 290 calibrations out of 374) to restrict the variability to the intrinsic characteristics of the methods.

We always considered sap flow observations obtained with the original parameters of the methods (e.g. Granier’s original calibration for TD), without applying the coefficients derived from the calibrations themselves. Some calibrations with TD gave measured K values (i.e. sap flow index, calculated from raw sapwood temperature differences) instead of measured SFD and, in these cases, K values were transformed to SFD using Granier’s original equation and calibration coefficients (Eq. 1, $a = 42.84 \text{ cm}^3\text{cm}^{-2}\text{h}^{-1}$, $b = 1.231$) (Granier & Une (1985)).

$$SFD = a \times K^b \quad (1.1)$$

For each calibration, we recorded the type of calibration material: whole plants, whole plants without roots or cut stem segments. We also assessed whether the sap flow method was properly applied using the best available protocol specified for each method. We considered a proper application of Dissipation methods when the probe was shorter than the sapwood depth and radial profile correction was applied, when the probe was approximately equal to the sapwood depth, or when the probe was longer than the sapwood depth and this effect was corrected for following Clearwater et al. (1999). To test whether our results could have been affected by this correction, we performed a preliminary analysis with the same structure as the main statistical model (cf. section 1.3.3) comparing TD calibrations with or without the Clearwater correction and we did not find significant effects on any of the metrics of calibration performance (cf. section 1.3.2) (data not shown). We considered a proper application of Pulse methods when wound correction was applied and either the probe had multiple measuring points along the sapwood or a radial sap flow profile correction was applied. We always considered Balance



1.2. Material and methods

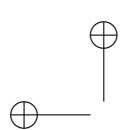
9

methods and Field methods as properly applied, because they always integrate (or account for) spatial variability of sap flow.

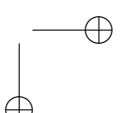
Finally, to analyze the influence of wood traits on calibration performance we used wood density, defined as fresh volume over oven-dry mass, and wood porosity type of the species employed in each study. Wood density was supplied in only a few studies (7 species ~ 80 calibration experiments ~ 4 studies). Assuming that for wood density between-species variability is typically larger than within-species variability (Siefert et al., 2015; Vilà-Cabrera et al., 2015), we retrieved wood density of each species from the TRY database (Kattge et al., 2011). Wood densities of *Carica papaya*, *Phoenix dactylifera* and *Vitis vinifera* were obtained from Kempe (2014), Fathi (2014) and Castelan-Estrada (2002), respectively, as they were not recorded in TRY. When wood density could not be found for a given species, we used the phylogenetically nearest species of the same genus if available in TRY (10 of 81 species; e.g. *Citrus sinensis* for *Citrus reticulata*). We could not estimate wood density for three taxa (*Humulus lupulus*, *Musa* sp. and *Siagrus romanzoffiana*). A correlation between calibration-specific and species-level wood density extracted from the TRY database ($r = 0.78$, $P < 0.01$, $n = 12$ calibrations, 6 species) indicates that species-level wood density values indeed are applicable for our purpose, but the results should be interpreted with caution. Finally, wood porosity was obtained from the InsideWood database (Wheeler (2011), (??)), using four categories: ring-porous, diffuse-porous (i.e. diffuse and semi-diffuse porous), conifer and monocots.

1.2.2 Calibration assessment

Although the reference methods always provide an estimate of sap flow through plants or stem segments, sap flow measurements can be reported as SF or SFD. It was not possible for us to interconvert between SF and SFD in all cases because sapwood areas were not always reported. This precluded a joint analysis of all the paired observations in the same linear model because units differ between SF and SFD. To overcome this problem and to maximize the amount of data considered in the analyses, we first



|

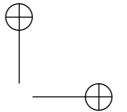


evaluated calibration performance using four complementary dimensionless metrics at the calibration level, which allowed us to analyze globally all calibrations regardless of the magnitude they reported (SF or SFD). In a second stage, we quantified the variability in the absolute errors in sap flow measurements across methods and flow ranges separately for SF and SFD methods. We did not expect differences between calibrations reported with SF or SFD because the inter-conversion between them only involves a scalar transformation. In addition, preliminary analyses confirmed that there was no significant difference between SF and SFD for any of the calibration performance metrics reported in this study (Table A2).

For the global analysis, the following metrics were calculated for each calibration (SF and SFD): the average ln ratio (Ln-Ratio) between measured and reference values as a measure of overall accuracy; the slope of the relationship between measured and reference sap flow to characterize proportional bias (Slope); the slope of the ln-ln relationship between measured and reference sap flow as a measure of linearity (Slope (ln-ln)); and Z Pearson’s Correlation to describe precision (Z-Cor) (Fig. 1.1). To calculate these metrics, we filtered out data points with measured or reference flows less or equal to 0. All calibration metrics and subsequent statistical models were performed in R 3.4.2 (R Core Team (2017)). For model-based metrics, we always checked residuals to ensure they satisfied normality and homoscedasticity assumptions. Accuracy was evaluated as the mean of the natural logarithm of the ratio between paired measurements (j) of each calibration (i):

$$Ln - Ratio_i = \frac{\sum_{j=1}^n \ln(\frac{measured_j}{reference_j})_i}{n_i} \quad (1.2)$$

where $measured_j$ and $reference_j$ are the paired measurements of sensor-estimated and reference flow, respectively, and n the number of paired measurements for each calibration i (see Fig. 1.1). The Ln-Ratio varies between $-\infty$ and $+\infty$, and equals 0 for a calibration with perfect mean accuracy (i.e. lack of systematic bias). We also expressed this metric as the exponential of Ln-ratio minus one multiplied by 100, as an indicator of accuracy



1.2. Material and methods

11

deviation (in %).

The slope of the linear relationship (Eq. 3) describes how the magnitude of the error changes (linearly) as a function of the reference flow. The slope of the ln–ln relationship (Eq. 4) captures the linearity between the measured and the reference flow. Both slope estimates were calculated for each calibration using a simple linear regression (lm - package stats):

$$\text{measured}_{ij} \sim \beta_{0i} + \beta_{1i} \text{reference}_{ij} + e_{ij} \quad (1.3)$$

$$\ln(\text{measured}_{ij}) \sim \beta'_{0i} + \beta'_{1i} \ln(\text{reference}_{ij}) + e_{ij} \quad (1.4)$$

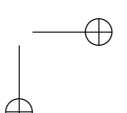
where β_{0i} and β'_{0i} are the intercepts and β_{1i} and β'_{1i} are the slopes for each calibration (i), and j indicates individual calibration points. Hereafter, we will refer to β_{1i} as *Slope* and to β'_{1i} as *Slope(ln – ln)*; slope values equal to 1 characterize measurements without proportional bias (Eq. 3) and with high linearity (Eq. 4), respectively.

We used Pearson’s correlation coefficients r between measured and reference flow of each calibration experiment (i) as a metric to describe the precision of the methods. The distribution of the resulting variable was skewed due to the large amount of correlation coefficients close to 1, so we used Fisher’s Z transformation (Eq. 5) to achieve normality:

$$Z - Cor_i = \frac{1}{2} \ln\left(\frac{1+r_i}{1-r_i}\right) \quad (1.5)$$

Low values of $Z - Cor$ correspond to low r correlations, and high values of $Z - Cor$ correspond to high r correlations and thus high precision (data set range $r = [0.0491 - 0.9999]$; $r = 0.0491 \sim z = 0.0491$; $r = 0.9999 \sim z = 5.1594$).

In the analysis of the absolute errors of sap flow measurements, we calculated the Normalized Root Mean Square Error (NRMSE) for each calibration (i) (Eq. 6), separately for SFD and SF methods, in order to obtain



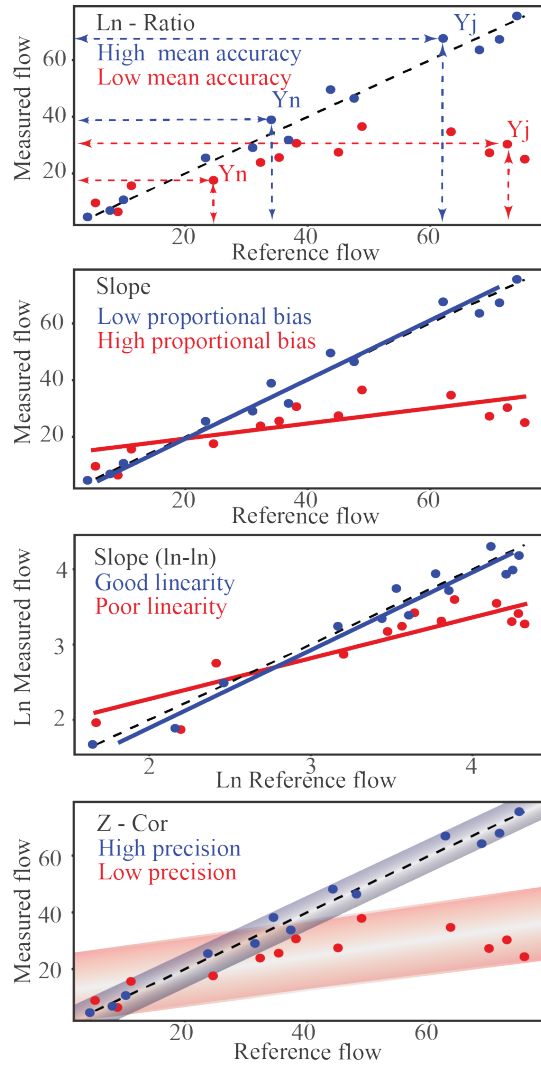
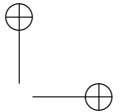


Figure 1.1: Graphical representation of the calibration performance metrics used in the analyses. Each panel presents the same simulated calibration points, representing plausible data. Blue dots represent an accurate, unbiased, linear and precise calibration, while red dots represent an inaccurate, biased, non-linear and imprecise calibration.

the percentage of absolute error at the mean range of each calibration (i).

$$NRMSE_i = \frac{(\sqrt{\frac{\sum_{j=1}^n (measured_j - reference_j)^2}{n}})_i \times 100}{range\ mean_i} \quad (1.6)$$

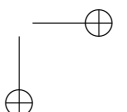
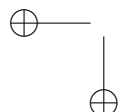


Subsequently, from the NRMSE and the mean range of each calibration, we fitted a linear model for each method allowing to quantify the absolute error (RMSE) at a given sap flow and also to obtain a RMSE at a reference flow (cf. section 2.3).

1.2.3 Statistical analyses

All the analyses were performed using linear mixed-effects models (LMM) with the package lmer (Bates, Mächler, Bolker, & Walker (2015)). Least-square means were estimated with package lsmeans (Lenth (2016)) and used to summarise the effects of fixed factors and to test contrasts among predictions. In all models, we used the variables Study and Species as partially crossed random effects (Schielzeth & Nakagawa (2013)), as we are interested in taking into account the variability associated with study and species, and also to analyze within- and between-group variability. We used Study as we expect experimental variability between researchers or laboratories, and Species because calibration performance has been reported to vary across species (S. Fuchs et al. (2017); D. Smith & Allen (1996); Steppe et al. (2015)). For each model, R_m^2 and R_c^2 (marginal and conditional coefficients of determination, respectively) based on Nakagawa & Schielzeth (2013) were calculated using the function r.squaredGLMM of the package MuMIn (Barton (2017)) in R. Intraclass Correlation Coefficients (ICC) were also calculated for the random factors to quantify the proportion of variance within and among groups (low ICC implies high intra-group variability).

In a first analysis, we were interested in assessing the differences in calibration metrics (Ln-Ratio, Slope, Slope (ln-ln), Z-Cor) between different families of methods (Family: Pulse, Dissipation, Balance and Field methods), because methods within a family share similar physical principles. We also analyzed differences between individual methods with a sufficient sample size (Method: CHP, T-max, HR, HFD, SHB, TD, TTD). As the calibration material determines, to a large extent, the experimental conditions, we also included this variable in our models (Material: whole plants, whole plants without roots or cut stem segments). For the analysis of absolute errors of



sap flow measurements, we modelled NRMSE as a function of Method and the Mean Range of SFD (or SF for Balance methods) in each calibration, as well as their interaction. We used the same random structure as in previous models.

Finally, we assessed how each calibration metric depended on Wood Density and Wood Porosity. A first model included all methods available, with Method interacting with Wood Density as predictors. In order to test Wood Porosity effects, we fitted separate models for CHP and TD calibrations, as these two methods were the only ones that had enough data (> 5 calibrations) for more than one type of porosity. Separate models were needed because not all wood porosity types were represented for all methods. In both models we also included Material as an explanatory cofactor, and the same random structure as in the first analysis explained above.

1.3 Results

Most of the published calibrations were performed with Pulse and Dissipation methods (Table 1.1). In particular, 61% of the total number of the properly applied calibrations were conducted using TD or CHP, followed by HFD and HR. SHB, T-max and TTD methods were less represented, with 8 – 14 calibrations each. The metrics extracted from the raw calibrations were highly variable within methods (Fig. 1.2). Calibration metrics often followed a quasi-normal distribution, but in most cases distributions were truncated or skewed, particularly for methods with fewer calibrations (Fig. 1.2).

1.3.1 Calibration performance compared among methods and families of methods

The average accuracy deviation across sap flow methods (properly applied) ranged between 14.2% for CHP and -40.5% for TD (Table 1.1). There were significant differences in accuracy (Ln-Ratio) among families of methods and for methods but not for calibration materials (Fig. 1.3). The Dissipation family in general and the TD and TTD methods in particular were the only

1.3. Results

15

Table 1.1: Analysis summary for the different methods and families of methods obtained from the LMM models (least-squares means). We provide the four dimensionless metrics: the Ln-ratio as a measure of accuracy, the accuracy deviation calculated as the exponential of the Ln-ratio minus one multiplied by 100, the Slope to characterize the proportional bias, the slope of the ln-ln-relationship, Slope (ln-ln), as a measure of linearity, and Z Pearson’s correlation (Z-Cor) to describe overall precision; n: number of calibrations; studies: number of studies of each method; species: number of different species; r is the correlation calculated as the tanh of Z-Cor.

Method	Family	n	studies	species	Ln-Ratio	Accuracy deviation %	Slope	Slope (ln-ln)	Z-Cor	r
CHP	Pulse	63	16	21	0.133	14.225	0.887	0.783	1.837	0.950
T-max	Pulse	11	5	6	-0.053	-5.162	0.614	0.697	1.755	0.942
HR	Pulse	23	6	7	-0.145	-13.498	0.845	0.841	2.000	0.964
HFD	Field	57	3	4	-0.073	-7.040	0.901	0.782	2.378	0.983
SHB	Balance	8	5	6	-0.242	-21.494	0.847	0.967	2.287	0.980
TD	Dissipation	115	18	35	-0.519	-40.488	0.683	1.066	1.711	0.937
TTD	Dissipation	14	2	6	-0.493	-38.921	0.669	0.985	1.464	0.899
all	Pulse	97	NA	30	0.012	1.167	0.844	0.787	1.874	0.954
all	Field	57	NA	4	-0.008	-0.820	0.896	0.762	2.322	0.981
all	Balance	8	NA	6	-0.244	-21.650	0.854	0.972	2.294	0.980
all	Dissipation	129	NA	37	-0.464	-37.153	0.681	1.052	1.666	0.931

cases for which the Ln-Ratio was significantly different from 0 ($p<0.001$) (Fig. 1.3), indicating systematic bias (underestimation).

Proportional bias, estimated by Slope, varied among methods and families of methods ($p<0.01$). Among families, Dissipation methods showed a significantly smaller Slope than Pulse and Field methods (Fig. 1.3(a)), which was largely driven by the low value of TD (Fig. 1.3(b)). Also, both Pulse and Dissipation families had slopes significantly different from 1 ($p<0.01$ and $p<0.001$, respectively), but only the slope of the TD method was significantly lower than 1 ($p<0.001$) (Fig. 1.3). As for the effects of calibration material, calibrations made with whole plants had a significant proportional bias (Slope < 1 , $p<0.001$) (Fig. 1.3). Calibration linearity, as denoted by Slope (ln-ln), varied across methods and families of methods ($p<0.001$). We observed higher values of Slope (ln-ln) for the TD method compared to CHP, T-max, HR and HFD. Consistently, the Dissipation family in general also had a higher Slope (ln-ln) than the Pulse and Field families (Fig. 1.3). CHP, T-max and HFD (and Pulse and Field methods in general) had a Slope (ln-ln) significantly lower than 1 (Table 1.1 and Fig. 1.3(b)), indicating a convex relationship between reference and measured flow. Calibrations performed with whole plants

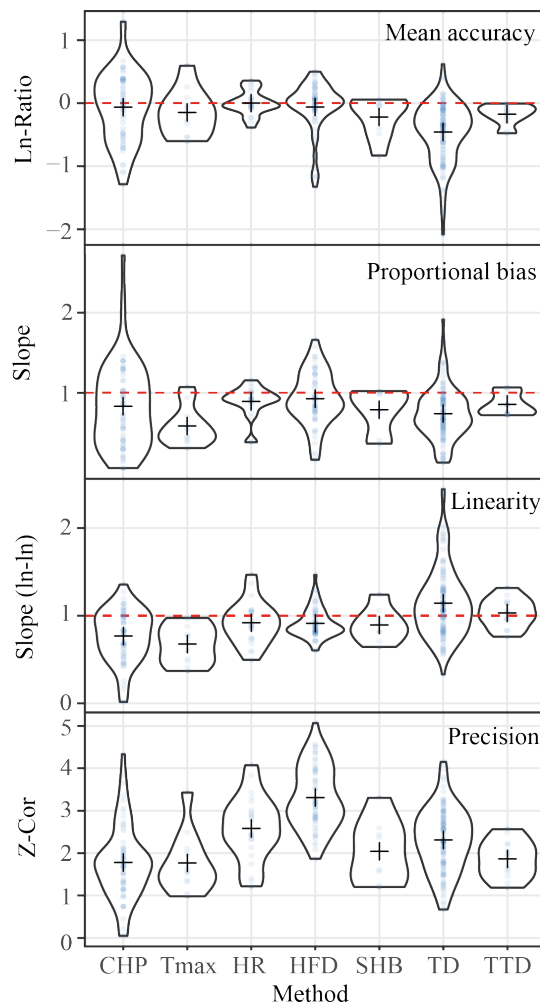


Figure 1.2: Distribution of the calibration performance metrics for each method. Dots represent the value of each individual calibration metric. Crosses represent the average of the metric for each method. Horizontal, dashed lines specify reference, perfect calibration values for a given metric.

suffered from lack of linearity, indicated by Slope (ln-ln) significantly lower than 1 (Fig. 1.3).

Precision (Z-Cor) was explained by both method and calibration material. The HFD method (and Field methods in general) provided significantly higher precision than either Pulse or Dissipation methods (particularly CHP,

1.3. Results

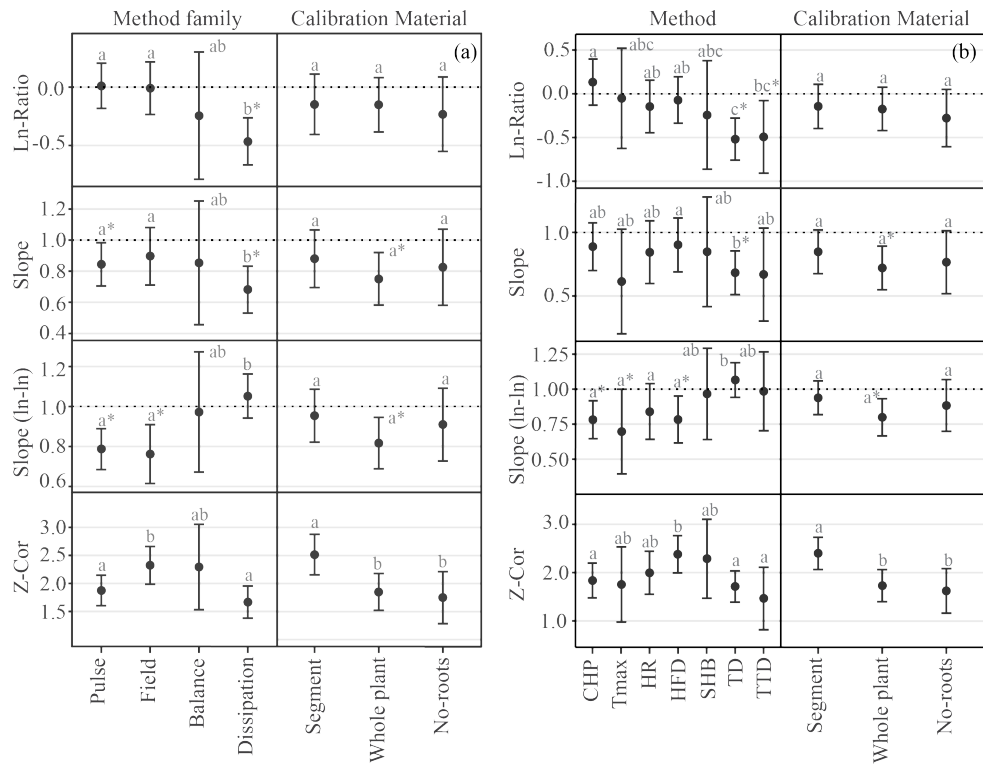


Figure 1.3: Predictions of the LMM models calculated from least-squares means of the four calibration metrics (Ln-Ratio as a proxy for mean accuracy, Slope for proportional bias, Slope (ln-ln) for linearity and Z-Cor for precision) for (a) different families of sap flow methods or for (b) different sap flow methods and for different calibration materials (Segment: stem segment; Whole plant: whole plant on a container or lysimeter; No-roots: whole plant without roots). 95% confidence intervals of the estimates are also shown. Different letters indicate significant differences between factors levels evaluated with Tukey’s test. Horizontal, dotted lines indicate reference, perfect calibration values for a given metric. Asterisks (*) indicate significant departure from those reference values.

TD and TTD) (Table 1.1 and Fig. 1.3(b)). Calibrations performed on stem segments provided higher precision than those conducted on whole plants (with or without roots) (Fig. 1.3).

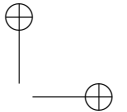
In all the previous models, little variability was explained by species (τ_{00} , species), relative to the higher variability associated to Study, particularly for the Ln-Ratio and Z-Cor models (τ_{00} , study, Table A3). This is consistent with the low ICC values observed for the species factor, indicating that there is more variability within than among species (Table A3).

In addition, the analysis of the normalized absolute error for the different methods showed that NRMSE decreased linearly with increasing measured sap flow in CHP, HFD and TTD methods and increased for T-max, SHB and TD (Table 1.2 and Fig. A2). For HR the increase in NRMSE with measured sap flow was not significant. For all the methods that measure SFD, the absolute error at a typical flow of $25 \text{ cm}^3 \text{ cm}^{-2} \text{ h}^{-1}$ ranged between $6.3 \text{ cm}^3 \text{ cm}^{-2} \text{ h}^{-1}$ for CHP and $10.7 \text{ cm}^3 \text{ cm}^{-2} \text{ h}^{-1}$ for the TTD method (Table 1.2).

1.3.2 Influence of wood traits

We did not find any significant influence of wood density on accuracy and linearity metrics (Fig. 1.4). Nonetheless, we observed a negative effect of wood density on proportional bias of HFD and TD calibrations ($p < 0.05$ and $p < 0.1$, respectively). In addition, a significant positive effect of wood density on the precision of HFD measurements was observed ($p < 0.001$), indicating that the higher the wood density, the higher the precision (Fig. 1.4).

We did not find any significant difference among wood porosity types in calibration metrics for studies using the TD or CHP methods. Nevertheless, the non-linearity (Slope (ln-ln) < 1) observed in general for the CHP method (Fig. 1.3(b)) was only significant for species with diffuse-porous wood, not for conifer species (Table 1.3).



1.4. Discussion

19

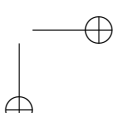
Table 1.2: Error analysis of different sap flow methods. The normalized root mean square error (NRMSE) is modelled as a function of method and the mean flow range for each calibration (and their interaction) using a LMM model with the same random structure as the main models (cf. section 2.3). β_0 and β_1 are the corresponding intercepts and slopes, respectively (β_0 expressed as % NRMSE; β_1 expressed as % NRMSE per change in $cm^3 cm^{-2} h^{-1}$ for SFD or as % NRMSE per change in $cm^3 h^{-1}$ for SF). This linear model, was also used to calculate a reference NRMSE at a sap flux equivalent to the percentile 50 of the range of the data in the calibrations (SFD: $25 cm^3 cm^{-2} h^{-1}$; SF: $1300 cm^3 h^{-1}$). The expected NRMSE and RMSE (in brackets, in $cm^3 cm^{-2} h^{-1}$, except for SHB that is in $cm^3 h^{-1}$) at a typical flow are also given.

Method	NRMSE			
	β_0	%	β_1	reference NRMSE (and RMSE)
CHP	27.03***		-0.08***	25.04% (6.26)
T-max	31.56.		0.25***	37.83% (9.46)
HR	9.38		0.81	29.59% (7.40)
HFD	30.33***		-0.12***	27.45% (6.86)
SHB	14.85		0.02***	42.95% (558.36)
TD	34.93***		0.10***	37.31% (9.33)
TTD	44.04***		-0.04***	42.94% (10.73)

Statistical significant levels: " ." p<0.1 ; "*" p<0.05; "**" p<0.01; "***" p<0.001.

1.4 Discussion

Our results show a large variability in the quality of sap flow calibrations, even within the same sap flow method (Fig. 1.2), highlighting the large variability among and even within studies. This implies that, even if methods are properly applied (as defined in section 2.1), sap flow measurements can still produce biased estimates of water transport rates in plants, and these errors will need to be considered in quantitative analyses based on this type of measurements. On average, however, all sap flow methods assessed here produced results that may be acceptable for qualitative use in most applications, as shown by the typical high correlation between measured and reference values ($r > 0.89$ for all methods and method families, Table 1.1). For quantitative use, no method appears to be suitable for all experimental contexts,



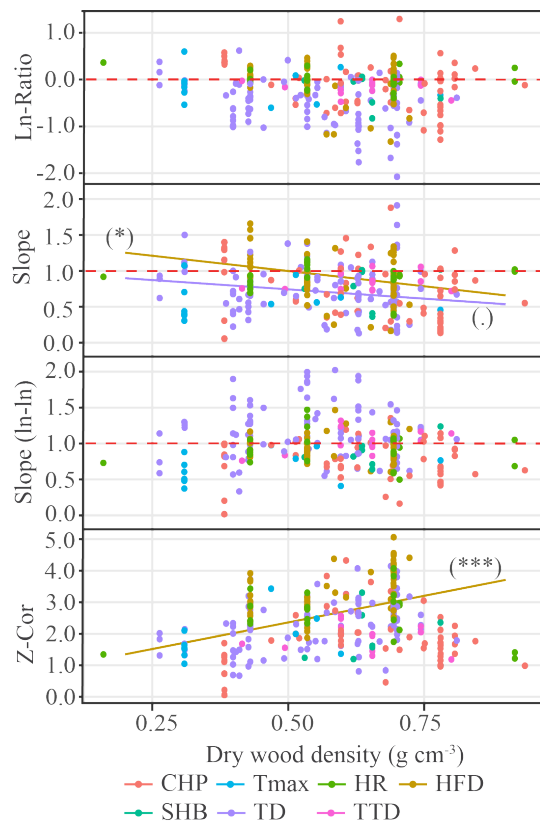


Figure 1.4: Relationship between the four calibration performance metrics (Ln-Ratio as a proxy for accuracy, Slope for proportional bias, Slope (ln-ln) for linearity, and Z-Cor for precision) and wood density, for different sap flow methods. Horizontal, dashed red lines indicate reference, perfect calibration values for a given metric. Regression lines are shown for significant effects only, and the corresponding level of significance (p-value: <0.1: (.), <0.05: (*), < 0.01: (**), < 0.001: (***) is also reported

and researchers need to consider both the inherent limitations of the methods and the need to perform study-specific calibrations (see Implications and recommendations, Table 1.4).

Table 1.3: Least-squares means and 95% CI calculated from the LMM models testing the effect of different wood porosity types (Wood porosity) on sap flow calibration performance metrics (Ln-Ratio as a proxy for accuracy, Slope for proportional bias, Slope (ln-ln) for linearity, and Z-Cor for precision) for CHP and TD methods. No differences were detected among wood anatomies. Significance levels indicate departure from an ideal calibration (Ln-Ratio = 0; Slope = 1; Slope (ln-ln) = 1)

Method	Wood porosity	n	Accuracy		Proportional bias		Linearity		Precision	
			Ln-Ratio	Slope	Slope (ln-Ln)	Z-Cor				
CHP	diffuse	48	-0.055 [-0.370 , 0.259]	0.795 [0.557 , 1.033].	0.799 [0.671, 0.927]	1.980 [1.729 , 2.231]				
CHP	conifers	15	0.066 [-0.603 , 0.734]	1.043 [0.459 , 1.627]	0.777 [0.469 , 1.085]	1.381 [0.775 , 1.988]				
TD	diffuse	81	-0.273 [-0.658 , 0.111]	0.752 [0.491 , 1.014].	1.126 [0.917 , 1.336]	1.672 [1.085 , 2.260]				
TD	ring	16	-0.405 [-0.866 , 0.056].	0.743 [0.410 , 1.077].	0.984 [0.681 , 1.286]	2.260 [1.572 , 2.947]				
TD	conifers	15	-0.396 [-0.873 , 0.080].	0.808 [0.468 , 1.147]	1.142[0.842 , 1.441]	1.606 [0.892 , 2.321]				

Statistical significant levels: * p<0.1 ; ** p<0.05; *** p<0.01; **** p<0.001.

1.4.1 Sap flow measurement errors across methods and methodological families

A relatively small part of the total variability in the quality of calibrations is related to methods and families of methods and, to a lesser extent, to the calibration material (fixed effects explain 8 – 28% of the variability in calibration metrics; see R_m^2 values in Table A3). Despite the high variability within methods, we detected significant differences between methods. Dissipation methods were the only methods for which accuracy was significantly lower than expected for an ideal calibration. This is consistent with previous reports (Braun & Schmid (1999); S. E. Bush, Hultine, Sperry, Ehleringer, & Phillips (2010); Caterina, Will, Turton, Wilson, & Zou (2014); (????); de Oliveira Reis, Campostrini, Sousa, & Silva (2006); S. Fuchs et al. (2017); Ping Lu & Chacko (1998); McCulloh et al. (2007); Montague & Kjelgren (2006); Rubilar, Hubbard, Yañez, Medina, & Valenzuela (2017); Steppe, De Pauw, Doody, & Teskey (2010); Taneda & Sperry (2008); Uddling, Teclaw, Pregitzer, & Ellsworth (2009)) and our synthesis confirms that most of the individual TD and all TTD calibrations underestimate sap flow systematically (Fig. 1.5). Interestingly, however, other studies have found the opposite result (Cain (2009); K. R. Hultine et al. (2010); P Lu (2002); Sperling et al. (2012); Sun, Aubrey, & Teskey (2012)) and simulation models (Hölttä, Linkosalo, Ri-

ikonen, Sevanto, & Nikinmaa (2015); Wullschleger et al. (2011)) suggest that it is difficult to state a priori whether TD will over- or underestimate flow, as the measurements obtained are highly dependent on wood properties and on flux conditions. Our results show that, globally, the conditions leading to underestimation are more frequent and support the existence of a proportional bias underlying this systematic underestimation by TD (Fig. 1.3). It must be also noted, however, that Dissipation methods have been tested against a much wider range of flow conditions compared to the rest of the methods (Fig. 1.5, Fig.6).

Calibration parameters of the TD method were originally considered to be universal but subsequent studies have claimed that species-specific calibrations are necessary to obtain correct sap flow measurements (S. Fuchs et al. (2017); Ping Lu et al. (2004); Steppe et al. (2010)). For a set of diffuse-porous species, using a pooled calibration also substantially improved TD (but not HFD) performance compared to measurements obtained with the original calibration (S. Fuchs et al. (2017)). However, our results show that species in general and wood porosity type in particular explain a small or even no proportion of the variability in the calibrations (Table 1.3 and A3). This implies that factors related to the experimental context and, possibly, to intraspecific variability in wood properties (cf. section 1.5.2) may have a large contribution to overall uncertainty. Therefore, our results suggest that calibration parameters for TD or HFD, obtained under different experimental contexts, may not be generalizable to species level, as also suggested by Fuchs et al. (2017).

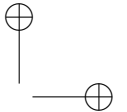
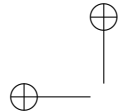
In addition to Dissipation methods, Pulse methods also suffer proportional bias, probably driven by overestimation at low flows, although this was significant for T-max only (i.e. positive intercepts in linear models fitted to calibration data; Fig. 1.5 and 1.6 and A3). It is well known that the equations of CHP and T-max cannot be solved at sap flows close to 0, and the calibration intercepts observed here (Fig. A3) are consistent with the detection thresholds reported for T-max ($\sim 10 \text{ cm}^3 \text{ cm}^{-2} \text{ h}^{-1}$; Steve Green et al. (2003)) and CHP ($2\text{-}4 \text{ cm}^3 \text{ cm}^{-2} \text{ h}^{-1}$; T. M. Bleby, Burgess, & Adams (2004));

Table 1.4: Synthesis of the potential sources of error and use adequacy for each method. Crosses indicates that the method is sensitive to the respective source of error (updated from Vandegehuchte and Steppe, 2013). Methods are classified according to their use effectiveness under different flow conditions: dark grey, light grey and white indicate highly, partially and no recommended use, respectively. When assessing use adequacy for high/low flows, dark and light gray indicate a Normalized Root Mean Square Error (NRMSE) less than a 22% and a 44%, respectively, calculated with the NRMSE model (Table 1.2). In Absolute flows use recommendation, dark grey shows methods with both accuracy (Ln-Ratio) and proportional bias (Slope) not significantly different from a perfect calibration. In Relative flows use recommendation, dark grey shows methods with linearity (Slope (ln-ln)) not significantly different from a perfect calibration and with reasonable precision. Potentiality of measuring small stems diameters (< 125mm) is also reported.

Method	Potential source of measure error								Effectiveness in measuring					
	Wounding	Radial velocity profile	Wood properties	Natural thermal gradients	Sensor installation	Sensor design	Baseline	Power input	Pulse length	Reverse flows	Low flows*	High flows*	Absolute flows	Relative flows
CHP	x	x	x	x	x				x					
T-max	x	x	x		x		x							
HR	x	x	x		x									
HFD	x	x		x	x	x	x	x						
SHB				x		x	x	x						
TD	x	x	x	x		x	x	x						
TTD	x	x	x	x		x	x	x						

* (Low/High: SFD methods: <5 / >80 $cm^3 cm^{-2} h^{-1}$; SF methods: <260 / >3900 $cm^3 h^{-1}$)

Steve Green et al. (2003)). Our results confirm and generalize a previously reported low-flow detectability problem for T-max (S. Green et al. (2009), Steve Green et al. (2003); Vandegehuchte & Steppe (2012b)), but we could not confirm it for CHP as described before (Barrett et al. (1995); Becker

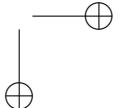


(1998); T. M. Bleby et al. (2004); Vandegehuchte & Steppe (2012b)). Despite overestimation at low flows, the average accuracy of CHP and T-max is good, which implies that low-flow overestimations may be compensated with underestimations at high flows. This is also shown by the lack of linearity observed in both methods (Slope ($\ln\text{-}\ln$) < 1 ; Fig. 1.3(b)).

Our analysis did not detect the saturation effect for the HR method at high flows that has been reported elsewhere (T. Bleby, McElrone, & Burgess (2008); S. Green et al. (2009); Steppe et al. (2015)). This is likely due to the fact that HR calibrations considered here include few observations in the region where this overestimation occurs ($> \sim 45 \text{ cm}^3 \text{ cm}^{-2} \text{ h}^{-1}$; Figs 5 and 6). Moreover, the high variability in the calibrations probably precluded detection of the saturation effect (Fig. 1.3 and 1.5) and of the apparent trend of increasing NRMSE with sap flow range for HR (Table 1.3 and Fig. A2). A lack of linearity can also be observed for HFD, consistent with the suggested tendency of this method to underestimate at high flows (Vandegehuchte & Steppe (2012c)).

Despite the large variability in precision within methods, our results show that calibrations performed with HFD give more precise results than those conducted using the CHP, TD and TTD methods. Although this result should be interpreted with care as it is based on 57 calibrations but only from 3 studies, the higher precision observed with HFD could lie in the second dimension included in the method, which could better capture the effect of anisotropy of the wood structure. This would also be consistent with the fact that SHB, a method that is assumed to integrate sap flow variability within the stem, was the method with the second highest precision on average, albeit precision was very variable for this method (Fig. 1.3(b)).

We did not detect differences in accuracy, proportional bias or linearity of the calibrations across calibration materials. However, compared to an ideal calibration, we did find proportional bias and lack of linearity in calibrations performed on whole plants, probably because these calibrations use large scales whose sensitivity and resolution are usually low, potentially affect-



1.4. Discussion

25

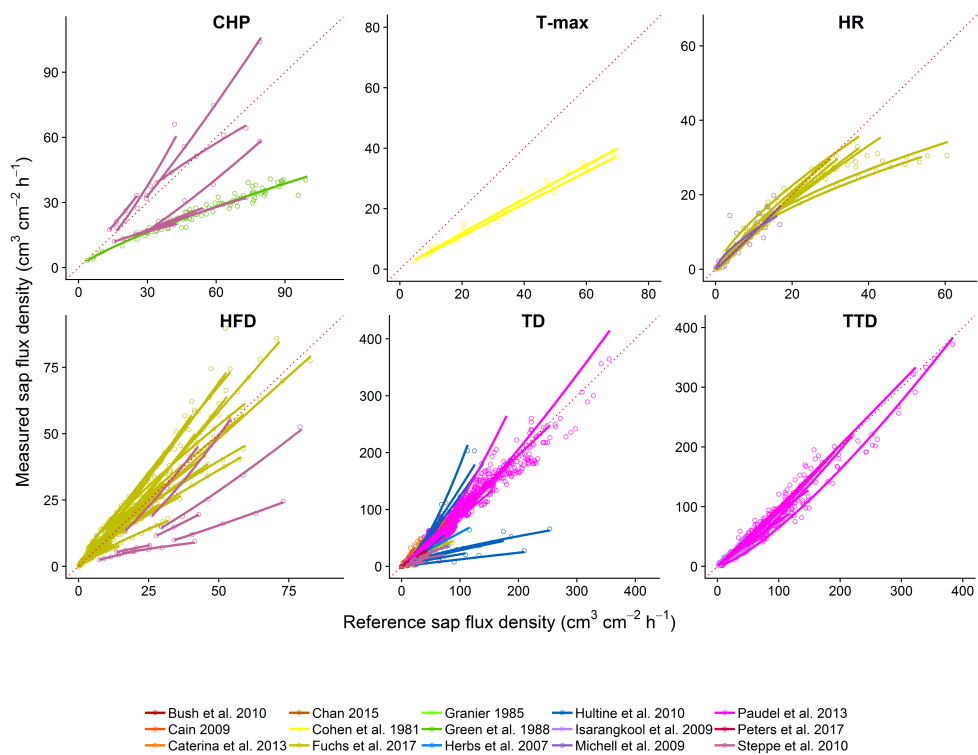


Figure 1.5: Relationship between measured and reference sap-flux density (SFD) for different sap flow methods, studies and calibrations. The fits of ln–ln regressions (Eq. 4) for each calibration are also depicted. Different colors represent different studies that report results in sap-flux density units. Scales vary across panels to facilitate intra method comparison. The red dotted line indicates the 1:1 relationship.

ing low-flow measurements and leading to artefactual overestimation at low flows. Poor linearity may also be due to non-linear changes in belowground hydraulic resistance as the sap flow increases (J. Martínez-Vilalta, Korakaki, Vanderklein, & Mencuccini (2007)). In cut plants, we may have two opposite effects, as cutting could eliminate belowground resistance (favoring flow) but add resistance due to putative embolism formation after cutting. Similarly, the higher precision of calibrations conducted on cut stems relative to those conducted on whole plants (with and without roots), likely reflects that cut stem calibrations are normally conducted in laboratories with precision scales and under controlled conditions that minimize experimental random errors.

1.4.2 The performance of sap flow calibrations is largely unrelated to species wood traits

Species-specific wood density and wood porosity type explained little variability in overall calibration performance, although we detected some effects of wood density for HFD and TD calibrations. Wood density affected HFD measurements by increasing precision, which could be related to the response time of the sensors. If we assume that maximum sapwood water content is reduced as wood density increases (Simpson (1993)), associated changes in thermal diffusivity could lead to a faster sensor response (Hölttä et al. (2015)), higher correlation between actual and measured flows. Wood density also showed a negative relationship with proportional bias for HFD and TD, a pattern that could be caused by the combined effects of wood density and water content on wood thermal diffusivity (Vandegehuchte & Steppe (2012c); Vergeynst et al. (2014)). The fact that we did not find clear effects of wood density on calibration accuracy and linearity, despite that wood density affects thermal diffusivity and hence heat transport (Wullschleger et al. (2011)), could be explained by two reasons. Firstly, we could not use the actual wood density for most of the calibrations, because it was not reported in the corresponding studies, and using species-level averages instead of the wood density of the plant material specifically used on the calibrations may mask the effect of wood density on calibration performance. Secondly, wood density in angiosperms appears to be only weakly correlated to some wood

1.4. Discussion

27

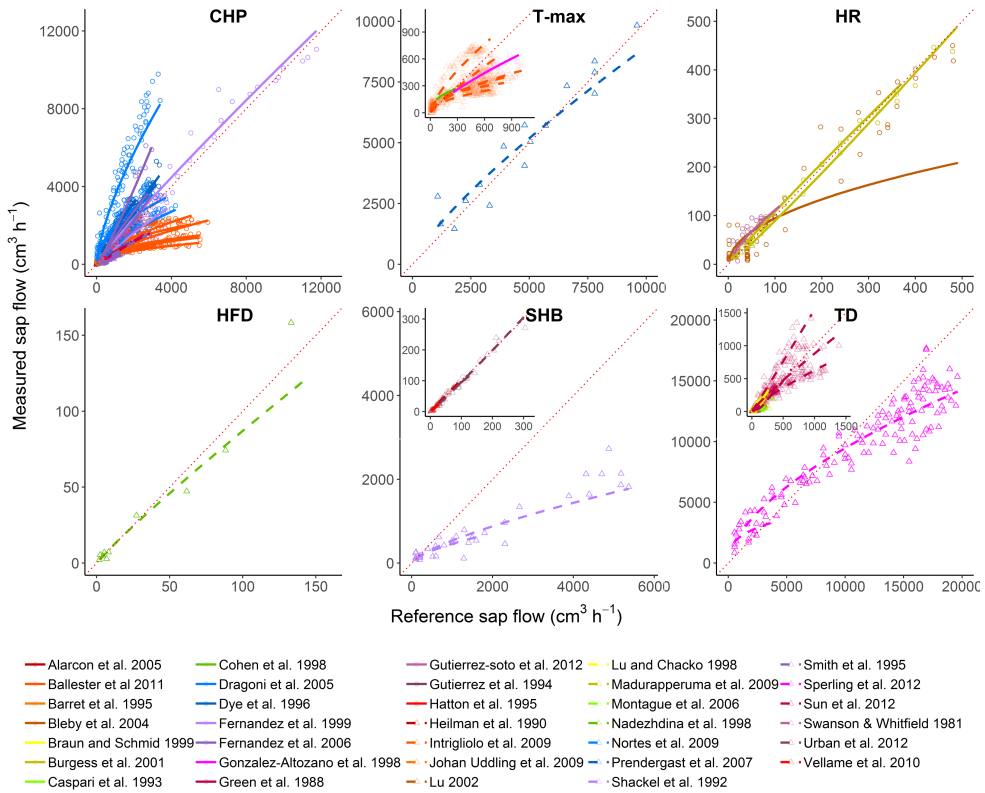


Figure 1.6: Relationship between measured and reference sap flow (SF) for different sap flow methods, studies and calibrations. The fits of ln-ln regressions (Eq. 4) for each calibration are also depicted. Different color symbols and line types represent different studies. Scales varies across panels to facilitate intra method comparison. Insets are shown in some panels (T-max, SHB, TD) to facilitate visualization when the flow ranges differed markedly among calibrations for the same method. The red dotted line indicates 1:1 relationship.

properties that could be important for sap flow calibrations, such as lumen fraction (Zanne et al. (2010)).

Our global analysis did not show clear and consistent differences in calibration quality between different wood porosity types (Table 1.2) as previously suggested by several studies for both CHP (S. R. Green & Clothier (1988)) and TD methods (S. E. Bush et al. (2010); Sun et al. (2012)). According to heat transport theory, we should expect declining performance from conifer to ring-porous species (i.e. from most homogenous to most heterogeneous wood). For CHP, we found that proportional bias (only marginally) and nonlinearity departed from an ideal calibration for diffuse-porous species, but these patterns did not differ significantly from those observed for conifers. Our results did not clearly support either an inferior performance of TD in ring-porous species compared to diffuse-porous or conifers, as could be expected from the reported underestimation driven by large sap flow gradients along sensor length or by the imperfect probe contact with hydroactive xylem in species with narrow sapwood (Michael J Clearwater et al. (1999); but see Wullschleger et al. (2011)). Wood porosity effects on sap flow calibrations have been inferred in individual studies from measurements in few species representative of each wood porosity type (S. E. Bush et al. (2010); Sun et al. (2012); Xie & Wan (2018)) and our inability to detect these effects here may be caused by the high variability in experimental context within our dataset. Furthermore, the effect of the different anatomies may be masked by high structural variability within wood porosity types, as for example the variation in latewood to earlywood in conifers (Fan, Guyot, Ostergaard, & Lockington (2018)) and we cannot discard that calibration performance could be related to quantitative anatomical traits not assessed in this study (cf. Xie & Wan (2018)). Although the low variability we observed at the species level suggests that quantitative anatomical traits might not explain much of the variability in sap flow calibrations, we encourage that quantitative wood traits are measured in the same plant material used to calibrate sap flow sensors to better understand the influence of wood properties on the variability of sap flow calibrations.

1.4. Discussion

1.4.3 Implications and recommendations

Our global analysis shows that even when the methods are applied following standard recommendations the quality of individual calibrations can be very low (Fig. 1.3). This result reflects, on one hand, systematic bias in TD and lack of linearity in CHP, two of the most widely used methods (Fig. A1) and, on the other hand, unknown sources of error related to experimental conditions and/or sample characteristics (Table 1.4). In our study, we could not account for all the experimental conditions to evaluate these sources of variability, except for the effect of the calibration material. Examples of factors that may affect calibrations when using the same type of calibration material include sensor design (S. Fuchs et al. (2017)), sensor installation (T. M. Bleby et al. (2004); Ping Lu & Chacko (1998); Ren et al. (2017)), variation in calculations of wood thermal properties (Looker et al. (2016)), zero flow determination (Looker et al. (2016); Peters et al. (2018)) or the mechanism of flow generation in cut stem calibrations (negative vs positive pressures) (S. Fuchs et al. (2017)) (Table 1.4). Previous reports, however, usually focus on only one of the sources of experimental error. Importantly, relevant methodological information that could be used to assess (and account for) these sources of error is frequently not reported (Peters et al. (2018); Steppe et al. (2015)). Clearly, further research into the effects of experimental conditions on the quality of different sap flow methods should be a priority, as well as more complete, standardized reporting of experimental conditions, including information on the sources of potential methodological errors listed in Table 1.4.

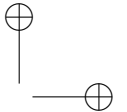
Our results show that calibrations may be needed to obtain correct absolute values of sap flow, even when Pulse methods are used (see also S. Fuchs et al. (2017); Steppe et al. (2010)). However, sap flow calibrations provide a snapshot of the performance of a given sap flow method under relatively stable conditions, which may greatly differ from those experienced by plants in the field. Moreover, our analysis could not address the methodological variability related to more dynamic effects such as errors caused by changes in sap-wood water content (Vergeynst et al. (2014)), long-term wounding or signal

dampening (Maranon-jimenez2018; Peters et al. (2018); A Wiedemann et al. (2013)). In this sense, more studies should assess calibration applicability to mid- or long-term measurements (e.g., Oliveras & Llorens (2001)), possibly combined with independent estimates of sapwood water content (Vandegeehuchte & Steppe (2012b)) and whether calibrations obtained from excised segments are valid for whole-plants.

Considering only their performance in calibration tests (i.e. no other logistic or technical issues, such as sensor, datalogging, or power constraints, which will be study-specific) we can provide some general recommendations on the use of sap flow methods (Table 1.4). The most widely used method, TD, appears to be consistently inaccurate, shows proportional bias and generally underestimates sap flow, by 40% on average (if used with its original calibration coefficients). However, it presents good linearity, which implies that this method can be used when sap flow responses to environmental variables and/or treatments are the primary focus of the study (i.e., good estimates of absolute sap flow values are not critical). In comparison, CHP, T-max and HFD all present a certain nonlinearity which may affect the estimation of these environmental responses. At least for CHP and T-max (specially for the latter) this pattern seems to be driven by overestimation at low flows and underestimation at high flows canceling out each other. This implies that both Pulse methods could be suitable for studies interested in absolute values of transpiration. For the HFD method, the nonlinearity could be influencing the estimations of radial sap flow patterns, as these measurements would need to correctly measure both high and low flows simultaneously. We also confirm that the HR method may not be suitable to measure high flows but it is probably the best method for detailed physiological studies involving low flows.

1.5 Conclusions

In conclusion, our global assessment contributes towards a proper incorporation of measurement errors in the interpretation of individual case studies



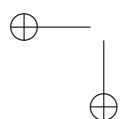
1.5. Conclusions

31

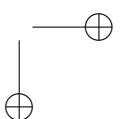
and in modelling studies aimed at upscaling sap flow data (T. J. Hatton et al. (1995); Hernandez-Santana et al. (2015)). Perhaps even more importantly, it paves the way towards improved intercomparison of sap flow datasets obtained with different methods to assess regional or global patterns in plant water use (e.g., the SAPFLUXNET initiative; Poyatos et al. (2016)). Although providing explicit correction factors for each method is beyond the scope of this paper, the typical accuracy deviations provided in Table 1.1 can be used as a first order correction when combining sap flow data from different methods (and no additional information on study-specific uncertainty sources is available).

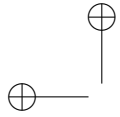
—

—

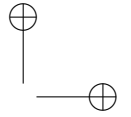


|



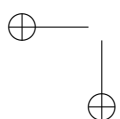


“thesis” — 2020/11/3 — | 9:01 — page 32 — #52

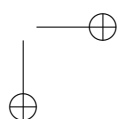


—

—



|



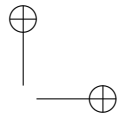
2

Global transpiration data from sap flow measurements: the SAPFLUXNET database

Rafael Poyatos, Víctor Granda, Víctor Flo, Jordi Martínez-Vilalta *et al.*

Abstract

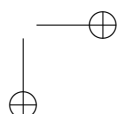
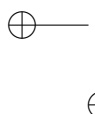
Plant transpiration links physiological responses of vegetation to water supply and demand with hydrological, energy and carbon budgets at the land-atmosphere interface. However, despite being the main land evaporative flux at the global scale, transpiration and its response to environmental drivers are currently not well constrained by observations. Here we introduce the first global compilation of whole-plant transpiration data from sap flow measurements (SAPFLUXNET, <https://sapfluxnet.creaf.cat/>). We harmonised and quality-controlled individual datasets supplied by contributors worldwide in a semi-automatic data workflow implemented in the R programming language. Datasets include sub-daily time series of sap flow and hydrometeorological drivers for one or more growing seasons, as well as metadata on the stand characteristics, plant attributes and technical details of the measurements. SAPFLUXNET contains 202 globally distributed datasets with sap flow time series for 2714 plants, mostly trees, of 174 species. SAPFLUXNET has a broad bioclimatic coverage, with woodland/shrubland and temperate forest biomes especially well-represented (80% of the datasets). The measurements cover a wide variety of stand structural characteristics and plant sizes. The datasets encompass the period between 1995 and 2018, with 50% of the datasets being at least 3 years long. Accompanying radiation and vapour pressure deficit data are available for most of the datasets, while on-site soil water content is available for 56% of the datasets. Many datasets contain data for species that make up 90% or more of the total stand basal area, allowing the estimation of stand transpiration in diverse ecological settings. SAPFLUXNET adds to existing plant trait datasets, ecosystem flux networks and remote sensing products to help increase our understanding of plant water use, plant responses to drought and ecohydrological processes. SAPFLUXNET version 0.1.5 is freely available from the Zenodo repository (<https://doi.org/10.5281/zenodo.3971689>, Poyatos et al. 2020a). The ‘sapfluxnetr’ R package, designed to access, visualise and process SAPFLUXNET data is available from CRAN.



2.1 Introduction

Terrestrial vegetation transpires ca. 45000 km³ of water per year (Schlesinger and Jasechko, 2014; Wang-Erlandsson et al., 2014; Wei et al., 2017), a flux that represents 40% of global land precipitation, 70% of total land evapotranspiration (Oki and Kanae, 2006), and is comparable in magnitude to global annual river discharge (Rodell et al., 2015). For most terrestrial plants, transpiration is an inevitable water loss to the atmosphere because they need to open stomata to allow CO₂ diffusion into the leaves for photosynthesis. Latent heat from transpiration represents 30–40% of surface net radiation globally (Schlesinger and Jasechko, 2014; Wild et al., 2015). Transpiration is therefore a key process coupling land-atmosphere exchange of water, carbon and energy, determining several vegetation-atmosphere feedbacks, such as land evaporative cooling or moisture recycling. Regulation of transpiration in response to fluctuating water availability and/or evaporative demand is a key component of plant functioning and one of the main determinants of a plant’s response to drought (Martin-StPaul et al., 2017; Whitehead, 1998). Despite its relevance for earth functioning, transpiration and its spatiotemporal dynamics are poorly constrained by available observations (Schlesinger and Jasechko, 2014) and not well represented in models (Faticchi et al., 2016; Mencuccini et al., 2019). An improved understanding on how plants regulate transpiration is thus needed to better predict future trajectories of land evaporative fluxes and vegetation functioning under increased drought conditions driven by global change.

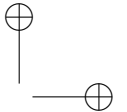
Conceptually, transpiration can be quantified at different organisational scales: leaves, branches and whole plants, ecosystems and watersheds. In practice, transpiration is relatively easy to isolate from the bulk evaporative flux, evapotranspiration, only from the leaf to the plant levels. In terrestrial ecosystems, evapotranspiration includes evaporation from the soil and from water-covered surfaces, including plants. Transpiration measurements on individual leaves or branches with gas exchange systems are difficult to upscale to the plant level (Jarvis, 1995). Likewise, transpiration measurements using whole-plant chambers (e.g. Pérez-Priego et al., 2010) or gravimetric methods



(e.g. weighing lysimeters) in the field are still challenging. At the ecosystem scale and beyond, evapotranspiration is generally determined using micrometeorological methods, catchment water budgets or remote sensing approaches (Shuttleworth, 2007; Wang and Dickinson, 2012). In some cases, isotopic methods and different algorithms applied to measured ecosystem fluxes can provide an estimation of transpiration at the ecosystem scale (Kool et al., 2014; Stoy et al., 2019).

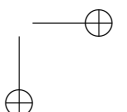
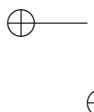
Transpiration drives water transport from roots to leaves in the form of sap flow through the plant’s xylem pathway (Tyree and Zimmermann, 2002), and this sap flow affects heat transport in the xylem. Taking advantage of this, thermometric sap flow methods were first developed in the 1930s (Huber, 1932) and further refined over the following decades (Čermák et al., 1973; Marshall, 1958) to provide operational measurements of plant water use. These methods have become widely used in plant ecophysiology, agronomy and hydrology (Poyatos et al., 2016), especially after the development of simple, easily replicable methods (e.g. Granier, 1985, 1987). Whole-plant measurements of water use using thermometric sap flow methods provide estimates of water flow through plants from sub-daily to interannual timescales, and have been mostly applied in woody plants (but see Baker and Van Bavel (1987) for measurements on herbaceous species). Xylem sap flow is measured semi-invasively (Brodersen et al., 2019) and can be upscaled to the whole plant, obtaining a near-continuous quantification of plant water use. Multiple sap flow sensors can be deployed, in almost any terrestrial ecosystem, to determine the magnitude and temporal dynamics of transpiration across species, environmental conditions or experimental treatments. All sap flow methods are subject to methodological and scaling issues, which may affect the quantification of absolute water use in some circumstances (Čermák et al., 2004; Köstner et al., 1998; Smith and Allen, 1996; Vandegehuchte and Steppe, 2013). Nevertheless, all methods are suitable for the assessment of the temporal dynamics of transpiration and of its responses to environmental changes or to experimental treatments (Flo et al., 2019).

The generalised application of sap flow methods in ecological and hydrological research in the last 30 years has thus generated a large volume of



data, with an enormous potential to advance our understanding of the spatiotemporal patterns and the ecological drivers of plant transpiration and its regulation (Poyatos et al., 2016). However, this large volume of data needs to be compiled and harmonised to enable global syntheses and comparative studies across species and regions. Across-species data syntheses using sap flow data have mostly focused on maximum values extracted from publications (Kallarackal et al., 2013; Manzoni et al., 2013; Wullschleger et al., 1998). Multi-site syntheses have focused on the environmental sensitivity of sap flow, using site means of plant-level sap flow or sap flow-derived stand transpiration (Poyatos et al., 2007; Tor-ngern et al., 2017). Since data sharing is only incipient in plant ecophysiology, sap flow datasets have not been traditionally available in open data repositories. Open data practices are now being implemented in databases, which fosters collaboration across monitoring networks in research areas relevant to plant functional ecology (Falster et al., 2015; Gallagher et al., 2020; Kattge et al., 2020) and ecosystem ecology (Bond-Lamberty and Thomson, 2010). The success of the data sharing and data re-use policies within the FLUXNET global network of ecosystem level fluxes has shown how these practices can contribute to scientific progress (Bond-Lamberty, 2018).

Here we introduce SAPFLUXNET, the first global database of sap flow measurements built from individual community-contributed datasets. We implemented this compilation in a data structure designed to accommodate time series of sap flow and the main hydrometeorological drivers of transpiration, together with metadata documenting different aspects of each dataset. We harmonised all datasets and performed basic semi-automated quality assurance and quality control procedures. We also created a software package that provides access to the database, allows easy visualisation of the datasets and performs basic temporal aggregations. We present the ecological and geographic coverage of SAPFLUXNET version 0.1.5, (Poyatos et al., 2020a) followed by a discussion of potential applications of the database, its limitations and a perspective of future developments.



2.2 The SAPFLUXNET data workflow

2.2.1 An overview of sap flow measurements

The main characteristics of sap flow methods have been reviewed elsewhere (Čermák et al., 2004; Smith and Allen, 1996; Swanson, 1994; Vandegehuchte and Steppe, 2013). Given the already broad scope of the paper, here we only provide a brief methodological overview, without delving into the details of the individual methods. Sap flow sensors track the fate of heat applied to the plant’s conducting tissue, or sapwood, using temperature sensors (thermocouples or thermistors), usually deployed in the plant’s main stem. Both heating and temperature sensing can be done either internally, by inserting needle-like probes containing electrical resistors (or electrodes for some methods) and temperature sensors into the sapwood, or externally; these latter systems being especially designed for small stems. Depending on how the heat is applied and the principles underlying sap flow calculations, sap flow sensors can be classified into three major groups: heat dissipation methods, heat pulse methods and heat balance methods (Flo et al., 2019). Heat dissipation and heat pulse methods estimate sap flow per unit sapwood area and they have been called ‘sap flux density methods’ (Vandegehuchte and Steppe, 2013); heat balance methods directly yield sap flow for the entire stem or for a sapwood section. Heat dissipation methods include the constant heat dissipation (HD; Granier 1985, 1987), the transient (or cyclic) heat dissipation (CHD; Do and Rocheteau, 2002) and the heat deformation (HFD; Nadezhina 2018) methods. Heat pulse methods include the compensation heat pulse (CHP; Swanson and Whitfield, 1981), heat ratio (HR; Burgess et al. 2001), T-max (HPTM; Cohen et al. 1981) and Sapflow+ (Vandegehuchte and Steppe, 2012) methods. Heat balance methods include the trunk sector heat balance (TSHB; Čermák et al. 1973) and the stem heat balance (SHB; Sakuratani, 1981) methods. The suitability of a certain method in a given application largely depends on plant size and the flow range of interest (Flo et al., 2019), but HD and CHP are the most widely used (Flo et al., 2019; Peters et al., 2018; Poyatos et al., 2016). Apart from these different methodologies, within

each sap flow method variants exist in sensor design and in data processing approaches, resulting in relatively high levels of methodological uncertainty comparable to those in other areas of plant ecophysiology.

The output from sap flow sensors is automatically recorded by dataloggers, at hourly or even higher temporal resolution. This output relates to heat transport in the stem and needs to be converted to meaningful quantities of water transport, such as sap flow per plant or per unit sapwood area. How this conversion is achieved varies greatly across methods, with some relying on empirical calibrations and others being more physically-based and requiring the estimation of wood thermal properties and other parameters (Čermák et al., 2004; Smith and Allen, 1996; Vandegehuchte and Steppe, 2013). Depending on the method and the specific sensor design, sap flow measurements can be representative of single points, linear segments along the sapwood, sapwood area sections or entire stems. Except for stem heat balance methods, these measurements need to be spatially integrated to account for radial (Berdanier et al., 2016; Cohen et al., 2008; Nadezhina et al., 2002; Phillips et al., 1996) and azimuthal (Cohen et al., 2008; Lu et al., 2000; Oren et al., 1999a) variation of sap flow within the stem to obtain an estimate of whole-plant water use (Čermák et al., 2004). At a minimum, an estimate of sapwood area is needed to upscale the measurements to whole-plant sap flow rates. Sap flow rates can thus be expressed per individual (i.e. plant or tree), per unit sapwood area (normalising by water-conducting area), and per unit leaf area (normalising by transpiring area).

Here we will use the term ‘sap flow’ when referring, in general, to the rate at which water moves through the sapwood of a plant and, more specifically, when we refer to sap flow per plant (i.e. water volume per unit time, Edwards et al., 1996). We acknowledge that the term ‘sap flux’ has also been proposed for this quantity (Lemeur et al., 2009), but more generally, ‘sap flux density’ (e.g. Vandegehuchte and Steppe, 2013) or just ‘sap flux’ are used to refer to ‘sap flow per unit sapwood area’. Since here we include methods natively measuring sap flow per plant or per sapwood area, throughout this paper we will use the more general term ‘sap flow’, and, when necessary, we

will indicate explicitly the reference area used: ‘sap flow per (unit) sapwood area’, ‘sap flow per (unit) leaf area’ or ‘sap flow per (unit) ground area’.

2.2.2 Data compilation

SAPFLUXNET was conceived as a compilation of published and unpublished sap flow datasets (Appendix Table A1) and thus the ultimate success of the initiative critically depended on the contribution of datasets by the sap flow community. An expression of interest showed that a critical mass of datasets with a wide geographic distribution could potentially be contributed and the results of this survey were used to raise the interest of the sap flow community (Poyatos et al., 2016). The data contribution stage was open between July 2016 and December 2017 although a few additional datasets were updated during the data quality control process and contain more recent data.

All contributed datasets had to meet some minimum criteria before they were accepted, both in terms of content and format. We required that all datasets contained sub-daily, processed sap flow data, representative of whole-plant water use under different hydrometeorological conditions. This meant that both the processing from raw temperature data to sap flow quantities and the scaling from single-point measurements to whole-plant data had been performed by the data contributor responsible for each dataset. Time-series of sap flow data and hydrometeorological drivers were required to be representative of one growing-season, setting, as broad reference, a minimum duration of 3 months. Sap flow could be either expressed as total flow rate per plant or per unit sapwood area. Contributors also needed to provide metadata on relevant ecological information of the site, stand, species and measured plants as well as on basic technical details of the sap flow and hydrometeorological time-series. Datasets had to be formatted using a documented spreadsheet template (cf. ‘sapfluxnet_metadata_template.xlsx’ in the Supplement) and uploaded to a dedicated server at CREAf, Spain, using an online form.

2.2.3 Data harmonisation and quality control: QC1

Once datasets were received, they were stored and entered a process of data harmonisation and quality control (Fig. 1, Supplement Fig. S1). This process combined automatic data checks with human supervision, and the entire workflow was governed by functions and scripts in the R language (R Core Team, 2019), including other related tools, such as R markdown documents and Shiny applications. All R code involved in this QC process was implemented in the `sapfluxnetQC1` package (Granda et al., 2016). To aid in the detection of potential data issues throughout the entire process (Fig. 1, Supplement Fig. S1), we implemented several elements of control: (1) automatic log files tracking the output of each QC function applied, (2) automatic creation and update of status files, tracking the QC level reached by each dataset, (3) automatic QC summary reports in the form of R markdown documents, (4) interactive Shiny applications for data visualisation, (5) documentation of manual changes applied to the datasets using manually-edited text files, (6) storage of manual data cleaning operations in text files, and (7) automatic data quality flagging associated with each dataset. All these items ensure a robust, transparent, reproducible and scalable data workflow. Example files for (2), (3) and (6) can be found in the Supplement.

The first stage of the data QC (QC1) performed several data checks (Supplement Table S1) on received spreadsheet files and produced an interactive report in an R markdown document, which signalled possible inconsistencies in the data and warned of potential errors. These data issues were addressed, with the help of data contributors, if needed. Once no errors remained, the dataset was converted into an object of the custom-designed ‘`sfn_data`’ class (Supplement Fig. S2, see also section 2.5), which contained all data and metadata for a given dataset (Appendix Tables A2–A6 list all variable names). Data and metadata belonging to all Level 1 datasets were further visually inspected using an interactive R Shiny application, and, if no major issues were detected, they were subjected to the second QC process, QC2.

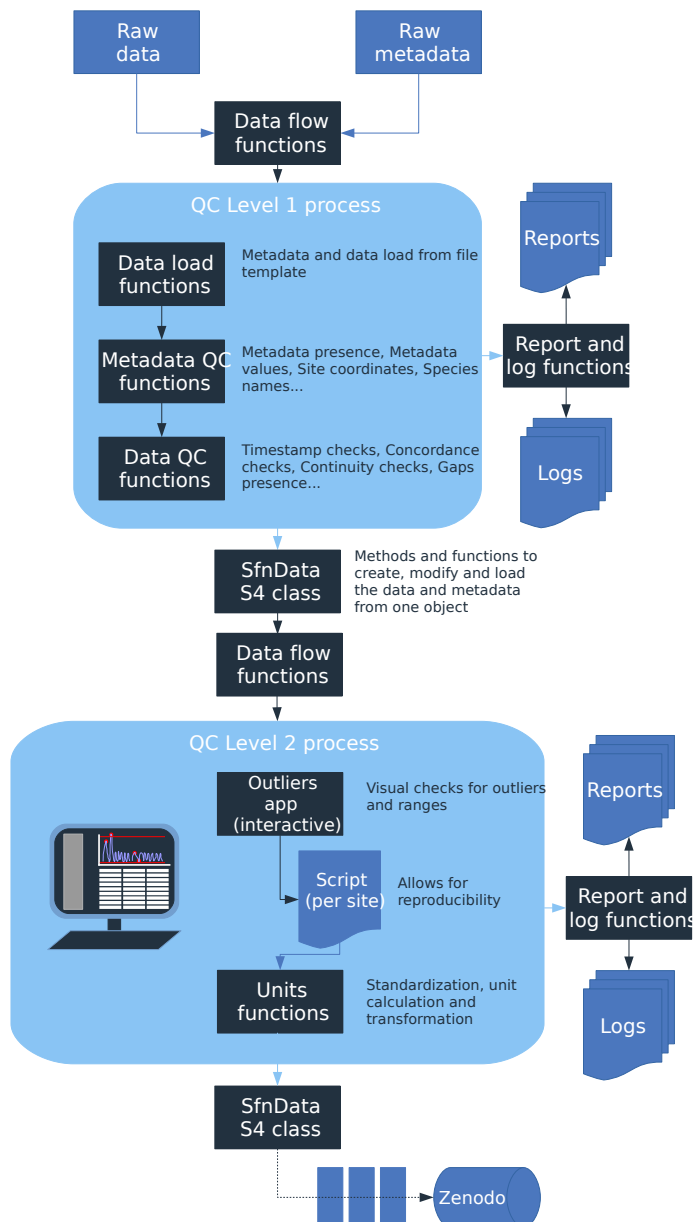


Figure 2.1: Overview of the SAPFLUXNET data workflow. Data files are received from data contributors, and undergo several quality-control processes (QC1 and QC2). Both, QC1 and QC2 produce an .RData object of the custom-designed sfn-data S4 class storing all data, metadata and data flags for each dataset. The progress and results of the QC processes are monitored through individual reports and log files. The final outcome, is stored in a folder structure with a either single .RData file for each dataset or a set of seven csv files for each dataset.

2.2.4 Data harmonisation and quality control: QC2

Datasets entering QC2 underwent several data cleaning and data harmonisation processes (Supplement Table S2). We first ran outlier detection and out of range checks; these checks did not delete or modify the data, only warned about any suspicious observation ('outlier' and 'range' warnings). The outlier detection algorithm was based on a Hampel filter, which also estimates a replacement value for a candidate outlier (Hampel, 1974). For the range checks, we defined minimum and maximum allowed values for all the time series variables, based on published values of extreme weather records and maximum transpiration rates (Cerveny et al., 2007; Manzoni et al., 2013). The outcome of outlier and range checks were visually inspected on the actual time series being evaluated using an interactive R Shiny application (Supplement Fig.S3). Following expert knowledge, visually confirmed outliers were replaced by the values estimated by the Hampel filter. Similarly, we replaced out of range values by NA if the variable was out of its physically allowed range (Supplement Fig.S3). Outlier and out of range 'warnings' for each observation (e.g. for each variable and timestep) were documented in two data flags tables, with the same dimensions as the corresponding data tables (Supplement Fig. S2). Likewise, those observations with confirmed problematic values, which were removed or replaced, were also flagged; further information can be found in the 'data flags' vignettes in the 'sapfluxnetr' package Granda et al. (Granda et al., 2019)

Final data harmonisation processes in QC2 involved unit transformations and the calculation of derived variables (Supplement Table S2). When plant sapwood area was provided by data contributors, we interconverted between sap flow rate per plant and per unit sapwood area. If leaf area was supplied, we also calculated sap flow per unit leaf area, but note that this transformation does not take into account the seasonal variation in leaf area. In QC2 we estimated missing environmental variables which could be derived from related variables in the dataset (Appendix, Table A6). We also estimated the apparent solar time and extraterrestrial global radiation from the provided timestamp and geographic coordinates using the R package 'solaR'

(Perpiñán, 2012). All estimated or interconverted observations were flagged as ‘CALCULATED’ in the ‘env_flags’ or ‘sap_flags’ table (Supplement Fig. S2).

2.2.5 Data structure

One of the major benefits of the SAPFLUXNET data workflow is the encapsulation of datasets in self-contained R objects of the S4 class with a predefined structure. These objects belong to the custom-designed ‘sfn_data’ class, which display different slots to store time series of sap flow and environmental data, their associated data flags, and all the metadata (Supplement Fig. S2). For further information please see the ‘sfn_data classes’ vignette in the ‘sapfluxnetr’ package (Granda et al., 2019). The code identifying each dataset was created by the combination of a ‘country’ code, a ‘site’ code and, if applicable, a ‘stand’ code and a ‘treatment’ code. This means that several ‘stands’ and/or ‘treatments’ can be present within one ‘site’ (Supplement Table S3).

At the end of the QC process, we generated a folder structure with a first-level storing datasets as either ‘sfn_data’ objects or as a set of comma-separated (csv) text files. Within each of these formats, a second-level folder groups datasets according to how sap flow is normalized (per plant, sapwood or leaf area); note that the same dataset, expressing different sap flow quantities, can be present in more than one folder (e.g. ‘plant’ and ‘sapwood’). Finally, the third level contains the data files for each dataset: either a single ‘sfn_data’ object storing all data and metadata, or all the individual csv files. More details on the data structure can be found in the ‘sapfluxnetr-quick-guide’ vignette in the ‘sapfluxnetr’ package (Granda et al., 2019).

2.3 The SAPFLUXNET database

2.3.1 Data coverage

The SAPFLUXNET version 0.1.5 database harbours 202 globally distributed datasets (Fig. 2a, Supplement Fig. S4 and Table S3), from 121 geographical

locations, with Europe, Eastern USA and Australia especially well represented. These datasets were represented in the bioclimatic space using the terrestrial biomes delimited by Whittaker (Fig. 2b), but note that, as any bioclimatic classification, it has its limitations. Datasets have been compiled from all terrestrial biomes, except for temperate rainforests, although some tropical montane sites have been included. Woodland/shrubland and temperate forest biomes are the most represented in the database adding up to 80% of the datasets (Fig. 2b). However, large forested areas in the tropics and in boreal regions are still not well represented (Fig. 2a,b). Looking at the distribution by vegetation type (Fig. 2c), evergreen needleleaf forest is the most represented vegetation type (65 datasets), followed by deciduous broadleaf forest (47 datasets) and evergreen broadleaf forest (43 datasets).

SAPFLUXNET contains sap flow data for 2714 individual plants (1584 angiosperms and 1130 gymnosperms), belonging to 174 species (141 angiosperms and 33 gymnosperms), 95 different genera and 45 different families (Supplement, Table S4-S5). All species but one, *Elaeis guineensis*, a palm, are tree species. *Pinus* and *Quercus* are the most represented genera (Fig. 3b). Amongst the gymnosperms, *Pinus sylvestris*, *Picea abies* and *Pinus taeda* are the three most represented species with data provided on 290, 178 and 107 trees, respectively (Fig. 3a). For the angiosperms, *Acer saccharum*, *Fagus sylvatica* and *Populus tremuloides* are the most represented species, with 162, 116 and 104 trees, respectively, although most *Acer saccharum* data come from a single study with a very large sample size (Fig. 3a). Some species are present in more than 10 datasets: *Pinus sylvestris*, *Picea abies*, *Fagus sylvatica*, *Acer rubrum*, *Liriodendron tulipifera* and *Liquidambar styraciflua* (Fig. 3a, Supplement Table S4).

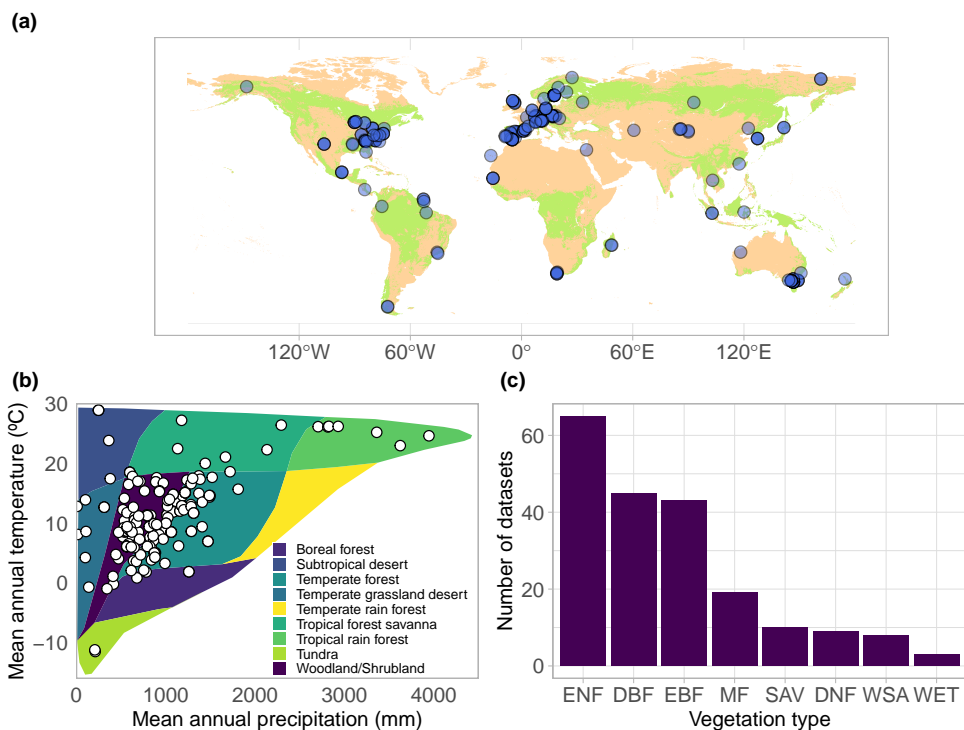


Figure 2.2: (a) Geographic, (b) bioclimatic and (c) vegetation type distribution of SAPFLUXNET datasets. In (a) woodland area from Crowther et al. (2015) is shown in green. In (b) we represent the different datasets according to their mean annual temperature and precipitation in a Whittaker diagram showing the classification of the main terrestrial biomes. In (c) vegetation types are defined according to the International Geosphere-Biosphere Programme (IGBP) classification (ENF: Evergreen Needleleaf Forest; DBF: Deciduous Broadleaf Forest; EBF: Evergreen Broadleaf Forest; MF: Mixed Forest; DNF: Deciduous Needleleaf forest; SAV: Savannas; WSA: Woody Savannas; WET: Permanent Wetlands).

2.3. The SAPFLUXNET database

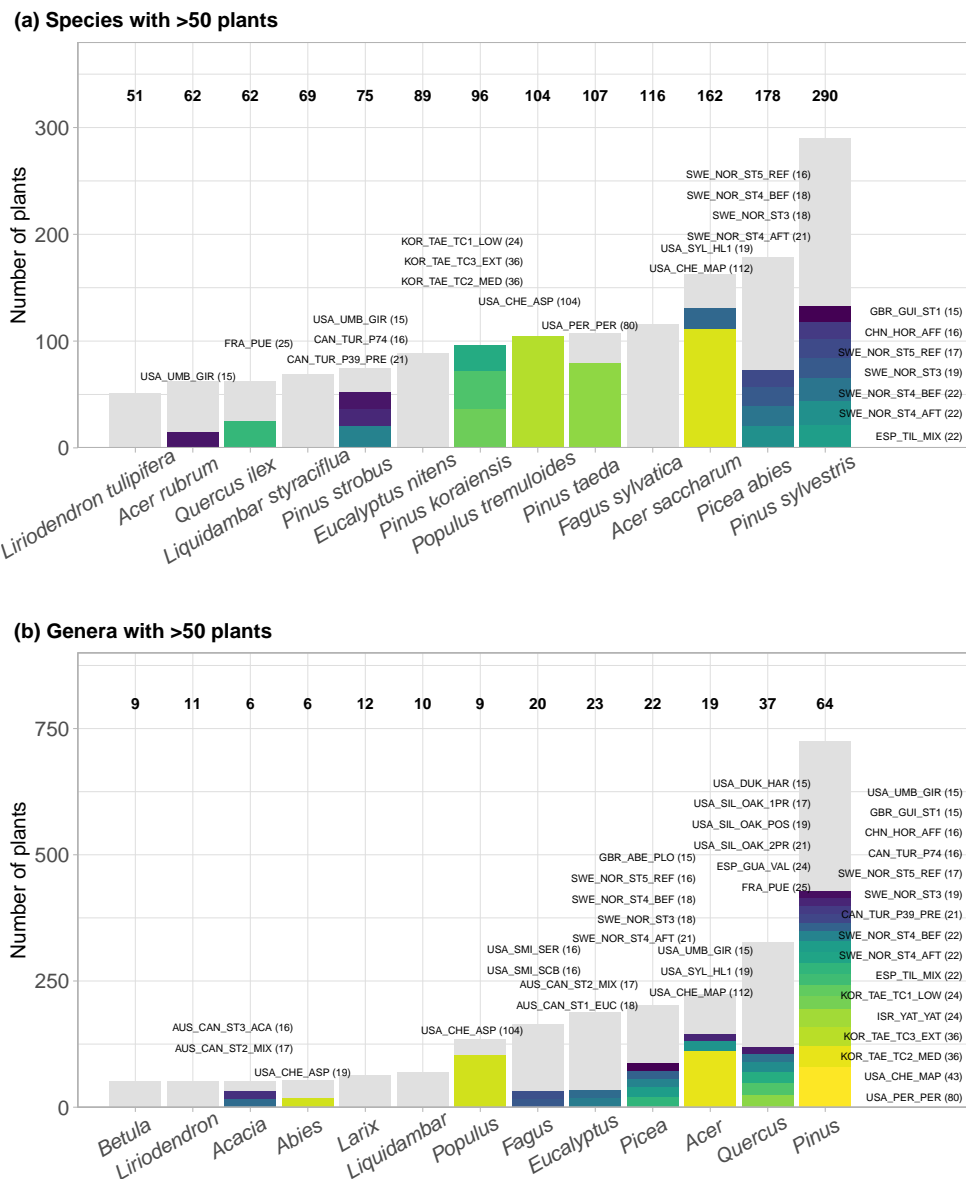


Figure 2.3: Taxonomic distribution of genera and species in SAPFLUXNET, showing (a) species and (b) genera with > 50 plants in the database. Total bar height depicts number of plants per species (a) or genera (b). Numbers on top of each bar show the number of datasets where each species (a) or genus (b) is present. Colours other than grey highlight datasets with 15 or more plants of a given species (a) or genus (b). Bar height for a given colour is proportional to the number of plants in the corresponding dataset, which is also shown in parentheses next to the dataset code.

2.3.2 Methodological aspects

For more than 90% of the plants, sap flow at the whole-plant level is available (either directly provided by contributors or calculated in the QC process); this is important for upscaling SAPFLUXNET data to the stand level (cf. section 4.2). Because the leaf area of the measured plants is often not available as metadata, sap flow per unit leaf area was estimated for only 18.6% of the individuals (Fig. 4). The heat dissipation method is the most frequent method in the database (HD, 66.4% of the plants), followed by the trunk sector heat balance (TSHB, 16.4%) and the compensation heat pulse method (CHP, 8.4%) (Fig. 4). This distribution is broadly similar to the use of each method documented in the literature, although the TSHB method is overrepresented here, compared to the current use of this method by the sap flow community (Flo et al., 2019; Poyatos et al., 2016). Some methods, especially those belonging to the heat pulse family and the cyclic (or transient) heat dissipation (CHD) method are mostly used in angiosperms, while the TSHB and the heat field deformation (HFD) methods are more frequently used in gymnosperms (Fig. 4).

Calibration of sap flow sensors and scaling from point measurements to the whole-plant can be critical steps towards accurate estimates of absolute sap flow rates. In SAPFLUXNET, most of the sap flow time series have not undergone a species-specific calibration, with the CHD method showing the highest percentage of calibrated time series (Table 1). This lack of calibrations may be relevant for the more empirical heat dissipation methods (HD and CHD), which have been shown to consistently underestimate sap flow rates (Flo et al., 2019; Peters et al., 2018; Steppe et al., 2010). Radial integration of single-point sap flow measurements is more frequent than azimuthal integration (Table 2), except for the CHD method. A large number of plants using the HD method, and all plants measured using the HPTM method, do not employ any radial integration procedure. In contrast, the CHP, HR, SHB, and TSHB methods are those which more frequently addressed radial variation in one way or another (Table 2). Azimuthal integration procedures are also more frequent when the TSHB method is used (Table 2).

2.3. The SAPFLUXNET database

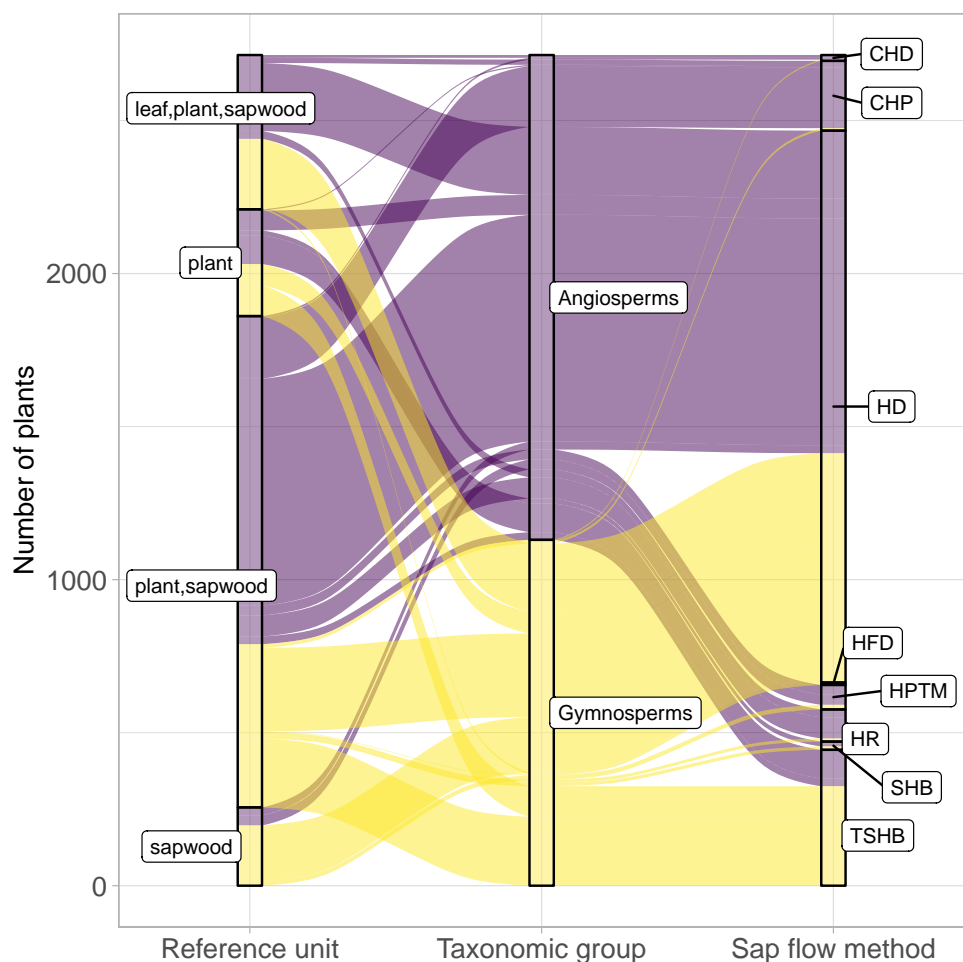


Figure 2.4: Distribution of plants in SAPFLUXNET according to major taxonomic group (angiosperms, gymnosperms), sap flow method (CHD:cycling heat dissipation; CHP: compensation heat pulse; HD: heat dissipation; HFD: heat field deformation; HPTM: heat pulse T-max (HPTM); HR: heat ratio (HR); SHB: stem heat balance; TSHB: trunk sector heat balance) and reference unit for the expression of sap flow (plant, sapwood area, leaf area). Combinations of reference units imply that data are present in multiple units.

2.3.3 Plant characteristics

Plant-level metadata is almost complete (99.5% of the individuals) for diameter at breast height (DBH), while sapwood area and sapwood depth, important variables for sap flow upscaling, are not available, or could not be

Table 2.1: Number of sap flow times series in SAPFLUXNET depending on whether they were calibrated (species-specific), non-calibrated or this information was not provided, for the different sap flow methods: cyclic (or transient) heat dissipation (CHD), compensation heat pulse (CHP), heat dissipation (HD), heat field deformation (HFD), heat pulse T-max (HPTM), heat ratio (HR), stem heat balance (SHB) and trunk sector heat balance (TSHB). The percentage of calibrated time series was expressed with respect to the total number of sap flow time series for each method.

Method	Calibrated	Non-calibrated	Not provided	% calibrated
CHD	6	13	0	31.6
CHP	29	42	157	12.7
HD	214	1491	98	11.9
HR	3	55	47	2.9
TSHB	7	433	4	1.6
HFD	0	8	0	0.0
HPTM	0	80	0	0.0
SHB	0	27	0	0.0

estimated, for 23% and 47% of the plants, respectively. Plant height and plant age are missing for 42% and 62% of the individuals, respectively. Sap flow data in SAPFLUXNET are representative of a broad range of plant sizes (Fig. 5a). The distribution of DBH showed a median of 25.0 cm and 20.4 cm for gymnosperms and angiosperms, respectively, with a long tail towards the largest plants, two *Mortoniodendron anisophyllum* trees from a tropical forest in Costa Rica that measured > 200 cm (Fig. 5a). The largest gymnosperm tree in SAPFLUXNET (176 cm in DBH) is a kauri tree (*Agathis australis*) from New Zealand. The distribution of plant heights is less skewed, with similar medians for angiosperms (17.6 m) and gymnosperms (17.5 m). The tallest plants are located in a tropical forest in Indonesia, where a *Pouteria firma* tree reached 44.7 m. Remarkably, of the 16 plants taller than 40 m, over 60% are Eucalyptus species. The tallest gymnosperm (36.2 m) is a *Pinus strobus* from NE USA.

Plant size metadata in SAPFLUXNET is complemented with plant-level data of sapwood and leaf area, that provide information on the functional areas for water transport and loss (Fig. 5a). Distributions of sapwood and leaf area show highly skewed distributions, with long tails towards the largest

2.3. The SAPFLUXNET database

Table 2.2: Number of plants in the SAPFLUXNET database using different radial and azimuthal integration approaches for the different sap flow methods: cyclic (or transient) heat dissipation (CHD), compensation heat pulse (CHP), heat dissipation (HD), heat field deformation (HFD), heat pulse T-max (HPTM), heat ratio (HR), stem heat balance (SHB) and trunk sector heat balance (TSHB).

Azimuthal integration					
Method	Measured	Sensor-integrated	Corrected, measured azimuthal variation	No azimuthal correction	Not provided
CHD	15	0	0	0	4
CHP	61	0	0	167	0
HD	216	0	520	1021	46
HFD	0	0	0	8	0
HPTM	0	0	0	80	0
HR	7	0	2	88	8
SHB	0	0	0	27	0
TSHB	0	25	191	219	9

Radial integration					
Method	Measured	Sensor-integrated	Corrected, measured radial variation	No radial correction	Not provided
CHD	0	0	6	13	0
CHP	222	0	6	0	0
HD	77	3	645	703	142
HFD	2	0	0	6	0
HPTM	0	0	0	80	0
HR	57	1	42	3	2
SHB	0	27	0	0	0
TSHB	0	338	8	89	9

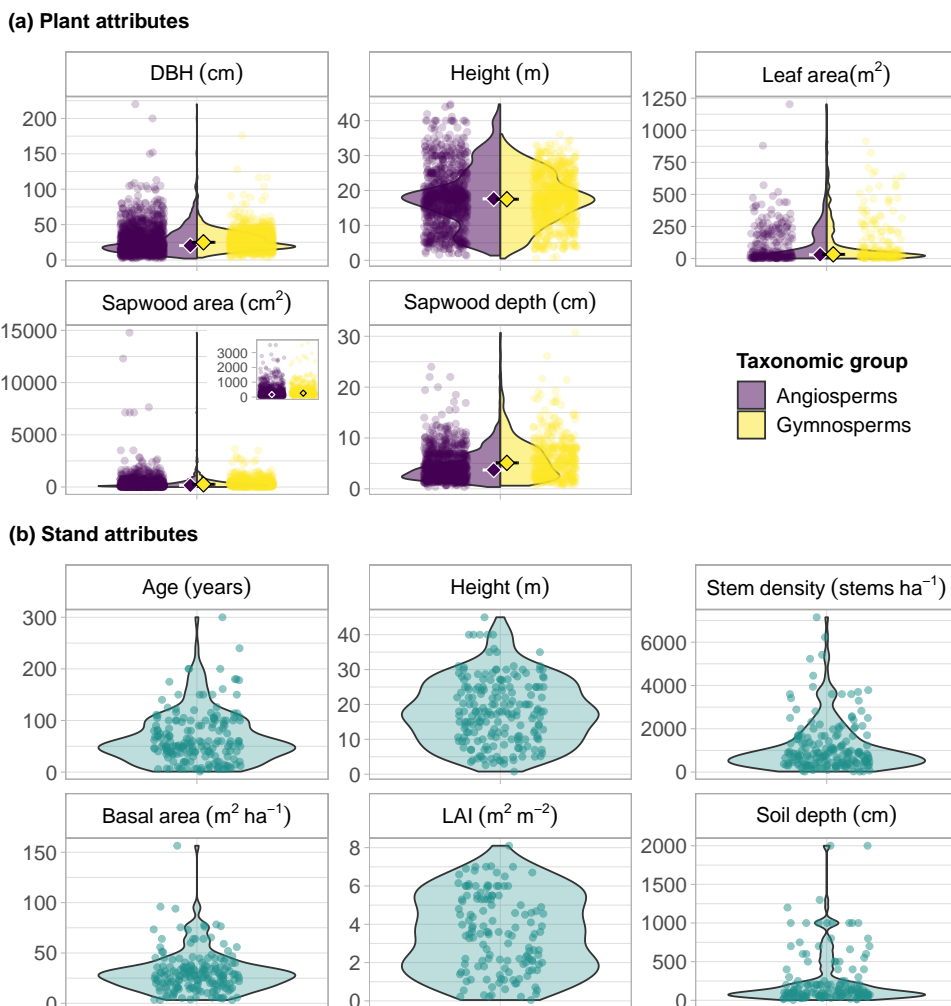


Figure 2.5: Characteristics of trees and stands in the SAPFLUXNET database. Panel (a) shows plant data and kernel density plots of the main plant attributes, coloured by taxonomic group (angiosperms and gymnosperms): diameter at breast height (DBH), plant height, sapwood area, sapwood depth and leaf area. The inset in the sapwood area panel zooms in values lower than 5000 cm^2 . Panel (b) shows stand data and kernel density plots of the main stand attributes: stand age, stand height, stem density, stand basal area, leaf area index (LAI) and soil depth.

values and slightly higher median values for gymnosperms (262 cm^2 and 33.0 m^2 for sapwood and leaf areas, respectively), compared to angiosperms (168 cm^2 and 29.9 m^2). Accordingly, median sapwood depth is also higher for

gymnosperms (5.1 cm) compared to angiosperms (3.7 cm). The largest trees (Mortoniiodendron, Pouteria, Agathis) with deep sapwood (17–24 cm) are also those with largest sapwood areas. Many large angiosperm trees from tropical (CRI_TAM_TOW, IDN_PON_STE, GUF_GUY_ST2; see Table S3 for dataset codes) and temperate forests (*Fagus grandifolia*, USA_SMIC_SCB) also show large sapwood areas (> 5000 cm²), but the plant with the deepest sapwood is a gymnosperm, an *Abies pinsapo* in Spain with 30.7 cm of sapwood depth.

2.3.4 Stand characteristics

Stand-level metadata include several variables associated with management, vegetation structure and soil properties. Half of the datasets originate from naturally regenerated, unmanaged stands, and 13.9% come from naturally regenerated but managed stands. Plantations add up to 32.2% and orchards only represent 4% of the datasets. Reporting of structural variables is mixed, with stand height, age, density and basal area showing relatively low missingness (6.4%, 11.4%, 12.9% and 13.4%, respectively); in contrast, soil depth and LAI are missing from 26.7% and 33.7% of the datasets.

SAPFLUXNET datasets originate from stands with diverse structural characteristics. Median stand age is 54 years and there are several datasets coming from >100 year-old forests (Fig. 5b). Stand height shows a similar range and distribution of values compared to individual plant height (Fig. 5a,b). The denser stands correspond to coppiced evergreen oak stands from Mediterranean forests (FRA_PUE, ESP_TIL_OAK), species-rich tropical forests (MDG_SEM_TAL) or relatively young temperate forests (e.g. FRA_HES_HE1_NON, USA_CHE_MAP). The sparsest stands (< 200 stems ha⁻¹) correspond to tree-grass savanna systems (Spain, Portugal, Australia, Senegal), dry woodlands (China), or oil palm plantations in Indonesia (IDN_JAM_OIL). Stands with the largest basal areas (> 70 m² ha⁻¹) are mostly dominated by broadleaf species, except for a *Picea abies* plantation in Sweden (SWE_SKO_MIN).

The distribution of leaf area index (LAI) shows a median of 3.5 m² m⁻², with the largest values observed in temperate (CZE_BIK, USA_DUK_HAR,

HUN_SIK) and tropical (GUF_GUY_GUY, COL_MAC_SAF_RAD) forests. The stands with the lowest LAI correspond to the sparse woodlands from Mediterranean and semi-arid locations and also those from forests near altitudinal or latitudinal tree-lines (FIN_PET, AUT_TSC). SAPFLUXNET datasets show a median soil depth of 100 cm, with only a dozen datasets originated from sites with soils deeper than 10 m (Fig. 5b).

The number of plants per dataset is highly variable, with most of the datasets (86%) containing data for at least 4 trees and 46% of the datasets having data for at least 10 trees (Fig. 6a, see also Fig. 9).

2.3.5 Temporal characteristics

The oldest datasets in SAPFLUXNET go back to 1995 (GBR_DEV_CON, GBR_DEV_DRO) while the most recent data reach up to 2018 (datasets from the ESP_MAJ cluster of sites). Several multi-year datasets are present in SAPFLUXNET (Fig. 6), with 50% of the datasets spanning a period of at least 3 years, and some datasets being extraordinarily long (16 years in FRA_PUE). Frequently, the datasets only cover the ‘growing season’ periods, or even shorter periods for some sites which were eventually included because they improved the ecological and geographic coverage of the database (e.g. ARG_MAZ, ARG_TRE as representative of deciduous Nothofagus forest in South Patagonia). In contrast, a few datasets show continuous records over multiple years (Fig. 6b). Amongst the longest datasets, most of them come from European or North American sites (Fig. 6), except some datasets from Israel (ISR_YAT_YAT, 7 years), Russia (RUS_FYO, 7 years), South Korea (KOR_TAE cluster of sites, 6 years) or New Zealand (NZL_HUA_HUA, 5 years).

SAPFLUXNET provides an unprecedented database to study the detailed temporal dynamics of plant transpiration across species and sites globally. Sub-daily records of sap flow (e.g. at least at hourly timesteps) are available for extended periods (Fig. 6b), allowing to address both seasonal and diel patterns in water use regulation by trees and how these temporal patterns change across species or years across terrestrial biomes, reflecting different

2.3. The SAPFLUXNET database

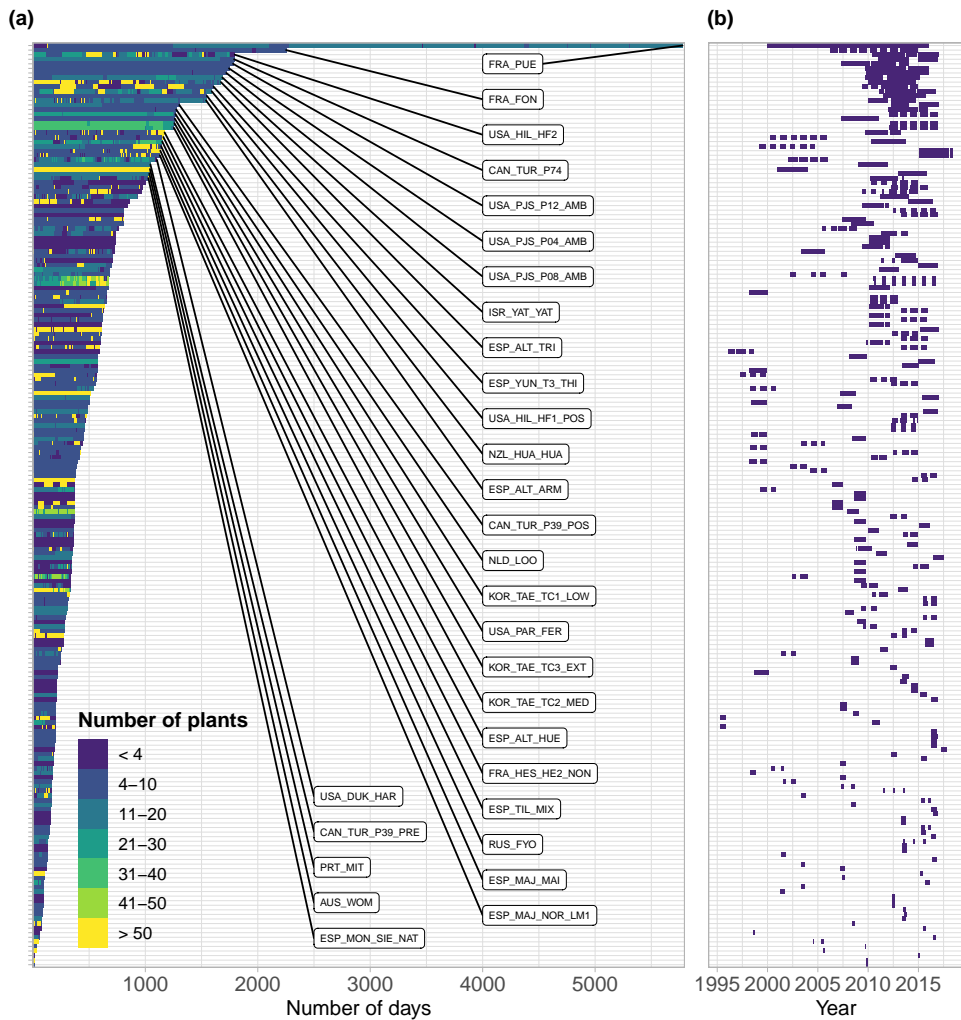


Figure 2.6: (a) Measurement duration of SAPFLUXNET datasets expressed in number of days with sap flow data and coloured by the number of plants measured on each day . The 30 longest datasets are labelled. For each dataset in panel (a), panel (b) shows its corresponding measurement period.

phenologies and water-use strategies. For instance, in Mediterranean forests, evergreen species such as *Quercus ilex*, *Arbutus unedo* and *Pinus halepensis* show moderate sap flow the whole year round, while the deciduous *Quercus pubescens* shows higher sap flow density during a shorter period and its water use is heavily reduced during a dry year (2012) (Fig. 7a). Temperate forests without water availability limitations show relatively high flows during the

growing season and similar diel sap flow patterns among species (Fig. 7b). In contrast, tropical forests show moderate to high sap flow rates during the entire year, with different dynamics in the intradaily water use regulation across species. For example, *Inga* sp. in a highly diverse wet tropical forest in Costa Rica, reduced sap flow during mid-day hours compared to co-existing species (Fig. 7c).

2.3.6 Availability of environmental data

All SAPFLUXNET datasets contain ancillary time series of the main hydrometeorological drivers of transpiration, accompanied by information on where these variables had been measured (Fig. 8a). Air temperature is available for all datasets. Although vapour pressure deficit (VPD) was originally absent in 38% of the datasets (Fig. 8a,b), we could estimate it for those sites providing air temperature and relative humidity data (QC Level 2, see section 2.3), and finally only 2 out of the 202 datasets have missing VPD information. For radiation variables, shortwave radiation was most often provided, compared to photosynthetically active and net radiation; only 8 out of 202 datasets do not have any accompanying radiation data. Most of these environmental variables were measured on-site, with precipitation being the variable most frequently retrieved from nearby meteorological stations (48% of the datasets) (Fig. 8a). Soil water content measured at shallow depth, typically between 0 and 30 cm below the soil surface, is provided for 56% of the datasets, while soil moisture from deep soil layers is available for only 27% of the datasets.

2.4 Potential applications

2.4.1 Applications in plant ecophysiology and functional ecology

There are multiple potential applications of the SAPFLUXNET database to assess whole-plant water use rates and their environmental sensitivity, both across species (e.g. Oren et al., 1999b) and at the intraspecific level (Poyatos et al., 2007). SAPFLUXNET will allow disentangling the roles of evaporative

2.4. Potential applications

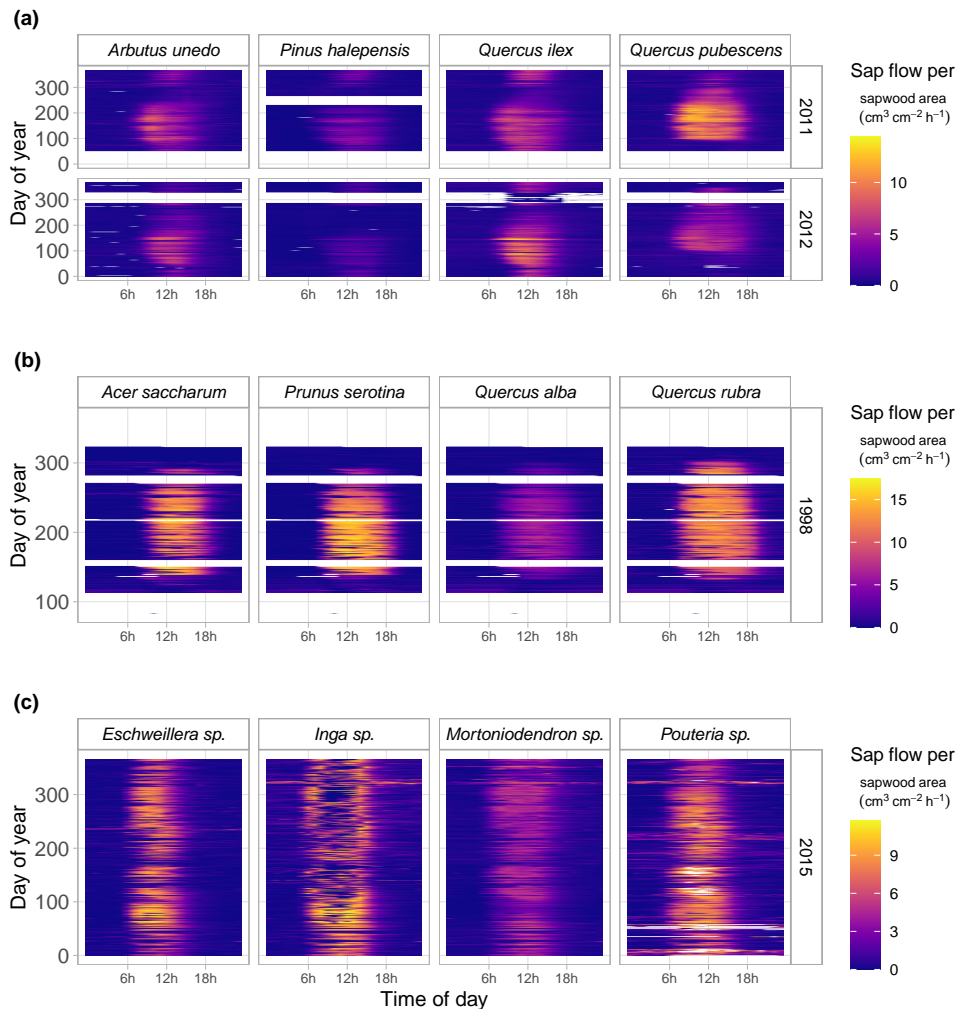


Figure 2.7: Fingerprint plots showing hourly sap flow per unit sapwood area (colour scale) as a function of hour of day (x-axis) and day of year (y-axis) for a selection of SAPFLUXNET sites with at least four co-occurring species. Panel (a) shows data from a Woodland/Shrubland forest in NE Spain (ESP_CAN), for an average (2011) and a dry (2012) year. Panel (b) shows data for a mesic Temperate forest (USA_WVF) and panel (c) shows data for a Tropical forest (CRI_TAM_TOW). For this latter site, only 4 of the 17 measured species are shown and some of them were only identified at the genus level.

demand and soil water content in controlling transpiration at the plant level, complementing recent studies looking at how water supply and demand affect

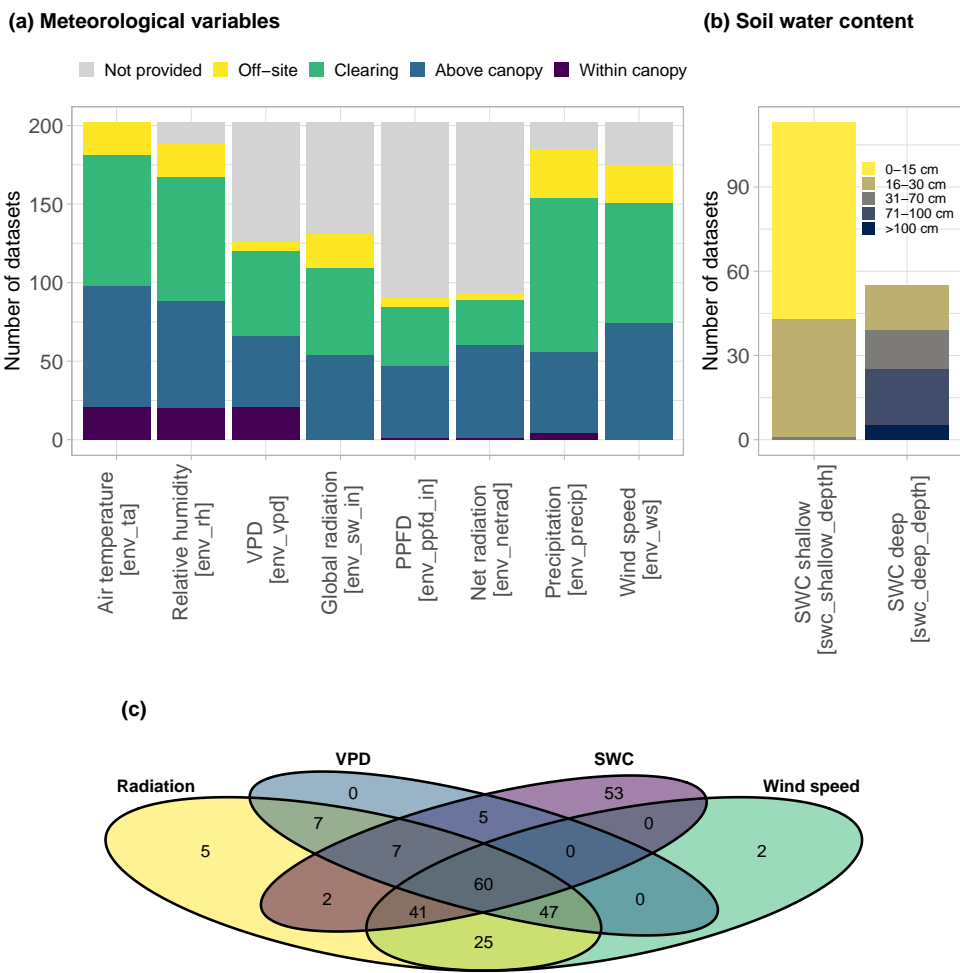


Figure 2.8: Summary of the availability of different environmental variables in SAPFLUXNET datasets. (a) Distribution of meteorological variables according to sensor location (in brackets, names of the variables in the database), (b) Distribution of soil moisture variables according to the measurement depth (in brackets, names of the variables in the database). (c) Venn diagram showing the number of datasets where each combination of different environmental variables are present, grouping shortwave, PPFD and net radiation under ‘Radiation’ variables.

evapotranspiration at the ecosystem level (Anderegg et al., 2018; Novick et al., 2016). The availability of global sap flow data at sub-daily time resolution and spanning entire growing seasons will allow focusing on how maximum

water use and its environmental sensitivity varies with plant-level attributes such as stem diameter (Dierick and Hölscher, 2009; Meinzer et al., 2005), tree height (Novick et al., 2009; Schäfer et al., 2000), hydraulic (Manzoni et al., 2013; Poyatos et al., 2007) and other plant traits (Grossiord et al., 2019; Kallarackal et al., 2013). SAPFLUXNET thus provides an unprecedented tool to understand how structural and physiological traits scale-up to whole-plant regulation of water fluxes (McCulloh et al., 2019), and how this integration determines drought responses (Choat et al., 2018) and post-drought recovery patterns (Yin and Bauerle, 2017). Analyses of the temporal dynamics of plant water use in response to specific drought events, as recently assessed for gross primary productivity (e.g. Schwalm et al., 2017), can also help to quantify drought legacy effects, including the reversibility of drought-induced losses of hydraulic conductivity at the plant level.

SAPFLUXNET will allow new insights into within-day patterns and controls in whole-plant water use, which can disclose the fine details of its physiological regulation. Circadian rhythms can modulate stomatal responses to the environment, potentially affecting sap flow dynamics (e.g. de Dios et al., 2015). Hysteresis in diel sap flow relationships with evaporative demand and time-lags between evaporative demand and sap flow, are two linked phenomena likely arising from plant capacitance and other mechanisms (O’Brien et al., 2004; Schulze et al., 1985), that also influence diel evapotranspiration dynamics (Matheny et al., 2014; Zhang et al., 2014). A major driver of time-lags is the use of stored water to meet the transpiration demand (Phillips et al., 2009), which can now be analysed across species, plant sizes or drought conditions using time series analyses, simplified electric analogies (Phillips et al., 1997, 2004; Ward et al., 2013) or detailed water transport models (Bohrer et al., 2005; Mirfenderesgi et al., 2016). Night-time water use can be substantial for some species (Forster, 2014; Resco de Dios et al., 2019). However, available syntheses rely on study-specific quantification of what constitutes nocturnal sap flow and do not address possible methodological influences (Zeppel et al., 2014). SAPFLUXNET will allow applying a consistent estimation of nocturnal sap flow and control for datasets that are less suitable for the quantification of night-time fluxes, as information on zero-flow deter-

mination is included in the metadata ('pl_sens_cor_zero', Appendix Table A5).

Sap flow data have been widely employed to assess changes in tree water use after biotic (e.g. Hultine et al., 2010) or abiotic (Oren et al., 1999a) disturbances. Likewise, sap flow data have been used to report changes in species and stand water use following experimental treatments involving resource availability modifications (e.g. Ewers et al., 1999) or density changes (i.e. thinning, Simonin et al., 2007). The SAPFLUXNET database includes datasets with experimental manipulations, applied either at the stand or at the individual level (Table 3). The main treatments present are related to thinning, water availability changes (irrigation, throughfall exclusion) and wildfire impact (Table 3), potentially facilitating new data syntheses and meta-analyses using these datasets (e.g. Grossiord et al., 2017).

Table 2.3: Number of datasets, plants and species by stand-level treatment in the SAPFLUXNET database.

Treatment	N sites	N plants	N species
None/control	155	2198	170
Thinning	18	332	18
Irrigation	9	36	4
Post-fire	6	18	4
CO ₂ fertilisation	3	28	2
Drought	3	9	2
Soil fertilisation	2	16	2
Post-mortality	1	22	5
Soil fertilisation and pruning	1	12	1
Soil fertilisation and thinning	1	12	1
Pruning and thinning	1	11	1
Soil fertilisation, pruning and thinning	1	11	1
Pruning	1	9	1

The combination of SAPFLUXNET with other ecophysiological databases can inform on the relative sensitivity of different physiological processes in response to drought, for example those related to growth and carbon assimilation (Steppe et al., 2015). Within-day fluctuations of stem diameter can be jointly analysed with co-located sap flow measurements to study the dynamics of stored water use under drought and its

contribution to transpiration (e.g. Brinkmann et al., 2016), and to infer parameters on tree hydraulic functioning using mechanistic models of tree hydrodynamics (Salomón et al., 2017; Steppe et al., 2006; Zweifel et al., 2007). These analyses could be carried out for a large number of species by combining SAPFLUXNET with data from the Dendroglobal database (<http://78.90.202.92/streess/databases/dendroglobal>); there are at least 18 SAPFLUXNET datasets with dendrometer data in Dendroglobal. This database and the International Tree-Ring Data Bank (Zhao et al., 2018) could also be used with SAPFLUXNET to investigate, at the species level, the link between radial growth and water use, including their environmental sensitivity (Morán-López et al., 2014), and how these two processes comparatively respond to drought (Sánchez-Costa et al., 2015). Moreover, given the tight link between water use and carbon assimilation, combining SAPFLUXNET with water-use efficiency from plant $\delta^{13}\text{C}$ data could potentially be used to estimate whole-plant carbon assimilation (Hu et al., 2010; Klein et al., 2016; Rascher et al., 2010; Vernay et al., 2020), a quantity that is difficult to measure directly, especially in field-grown, mature trees.

The two first PCA axes explained 60% of the variability of the 12 climatic variables (Appendix B Figure B.2). The niche of *P. halepensis* characterized with inter-annual variability (inter-annual variability-based niche) was 42% larger than the niche estimated with the average dataset (average-based niche). These differences implied that during the extreme climatic year, 93.3% of unaffected forests and 63.3% of highly affected forests were inside the *P. halepensis* niche estimated with inter-annual variability. These values diminished to 52.8% for unaffected forests and 21.2% for highly affected ones when niche was calculated with average climate (Figure 3.2).

2.4.2 Applications in ecosystem ecology and ecohydrology

SAPFLUXNET will provide a global look at plant water flows to bridge the scales between plant traits and ecosystem fluxes and properties (Reichstein et al., 2014). Vegetation structure, species composition and differential water use strategies among and within species scale-up to different seasonal patterns

of ecosystem transpiration, with a strong influence on ecosystem evapotranspiration and its partitioning. Global controls on evaporative fluxes from vegetation have been mostly addressed using ecosystem (Williams et al., 2012) or catchment evapotranspiration data (Peel et al., 2010). These studies have described global patterns in evapotranspiration driven by different plant functional types or climates, but they cannot be used to quantify and to explain the enormous variation in the regulation of transpiration across and within taxa.

The SAPFLUXNET database will provide a long-demanded data source to be used in ecohydrological research (Asbjornsen et al., 2011). Upscaling individual measurements to the stand level (Čermák et al., 2004; Granier et al., 1996; Köstner et al., 1998) is necessary to quantitatively compare sap-flow based transpiration with evapotranspiration and transpiration estimates at the ecosystem scale and beyond. Even though SAPFLUXNET was designed to accommodate sap flow data at the plant level, scaling to the ecosystem level is possible for many datasets. For a basic upscaling exercise using SAPFLUXNET data (Poyatos et al., 2020b), whole-plant sap flow can be normalised by individual basal area (as DBH is usually available in the metadata, cf. section 3.3), averaged for a given species and then scaled to stand level transpiration using total stand basal area and the fraction of basal area occupied by each measured species (see stand metadata, Table A3). For many datasets, sap flow data are available for the species comprising most of the stand basal area (often even 100%, Fig. 9), but species-based upscaling may be unfeasible in many tropical sites (Fig. 9b), where size-based scaling could be applied instead (e.g. da Costa et al., 2018). Further refinements of the upscaling procedure could be achieved by using trunk diameter distributions of the sap flow plots (Berry et al., 2018). This information, however, is not readily available in SAPFLUXNET, and other data sources (e.g. forest inventories, LIDAR data) or additional simplifying assumptions (i.e. applying the size distribution of measured individuals in the dataset) would be needed.

2.4. Potential applications

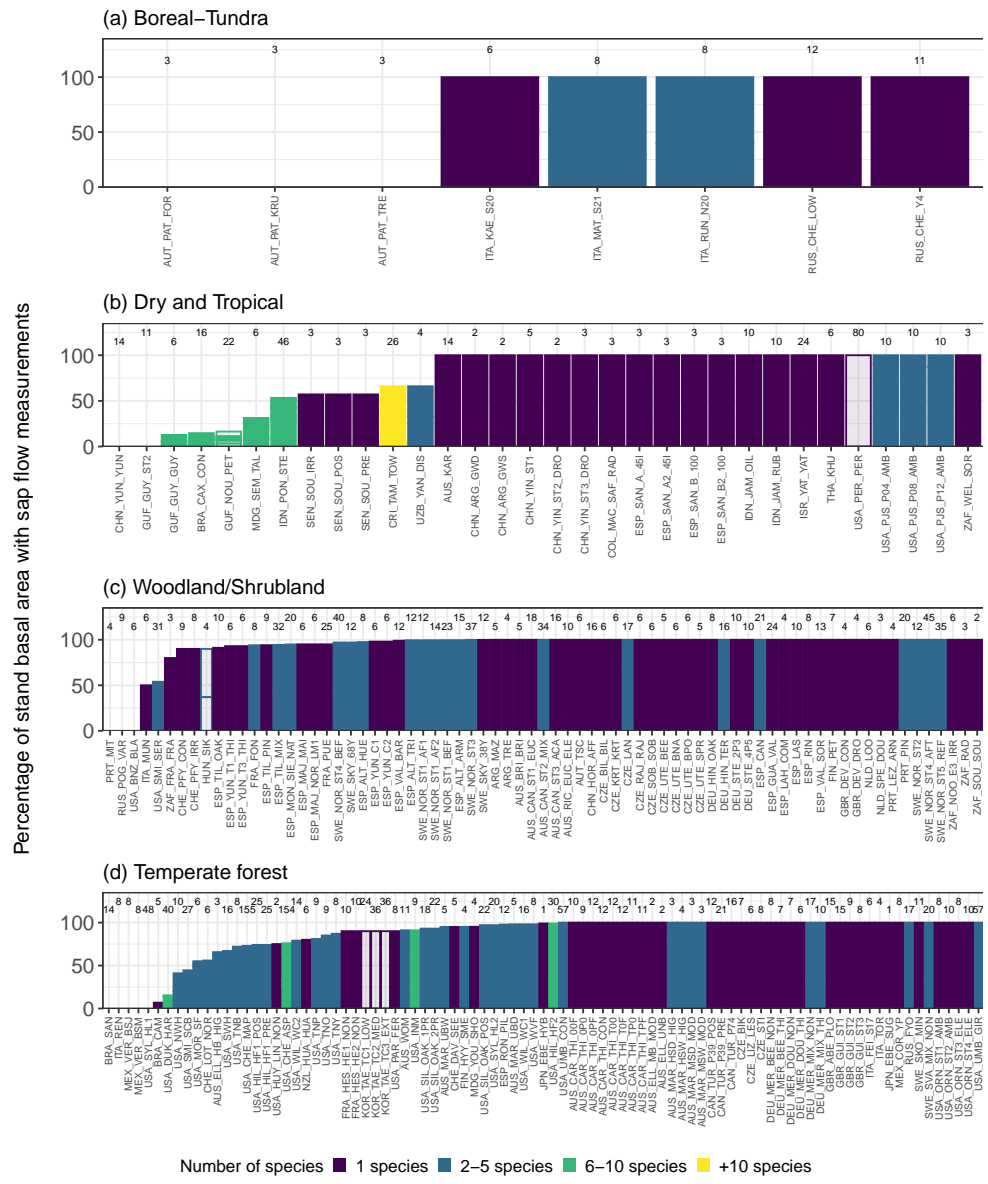


Figure 2.9: Potential for upscaling species-specific plant sap flow to stand-level sap flow using SAPFLUXNET datasets. Datasets are shown using an aggregated biome classification; ‘Dry and Tropical’ include: ‘Subtropical desert’, ‘Temperate grassland desert’, ‘Tropical forest savanna’ and ‘Tropical rain forest’. Each panel shows the percentage of total stand basal area that is covered by sap flow measurements for each species in the dataset. Datasets are also coloured by the number of species present. Numbers on top of each bar depict the total number of plants for a given dataset. Empty bars show datasets for which sap flow data expressed at the plant level were not available.

Stand-level transpiration estimates from a large number of SAPFLUXNET sites can contribute to improve our understanding of the role of forest transpiration in the context of stand water balance and its components at the ecosystem (e.g. Tor-ngern et al., 2018) and catchment levels (Oishi et al., 2010; Wilson et al., 2001). Importantly, SAPFLUXNET can contribute to better understand the global controls on vegetation water use (Good et al., 2017), including the biological and climatic controls on evapotranspiration partitioning into transpiration and evaporation components (Schlesinger and Jasechko, 2014; Stoy et al., 2019). There is some overlap between the FLUXNET network and SAPFLUXNET (47 datasets from FLUXNET sites). Hence, transpiration from SAPFLUXNET can also be used as a ‘ground-truth’ reference for transpiration estimates from remote sensing approaches (Talsma et al., 2018) and from eddy covariance data (Nelson et al., accepted). Extrapolating sap flow-derived stand transpiration to large spatial scales can be challenging due to landscape-scale variation in forest structure (Ford et al., 2007) or topography (Hassler et al., 2018), and to the low spatial representativeness of sap flow measurements (Mackay et al., 2010). A promising research avenue to help elucidate the role of vegetation in driving hydrological changes across environmental gradients (Vose et al., 2016) would be to combine species-specific stand transpiration data from SAPFLUXNET with stand structural and compositional data from forest inventories (e.g. sapwood area index, Benyon et al., 2015).

Understanding the patterns and mechanisms underlying species interactions with respect to water use within a community is necessary to predict tree species vulnerability to drought (Grossiord, 2019). Multispecies datasets from SAPFLUXNET (Table S4) can be used to assess competition for water resources among species, for example by identifying changes in seasonal water use across co-existing species and hence characterizing the spatiotemporal segregation of their hydrological niches (Silvertown et al., 2015). By providing a detailed seasonal quantification of tree water use, SAPFLUXNET could also complement isotope-based studies and contribute to interpret the large diversity in root water uptake patterns observed worldwide (Barbeta and Peñuelas, 2017; Evaristo and McDonnell, 2017) and to explain the differ-

ent seasonal origin of root-absorbed water across species and environmental gradients (Allen et al., 2019).

Plant water fluxes and hydrodynamics are amongst the most uncertain components of ecosystem and terrestrial biosphere models (Fatichi et al., 2016; Fisher et al., 2018). These models are now incorporating hydraulic traits and processes in their transpiration regulation algorithms (Mencuccini et al., 2019), but multi-site assessments of these algorithms are usually performed against evapotranspiration from eddy flux data (Knauer et al., 2015; Matheny et al., 2014). Model validation against sap flow data has been carried out typically in only one (Kennedy et al., 2019; Williams et al., 2001) or few (Buckley et al., 2012) sites. SAPFLUXNET can thus contribute to assess the performance of models simulating transpiration of stands or species within stands (e.g. De Cáceres et al., submitted.), for a large number of species and under diverse climatic conditions.

2.5 Limitations and future developments

2.5.1 Limitations

Sap flow data processing differs within and among methods, because different algorithms, calibrations or parameters involved in sap flow calculations may be applied. All of these methods contribute to methodological uncertainty (Looker et al., 2016; Peters et al., 2018) and this challenging methodological variability precludes the implementation of a complete, standardised data workflow from raw to processed data within SAPFLUXNET, as it is done for eddy flux data (Vitale et al., 2020; Wutzler et al., 2018). Commercial software for sap flow data processing from multiple methods is available (i.e. <http://www.sapflowtool.com/SapFlowToolSensors.html>) but it has not yet been widely adopted. Freely available data-processing software is only available for the HD method (Oishi et al., 2016; Speckman et al., 2020; Ward et al., 2017).

Sap flow measured with thermometric methods provides a precise estimate of the temporal dynamics of water flow through plants (Flo et al., 2019). However, their performance in measuring absolute flows is mixed. While some

well-represented methods in SAPFLUXNET such as the CHP yield accurate estimates (at least for moderate-to-high flows), the HD method, the most represented method by far, can significantly underestimate water flows (Flo et al., 2019). Because plant-level metadata contain information that document the conversion from raw to processed data (Appendix Table A5), a first-order correction for uncalibrated HD measurements based on available methodological assessments can be applied to allow intercomparability across methods. Nevertheless, given the high unexplained variability (i.e. by species and wood traits) in the performance of sap flow calibrations (Flo et al., 2019), these corrections should be applied with caution. The determination of zero flow conditions (baselining) can also have significant impacts on the quantification of absolute flow for several methods (Peters et al., 2018; Smith and Allen, 1996; Steppe et al., 2010). The different baselining approaches are also documented in the metadata to inform data syntheses and/or to selectively apply correction factors.

SAPFLUXNET has been designed to store whole-plant sap flow data, and therefore, sap flow measured at multiple points within an individual is not available in the database. Even though this spatial variation could be useful to describe detailed aspects of plant water transport (Nadezhina et al., 2009), focusing on plant-level data greatly simplifies the data structure. Hence, SAPFLUXNET only includes data already upscaled to the plant level by the data contributors. The main details of how this upscaling process was done for each dataset are provided together with other plant metadata (Table A5), but these metadata show that within-plant variation in sap flow is often not considered (Table 2). The impact of not accounting for radial and circumferential variability when scaling single-point measurements of sap flow to the whole-plant level can be important (Merlin et al., 2020), but the estimation of sapwood area can also cause large errors (Looker et al., 2016). SAPFLUXNET does not provide information on the method employed to quantify sapwood area (e.g. visual estimation with or without the application of dyes, indirect estimation through allometries at species or site levels) or on the accuracy of sapwood area data. This precludes uncertainty estimation at the individual level. Future developments in the SAPFLUXNET data

structure could include this information as metadata to better document the sensor-to-plant scaling process.

While SAPFLUXNET makes global sap flow data available for the first time, we note that spatial coverage is still sparse and some forested regions are underrepresented in the database (Fig. 2a). We note especially the relatively small number of datasets for boreal and tropical forests, two important biomes in terms of global water and carbon fluxes (Beer et al., 2010; Schlesinger and Jasechko, 2014). While many geographic gaps are caused by the absence of sap flow studies from such areas, some regions where sap flow studies have been conducted are still not represented in SAPFLUXNET. For example, the recent proliferation of Asian sap flow studies (Peters et al., 2018) has not translated into a high representativity of Asian datasets in SAPFLUXNET yet. Similarly, while the coverage of taxonomic and biometric diversity is unprecedented, SAPFLUXNET lacks data for the extremely tall trees (Ambrose et al., 2010) or for other growth forms such as shrubs (Liu et al., 2011), lianas (Chen et al., 2015) and other non-woody species (Lu et al., 2002).

2.5.2 Outlook

The public release of SAPFLUXNET has set the stage for a first generation of sap flow-based data syntheses. The work on these syntheses will fuel new ideas and tools for future improvements of the database, as for example new computing approaches for the processing and analysis of sap flow datasets. One example would be the development of robust imputation algorithms to gap-fill time series of sap flow and environmental data, which can take advantage of tools and datasets already developed by the ecosystem flux community (Moffat et al., 2007; Vuichard and Papale, 2015). The dissemination of SAPFLUXNET will encourage the use of machine-learning algorithms, only occasionally used to analyse sap flow datasets so far (e.g. Whitley et al., 2013). These approaches can also be used to identify the relative importance of different hydrometeorological drivers of transpiration (Zhao et al., 2019), or to produce global transpiration maps, by combining SAPFLUXNET with other data (Jung et al., 2019). This upscaling of stand transpiration to large

areas will also allow addressing broader questions at the regional and continental scale, such as the role of transpiration in moisture recycling (Staal et al., 2018).

The eventual success of this initiative, in terms of enabling data reuse, contributing towards the understanding and modelling of tree water use at local to global scales will likely encourage the sap flow community to contribute new datasets to future updates of the database. We expect that the development of open-source software for the processing of sap flow raw data (Speckman et al., 2020), its eventual widespread use by the sap flow community and the adoption of standardized calibration practices will increase the quality and intercomparability of future sap flow datasets. These new datasets will hopefully expand the temporal, geographical and ecological representativity of SAPFLUXNET when new data contribution periods can be opened in the future.

2.6 Data availability, access and feedback

In this paper we present SAPFLUXNET version 0.1.5 (Poyatos et al., 2020a), which contains some small metadata improvements on version 0.1.4, the first one to be made publicly available, in March 2020. Both versions supersede version 0.1.3 which was initially released to data contributors in March 2019. The entire database can be downloaded from its hosting webpage in the Zenodo repository (<https://doi.org/10.5281/zenodo.3971689>, Poyatos et al. 2020a). In this repository, we provide the database as separate .csv files and as .RData objects; see section 2.4. for details on data structure. Together with the initial publication of SAPFLUXNET in March 2019, we also released the sapfluxnet R package, available on CRAN, to enable easy access, selection, temporal aggregation and visualisation of SAPFLUXNET data. Feedback on data quality issues can be forwarded to the SAPFLUXNET initiative email address: `sapfluxnet@creaf.uab.cat`. All the information about SAPFLUXNET, including the publication of new calls for data contribution, can be found in the project website: [http://sapfluxnet.creaf.cat/./par](http://sapfluxnet.creaf.cat/./)

2.7 Conclusion

The SAPFLUXNET database provides the first global perspective of water use by individual plants at multiple timescales, with important applications in multiple fields, ranging from plant ecophysiology to Earth-system science. This database has been built from community-contributed datasets and is complemented with a software package to facilitate data access. Both the database and the software have been implemented following open science practices, ensuring public access and reproducibility. Data sharing has been a key component of the success of the FLUXNET network of ecosystem fluxes (Bond-Lamberty, 2018), and many databases in plant and ecosystem ecology now offer open data (Bond-Lamberty and Thomson, 2010; Falster et al., 2015; Gallagher et al., 2020; Kattge et al., 2020). SAPFLUXNET fully aligns with this philosophy. We expect that this initial data infrastructure will promote data sharing among the sap flow community in the future (Dai et al., 2018) and will allow the continued growth of the SAPFLUXNET database.

“thesis” — 2020/11/3 — 9:01 — page 70 — #90

3

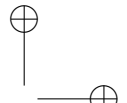
Climate and functional traits jointly mediate tree water use strategies

Victor Flo, Jordi Martínez-Vilalta, Maurizio Mencuccini^{1,3}, Victor Granda,
William R. L. Anderegg, Rafael Poyatos

72 3. Climate and functional traits jointly mediate tree water use strategies

Abstract

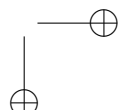
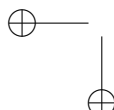
Tree water use is central to plant function and ecosystem fluxes. However, it is still unknown how organ-level water relations traits are coordinated to determine whole-tree water use strategies in response to drought, and if this coordination depends on climate. Here we used a global sap flow data base (SAPFLUXNET) to study the response of water use, in terms of whole-tree canopy conductance (G), to vapour pressure deficit (VPD) and to soil water content (SWC) for 142 tree species. We investigated the individual and coordinated effect of six water relations traits (vulnerability to embolism, Huber value, hydraulic conductivity, turgor-loss point, rooting depth and leaf size) on water use parameters, also accounting for the effect of tree height and climate (mean annual precipitation, MAP). Reference G and its sensitivity to VPD were tightly coordinated with water relations traits rather than with MAP. Species with efficient xylem transport had higher canopy conductance but also higher sensitivity to VPD. Moreover, we found that angiosperms had higher reference G and higher sensitivity to VPD than gymnosperms. Our results highlight the importance of trait coordination and the complications of defining a single, whole-plant resource use spectrum ranging from ‘acquisitive’ to ‘conservative’.



3.1 Introduction

Plant water use is a key component of the global water cycle (Katul et al., 2012). Plants regulate water use across a broad range of timescales to maintain a favourable water status under varying water availability (Feng et al., 2017). This regulation is the result of evolutionary processes together with environmental and biophysical constraints that have determined a huge diversity of species-specific water use strategies mediated by a particular suite of traits (Bacelar et al., 2012; Lu et al., 2020). These specific strategies determine plant survival under drought (Mitchell et al., 2013), species coexistence (Ehleringer et al., 1991; Jackson et al., 1995) and ecosystem CO₂ and water fluxes (Mencuccini et al., 2019a). Thus, a comprehensive understanding of how regulation of whole-plant water use relates to organ-level water relations traits would allow for a better characterization of plant responses to drought and improved prediction of climate change impacts on vegetation (Anderegg, 2015).

Among many other traits, the sensitivity of stomata to drought stress is a major regulator of plant water use over relatively short timescales (Martin-StPaul et al., 2017). In the absence of effective stomatal control under drought, water uptake by roots might not compensate water loss, resulting in high tensions in plants’ vascular system, which can trigger the entrance of air bubbles leading to xylem embolism (Tyree & Zimmermann, 2002). If embolism spreads to most of the xylem conduits, water transport becomes restricted and plants may eventually die from hydraulic failure (Tyree & Sperry, 1988; Choat et al., 2018). Through stomatal closure, plants reduce whole-plant canopy conductance (G) and therefore water loss and embolism risk, and maintain water status within tolerable limits, at the expense, however, of reducing gas exchange. Plants close stomata in response to drops in leaf and/or soil water potentials (see Martínez-Vilalta & Garcia-Forner, 2017) produced by increased atmospheric water demand (i.e., vapor pressure deficit; VPD) and reduced soil water availability (i.e., soil water content; SWC) (Jarvis, 1976; Grossiord et al., 2017). Stomatal responses have been largely described using semi-empirical models (Jarvis, 1976; Oren et al., 1999; Damour et al.,



74 3. Climate and functional traits jointly mediate tree water use strategies

2010) and optimality approaches relying on the coupling of photosynthesis and transpiration (Wang et al., 2020), with a recent focus on plant hydraulics (Sperry et al., 2016). Global syntheses of these two approaches exist (Lin et al., 2015; Hoshika et al., 2018) but they are only at the leaf level, and they do not consider the coordination of stomatal and hydraulic traits.

Coordination among stomatal sensitivity and other hydraulic and allocation traits is thought to underlie differences in water use strategies among species (Meinzer, 2002; Sperry et al., 2016; McCulloh et al., 2019). Because in woody plants water has to be transported from the soil through the xylem to supply leaf transpiration, the hydraulic properties of the xylem are key determinants of plant water relations and water use strategies. Particularly, maximum sapwood hydraulic conductivity (K_s ; Table 1) and vulnerability to xylem embolism (usually quantified as Ψ_{P50} ; i.e. the water potential at which half of K_s is lost) are key determinants of maximum transpiration rates (Manzoni et al., 2013). In addition, a vulnerable xylem (i.e. high $|\Psi_{P50}|$) has been related to higher canopy-level stomatal sensitivity to VPD across (Litvak et al., 2012) and within some species (Aspinwall et al., 2011). K_s and Ψ_{P50} have been hypothesized to define a safety-efficiency trade-off at the tissue level, by which species with high K_s (i.e., high water transport efficiency) are also more vulnerable to embolism (low $|\Psi_{P50}|$ and low safety) and vice versa (Venturas et al., 2017). However, this trade-off appears to be weak at the global scale across species, at least as captured with current measurement techniques (Gleason et al., 2016; Sanchez-Martinez et al., 2020). At the leaf level, another key component is the water potential at turgor-loss point (Ψ_{TLP}), which is tightly associated with drought tolerance and habitat water availability (Bartlett et al., 2012). Ψ_{TLP} is also closely related to water potential at complete stomatal closure (Brodribb & Holbrook, 2003; Martin-StPaul et al., 2017), and thus can be used as a proxy for quantifying the sensitivity of plant water use to changes in water availability.

Allocation ratios between the organs involved in water loss, transport and uptake are also important determinants of water use strategies. The ratio of cross-sectional sapwood area to leaf area or Huber value (Hv) is a major trait defining water use strategies because it expresses the water conducting

area per unit transpiring area. Increased Hv can contribute to reduce water potential gradients within the plant and therefore potentially compensate for a species vulnerable xylem (Mencuccini et al., 2019b). In addition, a high Hv has also been associated to strict stomatal control in conifers (Martínez-Vilalta et al., 2004; Poyatos et al., 2007) and to higher reference canopy conductance (Novick et al., 2009). Similarly, increasing rooting depth (R_{depth}) gives access to deeper water sources, which potentially allows maintaining less negative and stable water potentials as well as supporting high water use even under climates with high evaporative demand (Martínez-Vilalta & Garcia-Forner, 2017). At the leaf level, the importance of individual leaf size (L_s) for light penetration and crown architecture has been thoroughly studied (Sellers, 1985), but its influence on water use strategies has been little explored, despite the role of leaf evaporative cooling for thermoregulation (Wright et al., 2017). Large leaves with thick leaf boundary layers and an ineffective stomatal control of water loss (Jarvis & McNaughton, 1986), may need to sustain higher transpiration rates to maintain leaf temperature within operative limits under intense radiative heating and/or heat waves (e.g. Drake et al., 2018). This may lead to a trade-off between leaf thermoregulation and the conservation of water and/or hydraulic function (Fauset et al., 2018), especially in hotter sites (Aparecido et al., 2020).

Water use strategies are also mediated by plant height, community composition, and environmental conditions, particularly climate, topography and soil properties; as well as spatial and temporal variability in environmental conditions (Feng et al., 2018). Plant height increases hydraulic path length and hydraulic resistance, and thus plays a major role in the global coordination of several water use traits such as Ψ_{P50} or K_s (Liu et al., 2019), Hv (Mencuccini et al., 2019b) and reference canopy conductance (Novick et al., 2009). Likewise, increasing tree height has been related to enhanced sensitivity of canopy conductance to VPD for some species (Schäfer et al., 2000). Because soil water is a common resource belowground that is influenced by water uptake from many individuals and species, the community composition and diversity of water use strategies in an ecological community can also affect ecosystem fluxes and drought progression (Anderegg et al.,

76 3. Climate and functional traits jointly mediate tree water use strategies

2018, 2019). In addition, phylogeny may constrain flexibility in water use strategies independently of the environment, as it has been shown for example by the consistent differences in hydraulic traits between angiosperms and gymnosperms (Johnson et al., 2012; Bartlett et al., 2016) and by the strong phylogenetic conservatism reported for some hydraulic traits such as Ψ_{P50} and K_s at the global scale (Sanchez-Martinez et al., 2020).

In this study we explore water use strategies across tree species using a trait-based approach, which provides a simplified framework to understand species responses to drought at the global scale (Feng et al., 2018). Our ultimate aim is to better understand how water use strategies emerge from the covariation between traits and the influence of climate. To that end, we use a global database of sap flow measurements (SAPFLUXNET) to calculate whole-tree canopy conductance (G) for 142 tree species growing on 126 sites. We then parameterize the response of G to VPD and SWC at the species level and for major taxonomic groups (i.e. angiosperms and gymnosperms). Finally, we characterize the relationships between water use traits and key hydraulic and allocation traits among species (i.e. Ψ_{P50} , K_s , Hv , Ψ_{TLP} , R_{depth} , L_s and tree height), controlling also for the climatic effects produced by differences in precipitation. We hypothesize that (i) water use and water relations traits are coordinated to determine water use strategies at the species level, and (ii) species occupying drier habitats will tend to be more ‘conservative’ in their water use and also tend to have drought tolerance traits. (iii) After controlling for climatic effects, a safety-efficiency trade-off is visible at the scale of whole-plant water use, as opposed to the scale of individual xylem conduits.

3.2 Material and methods

We took a two-step approach to test the previous hypotheses. First, we modelled species-level whole-tree canopy conductance responses to evaporative demand and soil water availability to obtain species’ water use parameters, taking advantage of a recently-compiled global sap flow dataset. Next, we modelled the variability of those water use parameters as a function of

3.2. Material and methods

77

species' water relations traits, mean annual precipitation (MAP), tree height and broad functional types (i.e., angiosperms and gymnosperms).

Table 3.1: Description of variables and units in this study.

Variable	Description	Units
VPD	Vapour pressure deficit	kPa
SWC	Soil water content	$\text{m}_\text{water}^3 \text{m}_\text{soil}^{-3}$
REW	Relative extractable water	
Asw	Sapwood area	m^2
SF	Sap flow	$\text{cm}^3 \text{h}^{-1}$
SFD	Sap flux density	$\text{cm}^3 \text{cm}_\text{Asw}^{-2} \text{h}^{-1}$
G	Whole-tree canopy conductance	mol s^{-1}
G_Asw	Whole-tree canopy conductance per unit of sapwood area	$\text{mol m}_\text{Asw}^{-2} \text{s}^{-1}$
G'_Asw	Whole-tree stomatal conductance (i.e., G_Asw without aerodynamic conductance)	$\text{mol m}_\text{Asw}^{-2} \text{s}^{-1}$
MAP	Mean annual precipitation	mm
MAT	Mean annual temperature	$^\circ\text{C}$
PPET	Mean annual precipitation over potential evapotranspiration	mm mm^{-1}
H	Tree height	m
Ψ_{P50}	water potential at which half of K_s is lost	MPa
K_s	Maximum sapwood hydraulic conductivity	$\text{kg m}^{-1} \text{MPa}^{-1} \text{s}^{-1}$
Hv	Huber value: ratio of cross-sectional sapwood area to leaf area	$\text{cm}_\text{Asw}^2 \text{m}_\text{leaf}^{-2}$
Ψ_TLP	Water potential at leaf turgor-lost point	MPa
R_depth	Rooting depth	m
L_s	Individual leaf size	cm^2
T	Temperature	$^\circ\text{C}$
h	Plot altitude	m
G_REF	Reference G_Asw at VPD = 1 kPa and SWC = 0.5 $\text{m}^3 \text{m}^{-3}$	$\text{mol m}_\text{Asw}^{-2} \text{s}^{-1}$
β_VPD	G_Asw sensitivity to ln(VPD)	$\text{mol m}_\text{Asw}^{-2} \text{s}^{-1}$
β_SWC	G_Asw sensitivity to ln(SWC)	$\text{mol m}_\text{Asw}^{-2} \text{s}^{-1}$

3.2.1 Sap flow data

Data from 1929 trees belonging to 142 species on 126 plots without experimental treatments (Table S1) and meeting data quality criteria (see Data filtering

78 3. Climate and functional traits jointly mediate tree water use strategies

section below) were obtained from the global SAPFLUXNET database (Poyatos et al., 2020) (Fig. 1 and Table S2). For each species-site combination, we extracted sub-daily sap flux density (SFD; Table 1) or whole-tree sap flow (SF; 24 out of 126 data-sets) when tree sapwood areas (ASW) were not available. For these datasets, SF data were then transformed into SFD units by dividing SF values by tree ASW estimated with an allometric relationship. This relationship was obtained using all the SAPFLUXNET trees for which ASW data were available and taking diameter at breast height (DBH) and functional type (i.e., angiosperm or gymnosperm) as predictors ($R^2 = 0.78$; $n = 2262$). Sub-daily SFD time-series were aggregated to daytime SFD averages (i.e., 6am to 6pm solar time) using the `sfn_metrics` function of the `sapfluxnetR` package (Granda et al., 2020). Time-series obtained from non-calibrated thermal dissipation sensors were corrected for potential bias in absolute SFD by applying a multiplier of 1.405, according to the global synthesis of sap flow calibrations by Flo et al. (2019).

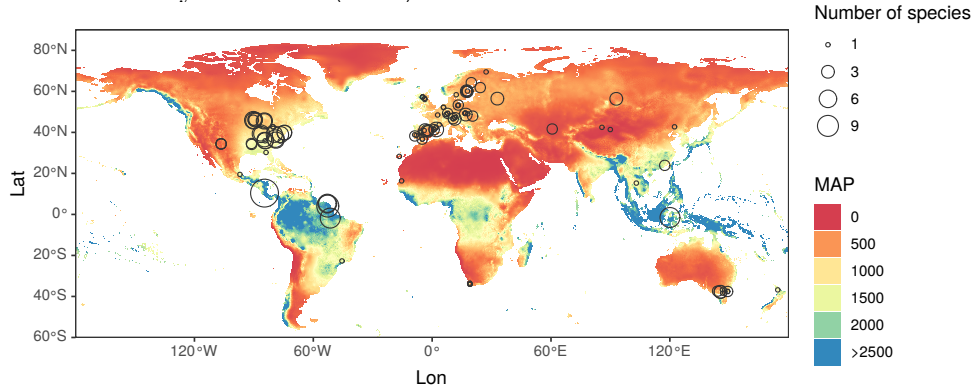


Figure 3.1: Distribution of the plots from the SAPFLUXNET database included in this study. Size of the dots represent the number of different species in the plot. Color gradient show mean annual precipitation (MAP).

3.2.2 Evaporative demand and soil water availability data

We used vapour pressure deficit (VPD) and soil water content (SWC) as proxies of evaporative demand and soil water availability, respectively. Similar to SFD, VPD was obtained from on-site sub-daily measurements from

SAPFLUXNET averaged to daytime values. Soil water content (SWC; v/v) was obtained from the 15–30 cm depth layer at 12 am from the ERA5-land re-analysis product (Copernicus Climate Change Service (C3S), 2019) at 9x9 km resolution. We used ERA5-land re-analyses instead of on-site SWC measures in order to maximize the number of plots and species included in the study, since SWC data were missing in 44% of the SAPFLUXNET data-sets included in this study. In addition, ERA5-land had longer time series (1980 to 2019). We validated the use of ERA5-land data using a linear mixed-model (LMM) regression between ERA5-land and on-site shallow SWC measurements by letting random intercepts and slopes of the response vary by site (n observations = 32815; n plots = 71; R^2 conditional = 0.97, R^2 marginal = 0.26).

To complement SWC, we also calculated relative extractable water (REW), as a normalized measure of soil water availability, as follows:

$$REW_{j,i} = \frac{SWC_{j,i} - SWC_{min}}{SWC_{max} - SWC_{min}} \quad (3.1)$$

where $REW_{j,i}$ and $SWC_{j,i}$ are plot (j) daily (i) values, and SWCmax and SWCmin, the overall maximum and minimum SWC measured at a plot, respectively. REW takes values between 0 and 1, being 0 the absolute plot lowest SWC and 1 being the highest.

3.2.3 Data filtering

We restricted the analysis to periods without potential phenological changes in leaf area to minimize variations in conductance unrelated to VPD and SWC changes. In the absence of detailed plot-specific observations, we excluded all data for periods comprised between 15 days prior to the first day with temperatures below 0°C and 30 days following the last day under 0°C, respectively, during the cold seasons of each plot site (similarly to Novick et al., 2016). To prevent potential artefacts due to unstable weather conditions in the calculation of whole-tree canopy conductance (Ewers & Oren, 2000) or in the estimation of model parameters, we filtered out days when SWC increased (rainy days), as well as days when daytime-averaged VPD was below

80 3. Climate and functional traits jointly mediate tree water use strategies

0.3 kPa (Anderegg et al., 2018). To ensure sufficiently contrasting conditions of evaporative demand and soil water availability, we also discarded species with both VPD ranges below 0.5 kPa and SWC ranges below 0.05 ($n = 8$ species).

After data filtering, the study covers a large geographic area being Europe and the east of North America especially well represented (Fig 1) and a wide range of climate conditions, with MAP values ranging from 14 mm to 3626 mm (mean \pm SD = 953 mm \pm 545 mm). Out of the 142 species used in the analyses, 116 were angiosperms and 26 gymnosperms. The number of trees per species ranges from 215 trees (*Pinus sylvestris*) to 1 (this being the case for 23 species) (Table S2). Tree species-level heights (H) range from 2 m (*Coprosma quadrifida*) to 40 m (*Carya glabra*) (mean \pm SD = 21 m \pm 9.75 m).

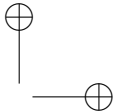
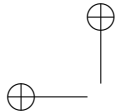
3.2.4 Whole-tree canopy conductance calculation

Daytime SFD was transformed from $[cm^3 cm_{Asw}^{-2} h^{-1}]$ to $[kg m_{Asw}^{-2} s^{-1}]$ and converted to daily whole-tree canopy conductance normalized per unit of sapwood area G_{Asw} using Phillips and Oren (1998) and unit transformations (eq.2).

$$G_{Asw,j,i,k} = \frac{115.8 + 0.4236 T_{j,i} \cdot SFD_{j,i,k}}{VPD_{j,i}} \cdot 44.6 \cdot \frac{273}{(273 + T_{j,i})} \cdot \frac{101.325 e^{0.00012 \cdot h_i}}{101.325} \quad (3.2)$$

Where $SFD_{j,i,k}$ is sap flux density value of each plot (j), day (i), and tree (k); $T_{j,i}$ is the temperature, $VPD_{j,i}$ is the daytime vapor pressure deficit and h is the altitude of each plot site. When h was not available it was obtained from The Shuttle Radar Topography Mission (SRTM) (Earth Resources Observation And Science (EROS) Center, 2017) ($n = 2$ plots).

The conductance obtained using eq. 2 is considered a good proxy of the tree-level stomatal conductance under the assumption that the canopy and the atmosphere are well-coupled, i.e., when the aerodynamic conductance is much larger than the stomatal conductance. Although this is generally assumed in sap flow studies for both needleleaf and even broadleaf species,

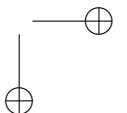


there is evidence that coupling may only be partial in some cases (Magnani et al., 1998; De Kauwe et al., 2017). Therefore, we also calculated whole-tree stomatal conductance (G'_{Asw}) by removing the contribution of aerodynamic conductance in a subset of plots-species (n plots = 64; n species = 47) where wind speed data were available in SAPFLUXNET (see supplementary material for details, Chu et al., 2018; Tan et al., 2019). We also related the environmental sensitivity of G'_{Asw} to the hydraulic and allocation traits (see Statistical analyses section below) to assess the potential impact of partial canopy-atmosphere coupling on our results.

3.2.5 Traits and climatic data

Species-level traits ($|\Psi_{P50}|$, Hv , K_s , $|\Psi_{TLP}|$, R_{depth} and L_s) were taken from HydraTry (Mencuccini et al., 2019b; Sanchez-Martinez et al., 2020) and the Global Leaf Size Dataset (Wright et al., 2017) (Table S2). $|\Psi_{P50}|$, Hv , K_s and L_s were log-transformed to achieve normality. In addition, we obtained tree species-level height (H) as the average of SAPFLUXNET actual tree heights, with the number of tree-days with available sap flow values as weighting factor. The height of the stand was used when the actual height of a tree was not available (792 out of 1929 trees).

To account for climatic effects on the species’ water use parameters and on water relation traits, we used mean annual precipitation (MAP), mean annual temperature (MAT) and an aridity index defined as precipitation over potential evapotranspiration (PPET) (Fig. 1, Fig. S6, Fig. S7). However, for simplicity, we only included MAP in the analyses since for the species in the study MAP was strongly correlated with PPET ($r = 0.94$) and MAT ($r = 0.76$), whereas PPET and MAT correlation was lower ($r = 0.56$). MAP and MAT were obtained for all study plots from the CHELSA data set (1x1 km resolution) (Karger et al., 2017) and averaged at the species level weighting by the number of tree-days. PPET were obtained from CGIAR-CSI Global Aridity index (Trabucco & Zomer, 2019).



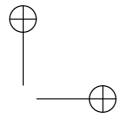
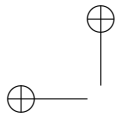
82 3. Climate and functional traits jointly mediate tree water use strategies

3.2.6 G_{Asw} sensitivity to soil water availability and water demand

In some species, G_{Asw} measurements were distributed very heterogeneously throughout the range of VPD or SWC. To avoid the issues associated with such unbalanced distributions we used binned data. Specifically, we calculated the average of G_{Asw} measurements comprised into 0.2 kPa VPD intervals and five bins spanning the plot-species specific SWC range. For each summarized G_{Asw} we defined a characteristic VPD and SWC as the average values of VPD and SWC of the data in the bin. The summarized values of G_{Asw} were fitted using LMM as a function of the logarithm of VPD ($\ln(\text{VPD})$) and the logarithm of SWC ($\ln(\text{SWC})$) as additive explanatory variables using uncorrelated random slopes for each species and a random intercept for each tree nested in each species. We log-transformed the independent variables to linearise the relationships and ensure normal residuals. LMMs were fitted using the lmer function from the lme4 R package (Bates et al., 2015). Using the coef function from lme4 we obtained species parameters β_{VPD} and β_{SWC} (i.e. species G_{Asw} sensitivity to VPD and to SWC, respectively), with higher values of β_{VPD} or β_{SWC} meaning stronger G reductions with increasing VPD or decreasing SWC, respectively. In addition, a reference G_{Asw} (G_{REF}) characterizing water use under standard conditions for each species, was predicted setting VPD = 1 kPa and SWC = 0.5 m³ m⁻³ (which is close to the average maximum of all sites). Complementary models were also fitted following the same procedure but with REW instead of SWC, so that soil water content variability was normalized across sites. Additional models were also fitted using canopy stomatal conductance (G'_{Asw}) as response variable. Finally, to remove parameter outliers, species with G_{REF} , β_{VPD} or β_{SWC} outside the 99.9 percentile of their normal distribution were excluded from subsequent analyses (2 out of 142 species excluded).

3.2.7 Statistical analyses

We tested whether water use regulation traits (G_{REF} , β_{VPD} and β_{SWC}) differ between angiosperms and gymnosperms using a simple linear model. Next, we

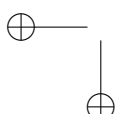


3.2. Material and methods

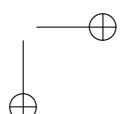
83

constructed bi-variate linear relationships between species' fitted parameters and species' water relations traits. Furthermore, we repeated these linear relationships by adding MAP and H as predictors and applying a stepwise model selection, to discern whether the effect of the traits remained significant once these new variables were added to the model. In all the analyses we used the number of species' tree-days as a weighting factor.

Finally, we performed a path analysis using the SEM function of the lavaan R package (Rosseel, 2012). Path analysis accounts for direct and indirect dependencies among variables. To account for the coordinated effect of the species' relations traits and to maximize the number of species (106 species), we imputed species' trait missing values (Table S2) using the imputePCA function of the package missMDA (Josse & Husson, 2016) and then performed a Principal Component Analysis (PCA) to extract the two main principal components (Fig. S1). A single path model was built including the three parameters describing G_{Asw} behaviour (G_{REF} , β_{VPD} and β_{SWC}) as response variables and using MAP, H and the two dimensions of the traits' PCA as explanatory variables. In addition to direct relationships, indirect effects of MAP and H on the fitted parameters were also included through their effect on the PCA dimensions (Liu et al., 2019). We also accounted for the effect of MAP on H. We included the number of tree-days per species as a weighting factor in the model. We performed a model selection procedure to include only paths with at least moderately strong support ($P < 0.1$). Finally, we also checked that the fit of the final model was not significantly different from the saturated model using the lavTestLRT function of the lavaan R package (Rosseel, 2012) with Satorra and Bentler (2001) approximation. All variables were standardized before fitting the path models. All the analyses of the study were performed in R3.6.1 (R Core Team, 2018).



|



84 3. Climate and functional traits jointly mediate tree water use strategies

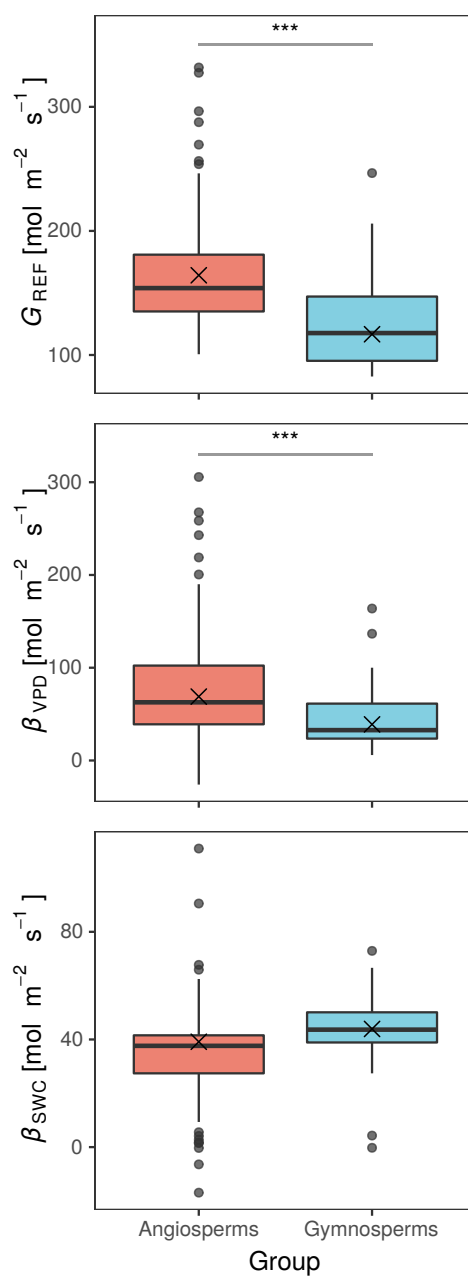


Figure 3.2: Boxplots of water use parameters for both Angiosperms and Gymnosperms. Crosses are weighted means of the parameters.

3.3 Results

3.3.1 Water use parameters and differences between angiosperms and gymnosperms

The model used to obtain water use parameters explained a 59.8% of the total conditional variance in the original data. Reference conductance (G_{REF}) across species ranged between $82.4 \text{ mol m}_{Asw}^{-2} s^{-1}$ (*Juniperus monosperma*) and $333 \text{ mol m}_{Asw}^{-2} s^{-1}$ (*Acacia longifolia*), β_{VPD} between $-26 \text{ mol m}_{Asw}^{-2} s^{-1}$ (*Avicennia marina*) and $306 \text{ mol m}_{Asw}^{-2} s^{-1}$ (*Ulmus americana*) and β_{SWC} between $-17.3 \text{ mol m}_{Asw}^{-2} s^{-1}$ (*Acer saccharum*) and $112 \text{ mol m}_{Asw}^{-2} s^{-1}$ (*Acacia longifolia*) (Fig. S2 – S3 – S4). Most species showed declining G with increasing VPD (positive β_{VPD}) and increasing G with increasing SWC (positive β_{SWC}).

Species showing opposite responses were two temperate (*Acer saccharum*, *Quercus petraea*), one tropical (*Ampelocera macrocarpa*) and a mangrove (*Avicennia marina*) species that showed negative sensitivities to one of the variables (Fig. S2). Mean G_{REF} and β_{VPD} were significantly higher for angiosperms than for gymnosperms (Fig. 2). However, there were no differences in β_{SWC} between angiosperms and gymnosperms. Across all species (including angiosperms and gymnosperms), G_{REF} and β_{VPD} were strongly and positively correlated ($r = 0.75$; with a weighted slope of 0.67; Fig. S5), being the species with high G_{REF} more sensitive to VPD, but strong correlations were not found between G_{REF} and β_{SWC} or between β_{VPD} and β_{SWC} ($|r| < 0.34$ in both cases). When comparing water use parameters calculated considering and not considering aerodynamic conductance, we found that G_{REF} was strongly correlated to G'_{REF} ($r = 0.8$); however, β_{VPD} and β'_{VPD} were poorly correlated ($r = 0.26$) while β_{SWC} and β'_{SWC} showed no significant correlation.

86 3. Climate and functional traits jointly mediate tree water use strategies

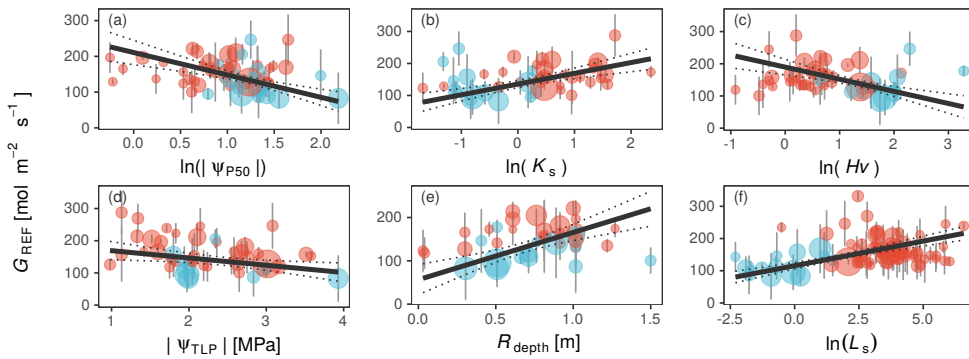


Figure 3.3: Bi-variate relationships between G_{REF} water relations traits. Individual water relation traits are shown in different panels: (a) logarithm of absolute water potential at 50% water conductivity loss, (b) logarithm of maximum sapwood water conductivity, (c) logarithm of Huber value, (d) absolute water potential at turgor-loss point, (e) rooting depth and (f) logarithm of individual leaf area. Black continuous lines depict significant linear relationships (Table 2) and the dashed lines represent the 95% confidence intervals of the models. Red dots are angiosperms and blue dots are gymnosperms. Size of the points is equivalent to the number of tree-days of the species. Vertical lines are the posterior standard deviation of the parameters calculated using REsim function of merTools package (Knowles & Frederick, 2016).

3.3.2 Coordination with hydraulic and allocation traits

In the bi-variate models relating G_{REF} with hydraulic and morphological traits, we found that G_{REF} showed a negative relationship with $|\Psi_{P50}|$, Hv and $|\Psi_{TLP}|$ (Table 2 and Fig. 3a,c,d), whereby species more resistant to embolism, with higher allocation to the sapwood relative to leaves and with more negative turgor-loss pressures showed lower G_{REF} . Furthermore, G_{REF} was positively related to K_s , R_{depth} and L_s (Table 2 and Fig. 3b,e,f), with species with efficient xylem, deeper roots and bigger leaves showing higher G_{REF} . For these traits, L_s was the one explaining the largest fraction of G_{REF} variability ($R^2 = 0.39$). With the exception of Ψ_{TLP} , these relationships remained significant also for G'_{Asw} (Table S3).

β_{VPD} was negatively related with $|\Psi_{P50}|$ and Hv and positively with K_s (Table 2 and Fig. 4a,b,c), i.e., species with less safe and more efficient xylem present higher sensitivity to VPD, and hence more strict stomatal control

3.3. Results

87

Table 3.2: Results of the bi-variate linear models relating water use parameters (G_{REF} , β_{VPD} , β_{SWC}) and water relations traits. Parameters are explained by individual traits using simple linear models using number of species-days as weighting factor.

Water use parameter	Water relations Traits	N species	Intercept	Slope	R^2
G_{REF}	$\ln(\Psi_{P50})$	55	210.701***	-62.724 ***	0.282
	$\ln(K_s)$	43	135.527***	33.614 ***	0.338
	$\ln(Hv)$	49	189.439***	-37.602 ***	0.285
	$ \Psi_{TLP} $	48	191.764***	-22.702 *	0.112
	R_{depth}	37	56.204**	109.296 ***	0.366
	$\ln(L_s)$	86	115.537***	15.28 ***	0.391
β_{VPD}	$\ln(\Psi_{P50})$	55	109.201***	-47.716 ***	0.240
	$\ln(K_s)$	43	50.199***	20.427 **	0.180
	$\ln(Hv)$	49	96.503***	-33.817 ***	0.363
	$ \Psi_{TLP} $	48	80.321***	-12.209 .	0.040
	R_{depth}	37	-2.190 ns	80.383 ***	0.260
	$\ln(L_s)$	86	34.577***	11.219 ***	0.327
β_{SWC}	$\ln(\Psi_{P50})$	55	16.103 ns	19.327 *	0.059
	$\ln(K_s)$	43	42.113***	-5.021 ns	0.000
	$\ln(Hv)$	49	23.952**	13.586 *	0.088
	$ \Psi_{TLP} $	48	40.468**	1.052 ns	0.000
	R_{depth}	37	53.851***	-28.471 .	0.051
	$\ln(L_s)$	86	51.112***	-4.095 **	0.087

Statistical significant levels: “.” p<0.1 ; “*” p<0.05; “**” p<0.01; “***” p<0.001; ns not significant.

88 3. Climate and functional traits jointly mediate tree water use strategies

as atmospheric water demand increases. β_{VPD} was also positively related to R_{depth} and L_s (Table 2 and Fig. 4e,f), indicating that deeper roots and larger leaves were associated to higher stomatal sensitivity to VPD. Absolute turgor-loss point ($|\Psi_{TLP}|$) was weakly negatively related with β_{VPD} (p value = 0.093; Table 2). Hv and L_s were the traits explaining most of β_{VPD} variability ($R^2 = 0.36$ and $R^2 = 0.33$, respectively). With the exception of Ψ_{TLP} , these relationships remained significant also for G'_{Asw} (Table S3).

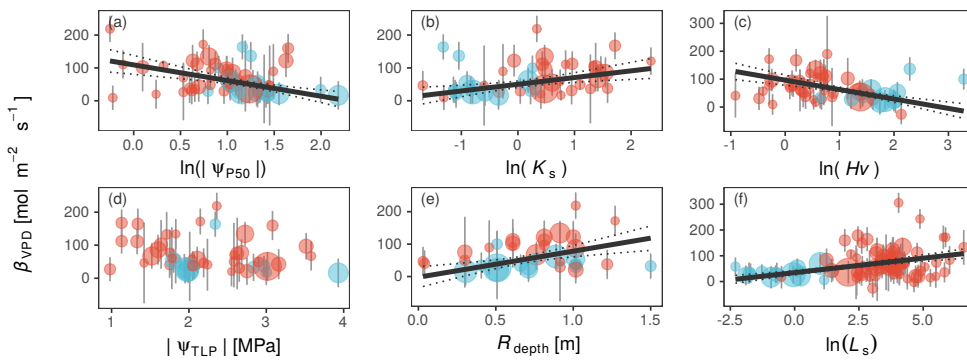


Figure 3.4: Bi-variate relationships between β_{VPD} water relations traits. Individual water relation traits are shown in different panels: (a) logarithm of absolute water potential at 50% water conductivity loss, (b) logarithm of maximum sapwood water conductivity, (c) logarithm of Huber value, (d) absolute water potential at turgor-loss point, (e) rooting depth and (f) logarithm of individual leaf area. Black continuous lines depict significant linear relationships (Table 2) and the dashed lines represent the 95% confidence intervals of the models. Red dots are angiosperms and blue dots are gymnosperms. Size of the points is equivalent to the number of tree-days of the species. Vertical lines are the posterior standard deviation of the parameters calculated using REsim function of merTools package (Knowles & Frederick, 2016).

β_{SWC} was positively related to $|\Psi_{P50}|$ and Hv (Table 2 and Fig. 5a,c), i.e., species with higher resistance to embolism and larger ratios of sapwood to leaf area were more sensitive to soil water depletion. In addition, species with larger leaves (L_s) and, marginally (p value = 0.095), with deeper roots (R_{depth}) were less sensitive to soil water stress (Table 2 and Fig. 5e,f). In general, water relations traits explained a lower proportion (at most 9%) of the variability in β_{SWC} than of G_{REF} or β_{VPD} . However, we should treat

3.3. Results

89

relationships between β_{SWC} and $|\Psi_{P50}|$, Hv and R_{depth} with caution, since they all become non-significant when aerodynamic conductance was taken into account (Table S3) or when REW was used instead of SWC (Table S3). Furthermore, when REW was used instead of SWC, all soil moisture sensitivity-trait relationships became non-significant (Table S4).

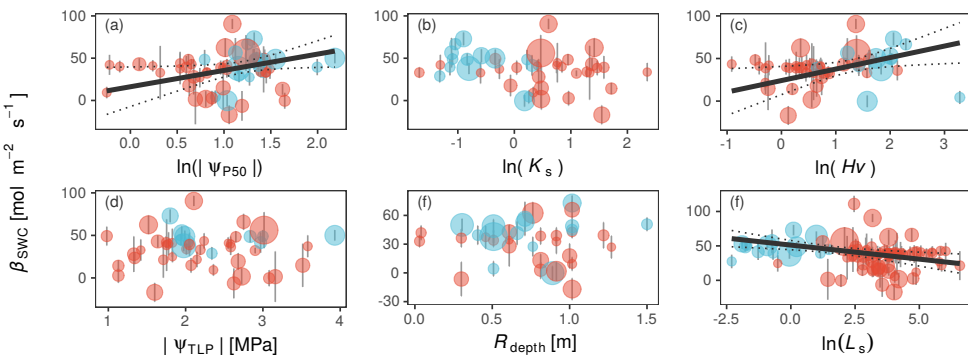


Figure 3.5: Bi-variate relationships between β_{SWC} water relations traits. Individual water relation traits are shown in different panels: (a) logarithm of absolute water potential at 50% water conductivity loss, (b) logarithm of maximum sapwood water conductivity, (c) logarithm of Huber value, (d) absolute water potential at turgor-loss point, (e) rooting depth and (f) logarithm of individual leaf area. Black continuous lines depict significant linear relationships (Table 2) and the dashed lines represent the 95% confidence intervals of the models. Red dots are angiosperms and blue dots are gymnosperms. Size of the points is equivalent to the number of tree-days of the species. Vertical lines are the posterior standard deviation of the parameters calculated using REsim function of merTools package (Knowles & Frederick, 2016).

Ecological factors associated with water use parameters and coordination When the coordination between water use parameters and water relations traits was assessed while also accounting for the effects of MAP (mean annual precipitation) and H (tree species-level mean height), most of the relationships described in the previous section remained significant, with only three exceptions. The relationships that were no longer observed corresponded to the effect of Ψ_{TLP} on G_{REF} and the effects of $|\Psi_{P50}|$ and Hv on β_{SWC} (Table 3). In these models, MAP was the variable that explained most of the variability in stomatal responses to soil water (β_{SWC}), with generally lower

90 3. Climate and functional traits jointly mediate tree water use strategies

Table 3.3: Results of the bi-variate linear models relating water use parameters (G_{REF} , β_{VPD} , β_{SWC}), water relations traits, climate and tree height. Water use parameters are explained using simple linear models with number of species-days as weighting factor. β column values are the slopes for each explanatory variable. N species = number of species included. NI = not included variable after model selection.

Water use parameter	Water relations Traits	N species	Intercept	β_{trait}	β_{MAP}	β_{H}	R^2
G_{REF}	$\ln(\Psi_{P50})$	54	173.6 ***	-48.549 **	NI	1.418 *	0.325
	$\ln(K_s)$	42	109.773 ***	30.731 ***	NI	1.822 *	0.423
	$\ln(Hv)$	43	162.178 ***	-32.21 **	NI	1.448 .	0.332
	$ \Psi_{\text{TLP}} $	47	66.861 ***	NI	0.057 *	1.962 *	0.346
	R_{depth}	36	41.932 *	88.301 ***	NI	1.802 *	0.448
	$\ln(L_s)$	80	98.531 ***	13.389 ***	NI	1.384 **	0.450
β_{VPD}	$\ln(\Psi_{P50})$	54	70.665 ***	-32.97 **	NI	1.468 *	0.317
	$\ln(K_s)$	42	25.16 *	17.444 **	NI	1.768 **	0.303
	$\ln(Hv)$	43	73.255 ***	-28.931 ***	NI	1.197 *	0.408
	$ \Psi_{\text{TLP}} $	47	16.363 .	NI	NI	2.502 ***	0.291
	R_{depth}	36	-18.282 ns	56.571 *	NI	2.034 **	0.412
	$\ln(L_s)$	80	16.099 *	8.955 ***	NI	1.512 ***	0.429
β_{SWC}	$\ln(\Psi_{P50})$	54	62.606 ***	NI	-0.029 *	NI	0.088
	$\ln(K_s)$	42	73.319 ***	NI	-0.038 **	NI	0.142
	$\ln(Hv)$	43	50.25 **	10.221 ns	-0.026 .	NI	0.149
	$ \Psi_{\text{TLP}} $	47	55.33 ***	NI	NI	-0.903 *	0.067
	R_{depth}	36	62.889 ***	NI	-0.037 **	NI	0.213
	$\ln(L_s)$	80	44.671 ***	-5.002 **	0.025 *	-0.749 *	0.142

Statistical significant levels: “.” p<0.1 ; ** p<0.05; *** p<0.01; **** p<0.001; ns not significant.

sensitivity to SWC in locations with high MAP (Table 3), although this effect reversed in the L_s model. However, when models were calculated using β'_{SWC} , MAP effects were all negative (Table S5). On the other hand, MAP was largely unrelated to G_{REF} and β_{VPD} in most of the G_{REF} and β_{VPD} models (Table 3). Finally, our results show that taller trees tend to have higher G_{REF} and higher sensitivity to VPD (β_{VPD}), however, when G_{REF} was obtained from G'_{Asw} (i.e. G'_{REF}), H was not selected in the final models (Table S5). The relationship between H and soil drought sensitivity (β_{SWC}) was less clear, since it was significantly negative in only two of the models (Table 3), suggesting higher sensitivity to soil drought in shorter trees. However when aerodynamic coupling was taken into account, the relationship was inverted and taller trees had higher sensitivity to SWC (Table S5).

The two main dimensions of the PCA analyses describing water relations trait coordination explained a 69.8% of the total variance (Fig. S1). The primary PCA dimension (Dim1; 56.8% of variance) could be interpreted as a safety-efficiency trade-off axis, whereby positive values are related to elevated K_s , large L_s , deep roots, low Hv and low $|\Psi_{P50}|$. The second PCA dimension (Dim2; 13% of variance) was associated to leaf turgor-loss pressure (Ψ_{TLP}), with positive values related to high $|\Psi_{TLP}|$ levels and, to a lower extent, deeper roots.

In the path analyses, efficiency traits (positive PCA Dim1 values) were significantly related to high annual precipitation (high MAP) and to taller trees (large H) (Fig. 6). Also, H increased with MAP. G_{REF} was positively associated with Dim1 (Fig. 6) and taller trees also had marginally higher G_{REF} (Fig. 6). Similarly, higher β_{VPD} (i.e., higher VPD sensitivity) was positively related to efficient water transport (Dim1) and to H (Fig. 6). Sensitivity to SWC (β_{SWC}) showed a marginal, negative relationship with Dim1, so that sensitivity increased with xylem resistance to embolism (Fig. 6). Finally, G_{REF} co-varied positively with β_{VPD} and β_{SWC} , implying that as G_{REF} increases so do β_{VPD} and β_{SWC} (Fig. 6, Fig. S5). The second dimension of the PCA was not included in the final path model, suggesting a lack of coordination between Ψ_{TLP} and water use parameters.

92 3. Climate and functional traits jointly mediate tree water use strategies

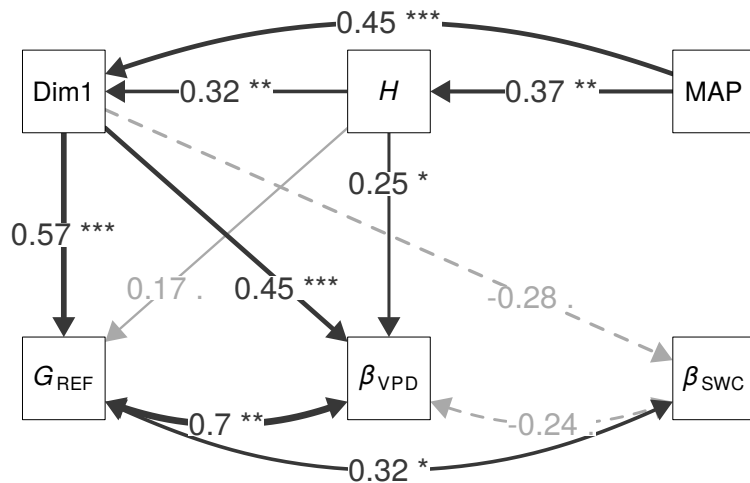
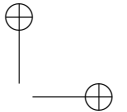


Figure 3.6: Path analyses of species-specific water use parameters explained by mean annual precipitation (MAP), tree height (H) and coordinated hydraulic traits Dim1. Dim1 is the hydraulic traits’ PCA dimension 1 (Fig. S1). Positive Dim1 values are mainly related to efficient water use strategies, while negative to safety strategies. Dim2 was not selected in the final model. Arrow labels are standardized parameters. Continuous lines are positive relationships while dashed lines are negative relationships. Black and grey lines are significant and marginally significant relationships, respectively. Statistical significant levels: .., $P < 0.1$; *, $P < 0.05$; **, $P < 0.01$; ***, $P < 0.001$

3.4 Discussion

In this study, we present a novel analysis linking organ-level traits with whole-plant water use strategies at the global scale, made possible by the compilation of the first global sap flow database. We provide evidence of a coordination between water relations traits and water use parameters (G_{REF} , β_{VPD} and β_{SWC}), while accounting for the effects of climate and tree size. Some water use and trait associations were explained by climate affiliations of species, but most relationships between water use and water relations traits remained after accounting for climate and tree size effects. As any synthesis effort of this magnitude based on diverse data sources, our study presents several limitations. First, sap flow data used to estimate G carry some uncertainty issues, although these may be less relevant for assessing environmental responses as



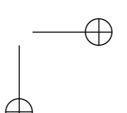
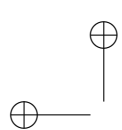
we do here than for characterizing absolute values (Flo et al., 2019). Second, SAPFLUXNET may have an incomplete coverage of global forest ecosystems (Fig. 1, Poyatos et al., 2020). Third, highly non-linear or threshold-based SWC responses may be difficult to capture, especially when having to resort to reanalysis data. Fourth, other ecological processes such as partial canopy-atmosphere coupling or intra-specific variability in traits and/or water use regulation may influence our results.

3.4.1 Climate influence on water use strategies across species

Our results showed no direct effect of mean annual precipitation (MAP) on G_{REF} and β_{VPD} , but instead indirect MAP effects on water use strategies mediated through hydraulic and allocation traits (Fig 6 and Fig. S6), suggesting that MAP constrains feasible water relations traits (Bourne et al., 2017; Liu et al., 2019), which then directly determine water use rate and β_{VPD} . The direction of these effects is consistent with previous studies showing that β_{VPD} increased with aridity in rainforest species (Cunningham, 2004; but see Grossiord et al., 2019) and at continental scales across ecosystems and functional types (Novick et al., 2016), but these studies did not disentangle direct from indirect effects. Although the global controls on β_{SWC} were less clear in our analyses, in part due to the influence of aerodynamic coupling (cf. Table 3 and S5), climate effects on this variable also appeared to be largely indirect (Fig. 6). Therefore, our results underscore the importance of using water relations traits, rather than climate when addressing species whole-tree water use strategies and ecosystem flux sensitivities to VPD.

3.4.2 Water use parameters

Water use parameters differed widely among species (Fig. S2) and defined a gradient of water use sensitivities to drought stress. Within the gradient of parameters, angiosperms and gymnosperms showed distinct whole-plant water use strategies (Fig. 2). We found that gymnosperms have generally more ‘conservative’ water use strategies in terms of lower G_{REF} but not in terms of enhanced sensitivity to VPD or SWC. Similarly, previous studies also



94 3. Climate and functional traits jointly mediate tree water use strategies

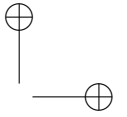
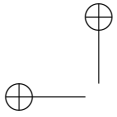
showed lower sensitivity to VPD in gymnosperms compared to angiosperms (Johnson et al., 2012; Lin et al., 2015), which could be associated to higher safety margins (Choat et al., 2012; Anderegg et al., 2016). The ‘conservative’ G_{REF} strategy of gymnosperms could be explained by group-specific trait syndromes associated to water relations traits (Fig. S8), wood anatomy (Venturas et al., 2017), and lower photosynthetic rates, stomatal conductance or leaf N concentrations (Lusk et al., 2003).

G_{REF} and β_{VPD} showed a strong positive correlation across species (Fig. S5) similar to the one found by Oren et al. (1999). This implies stronger VPD control on transpiration in species with higher water use under optimal conditions (higher G_{REF}). However, our global cross-species analyses might mask finer variations, as β_{VPD} (or $\beta_{\text{VPD}} / G_{\text{REF}}$) is expected to be lower across species from dry sites (Oren et al., 1999) or along a decreasing gradient of SWC within species (Domec & Johnson, 2012; Zhang et al., 2012; but see Poyatos et al., 2007). Nevertheless, this result suggests that G_{REF} can be a suitable proxy of whole-tree canopy conductance sensitivity to VPD, as it is at the leaf (Oren et al., 1999) or ecosystem (Grossiord et al., 2020) levels.

The lack of correlation found between the sensitivity to SWC calculated with and without aerodynamic conductance, indicates that canopy coupling could be important in calculating β_{SWC} and that in order to predict and model plant water responses to soil water dynamics, we likely have to explicitly consider aerodynamic and boundary layer conductances. In addition, these land-atmosphere interactions might be crucial in diagnosing and modelling the soil moisture controls over other ecosystem processes such as the carbon cycle (Green et al., 2019; Kannenberg et al., 2020).

3.4.3 Coordination between water use parameters and water relations traits

Our results support the hypothesis of a strong coordination between G_{REF} and individual hydraulic and allocation traits. G_{REF} aligns with ‘efficiency’ traits (K_s) in the hydraulic safety-efficiency axis, and is thus negatively related to



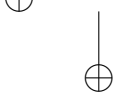
3.4. Discussion

95

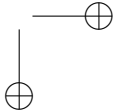
‘safety’ traits (particularly Ψ_{P50}). These results are consistent with the overall proposed coordination between plant hydraulics and gas exchange (Meinzer, 2002; Sperry et al., 2002; Mencuccini, 2003; Maherali et al., 2006; Henry et al., 2019) and with the notion that species operate close to their maximum transport capacity sustained by their hydraulic system (Manzoni et al., 2013). Large individual leaf areas were also related to higher G_{REF} , probably due to higher leaf hydraulic conductance mediated by wider conduits (Schreiber et al., 2016; Ding et al., 2020). The positive association of elevated G_{REF} with deeper roots points out the requirement of deep rooting to supply water for keeping high transpiration rates, and is also found in the coordination between R_{depth} , Ψ_{P50} and K_s (Mursinna et al., 2018).

Coordination between whole-tree water use sensitivity to VPD (β_{VPD}) and to SWC (β_{SWC}) with organ-level water relations traits had not been assessed before at a global scale. All the studied water relations traits (except Ψ_{TLP}) appear to be related to β_{VPD} , whereby the species with more ‘efficient’ or less “safe” traits tend to be those which show higher β_{VPD} . These results are consistent with previous studies relating stomatal responses and water relation traits (Lu et al., 2020) and with the stomatal gas exchange optimization theory (see Tyree & Sperry, 1988; Wang et al., 2020). By contrast, after controlling for climate and tree height, conductance sensitivity to SWC (β_{SWC}) was only (negatively) related to L_s . Notably, β_{SWC} was unrelated to Ψ_{TLP} , in contrast to Maréchaux et al. (2018), that evidenced more negative Ψ_{TLP} related to lower reductions in sap flow with decreasing SWC. This absence of relationship, including the weak $\beta_{VPD} - \Psi_{TLP}$ correlation, could be attributed to noise and uncertainty in Ψ_{TLP} measures (Meinzer et al., 2014) or with Ψ_{TLP} plasticity (Bartlett et al., 2012; Rosas et al., 2019). In addition, the lack of relationship between β_{SWC} and R_{depth} could be explained by the complexity of rooting depth dependency on soil water infiltration, tree height and climate (Fan et al., 2017).

We also explored the coordinated effect of water relations traits on water use parameters and accounted for direct and indirect climate and tree height effects through the PCA and the path model. Based on our results, water use strategies would be, in terms of G_{REF} , consistent with the Reich



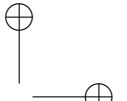
|



96 3. Climate and functional traits jointly mediate tree water use strategies

(2014) notion of a whole-plant resource use spectrum, ranging from ‘conservative’ to ‘acquisitive’ species. However, in terms of absolute sensitivity to VPD, our results go against this idea, since acquisitive species (with high G_{REF}) are also more sensitive to VPD (more ‘conservative’). Therefore, our study would support a more physiological interpretation of water use strategies that stresses trait coordination. According to this interpretation, plants with ‘safer’ hydraulic systems (high resistance to embolism) are able to function at higher water tensions without requiring a strict water use regulation, implying that they can show a more ‘acquisitive’ regulation of water use so that they can benefit from having a wider range of conditions to operate safely. In other words, high transport capacity in the xylem (K_s) is associated with high canopy conductance (G_{REF}) and a vulnerable (sensitive) xylem is also associated with a stricter regulation of gas exchange. However, a vulnerable xylem reduces safety, and is usually interpreted as part of an ‘acquisitive’ strategy, whereas a strict regulation of water use prevents hydraulic failure and hence corresponds to a ‘conservative’ strategy. This view is also consistent with the positive relationship between Ψ_{P50} and Ψ_{TLP} , even if it saturates at relatively low water potentials (cf. Martin-StPaul et al., 2017). These results highlight the complications of defining a single, whole-plant resource use spectrum ranging from ‘acquisitive’ to ‘conservative’ species (sensu Reich, 2014), and points to the need of considering different organs and functional axes when assessing whole-plant functional integration.

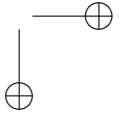
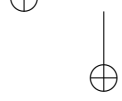
Regarding tree’s height, it was coordinated directly and indirectly –through water relations traits– with water use parameters (Table 3 and Fig. 6), in a way that taller trees displayed more ‘efficient’ water use strategies. Alignment of water relations traits and H was consistent with results found by Liu et al. (2019), relating maximum plant size with Ψ_{P50} , K_s or Hv at the global scale across species and life forms. These complex direct and indirect H relationships might be driven by ecosystem water availability (Fig. 6) and low freezing risk (Olson et al., 2018), which allows for increased water use through efficient water transport (e.g. high K_s or Hv), compensating the increase of resistance due to the enlarged water path of taller trees (Barnard & Ryan, 2003; Liu et al., 2019; Mencuccini et al., 2019b). Furthermore,



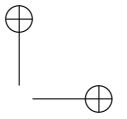
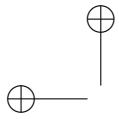
H could also affect differential sensitivity to VPD and SWC in tall trees (Giardina et al., 2018), as their canopy would be more exposed to VPD, requiring higher β_{VPD} , and would potentially have more developed root systems, which would decrease β_{SWC} .

3.4.4 Conclusions

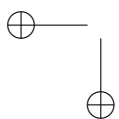
Understanding tree water use strategies at the global scale is crucial to better predict ecosystem water cycles and drought vulnerability of species and ecosystems. Here we demonstrate that there is a global spectrum of water use strategies determined by the coordination of hydraulic and allocation traits, rather than by climate. In particular, species-specific G_{REF} and β_{VPD} (but not β_{SWC}) are closely related to the species-specific water relations traits. We have also shown significant differences between angiosperm and gymnosperm water use strategies, showing greater water use and sensitivity to VPD in angiosperms than gymnosperms, a finding that could be related to distinct water relations traits syndromes (Fig. S8). Our trait-based approach allowed for a simplified global mapping of water use strategies. The use of simple measurable traits (e.g. leaf size) altogether with functional grouping can lead to a better approximation of species reference water conductance and its sensitivity to VPD. Recently developed global maps of traits (Moreno-Martínez et al., 2018; Trugman et al., 2020) would permit the inclusion of such water use strategies in Land Surface and Earth System Models potentially improving ecosystem carbon and water fluxes predictions.



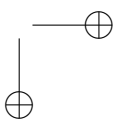
“thesis” — 2020/11/3 — | 9:01 — page 98 — #118



— —



|



References

- Abeli, T. et al. 2014. Effects of marginality on plant population performance. - *J. Biogeogr.* 41: 239–249.
- Ackerly, D. D. 2003. Community Assembly , Niche Conservatism , and Adaptive Evolution in Changing Environments. - *Int. J. Plant Sci.* 164: 164–184.
- Ackerly, D. D. et al. 2010. The geography of climate change: Implications for conservation biogeography. - *Divers. Distrib.* 16: 476–487.
- Adler, P. B. et al. 2013. Trait-based tests of coexistence mechanisms. - *Ecol. Lett.* 16: 1294–1306.
- AEMET (Spanish Meteorological Agency) 2014. Avance climatológico mensual mes de septiembre 2014 en la Región de Murcia.
- AEMET (Spanish Meteorological Agency) and IP (Portuguese Meteorological Institute) 2011. Iberian climate atlas. Air temperature and precipitation (1971-2000) (MR y M Ministerio de Medio Ambiente, Ed.).
- Aitken, S. N. et al. 2008. Adaptation, migration or extirpation: climate change outcomes for tree populations. - *Evol. Appl.* 1: 95–111.
- Alexander, J. M. et al. 2016. When Climate Reshuffles Competitors: A Call for Experimental Macroecology. - *Trends Ecol. Evol.* 31: 831–841.
- Allen, C. D. and Breshears, D. D. 1998. Drought-induced shift of a forest – woodland ecotone: Rapid landscape response to climate variation. - *Ecology* 95: 14839–14842.

1003. Climate and functional traits jointly mediate tree water use strategies

Allen, C. D. et al. 2010. A global overview of drought and heat-induced tree mortality reveals emerging climate change risks for forests. - *For. Ecol. Manage.* 259: 660–684.

Allen, C. D. et al. 2015. On underestimation of global vulnerability to tree mortality and forest die-off from hotter drought in the Anthropocene. - *Ecosphere* 6: art129.

Anderegg, W. R. L. et al. 2012. The roles of hydraulic and carbon stress in a widespread climate-induced forest die-off. - *Proc. Natl. Acad. Sci.* 109: 233–237.

Anderson, R. P. et al. 2002. Using niche-based GIS modeling to test geographic predictions of competitive exclusion and competitive release in South American pocket mice. - *Oikos* 98: 3–16.

Anne, P. 1945. Carbone organique (total) du sol et de l’humus. - *Ann. Agron.* 15: 161–172.

Araújo, M. B. and Guisan, A. 2006. Five (or so) challenges for species distribution modelling. - *J. Biogeogr.* 33: 1677–1688.

Araújo, M. B. and New, M. 2007. Ensemble forecasting of species distributions. - *Trends Ecol. Evol.* 22: 42–47.

Araújo, M. B. et al. 2013. Heat freezes niche evolution (D Sax, Ed.). - *Ecol. Lett.* 16: 1206–1219.

Araújo, M. B. et al. 2019. Standards for distribution models in biodiversity assessments. - *Sci. Adv.* 5: eaat4858.

Ashraf, M. et al. 2011. Drought Tolerance: Roles of Organic Osmolytes, Growth Regulators, and Mineral Nutrients. - *Adv. Agron.* 111: 249–296.

Austin, M. 1971. The role of regression analysis in plant ecology. - *Proc. Ecol. Soc. Aust.* 6: 63–75.

Austin, M. P. et al. 1990. Measurement of the Realized Qualitative Niche: Environmental Niches of Five Eucalyptus Species. - *Ecol. Monogr.* 60:

161–177.

Barbet-Massin, M. et al. 2012. Selecting pseudo-absences for species distribution models: How, where and how many? - *Methods Ecol. Evol.* 3: 327–338.

Barry, J. P. et al. 1995. Climate-Related, Long-Term Faunal Changes in a California Rocky Intertidal Community. *Science*. 267: 672–675.

Barve, N. et al. 2011. The crucial role of the accessible area in ecological niche modeling and species distribution modeling. - *Ecol. Modell.* 222: 1810–1819.

Belyea, L. R. and Lancaster, J. 1999. Assembly Rules within a Contingent Ecology. - *Oikos* 86: 402.

Benito Garzón, M. et al. 2011. Intra-specific variability and plasticity influence potential tree species distributions under climate change. - *Glob. Ecol. Biogeogr.* 20: 766–778.

—
Bernard-Verdier, M. et al. 2012. Community assembly along a soil depth gradient: Contrasting patterns of plant trait convergence and divergence in a Mediterranean rangeland (H Cornelissen, Ed.). - *J. Ecol.* 100: 1422–1433.

Bertrand, R. et al. 2012. Disregarding the edaphic dimension in species distribution models leads to the omission of crucial spatial information under climate change: The case of *Quercus pubescens* in France. - *Glob. Chang. Biol.* 18: 2648–2660.

Bertrand, R. et al. 2016. Ecological constraints increase the climatic debt in forests. - *Nat. Commun.* 7: 12643.

Bigler, C. et al. 2006. Drought as an inciting mortality factor in scots pine stands of the Valais, Switzerland. - *Ecosystems* 9: 330–343.

Blonder, B. et al. 2014. The n-dimensional hypervolume. - *Glob. Ecol. Biogeogr.* 23: 595–609.

1023. Climate and functional traits jointly mediate tree water use strategies

Blonder, B. et al. 2015. Linking environmental filtering and disequilibrium to biogeography with a community climate framework. - *Ecology* 96: 972–985.

Blonder, B. et al. 2017. Predictability in community dynamics. - *Ecol. Lett.* 20: 293–306.

Bowler, D. and Böhning-Gaese, K. 2017. Improving the community-temperature index as a climate change indicator. - *PLoS One* 12: 1–17.

Boyce, M. S. et al. 2002. Evaluating resource selection functions. - *Ecol. Modell.* 157: 281–300.

Bramer, I. et al. 2018. Advances in Monitoring and Modelling Climate at Ecologically Relevant Scales. - *Adv. Ecol. Res.* 58: 101–161.

Braun-Blanquet, J. and Bolòs, O. 1957. The plant communities of the Central Ebro Basin and their dynamics. - *An. la Estac. Exp. Aula Dei* 5: 1–266.

Breiner, F. T. et al. 2017. Including environmental niche information to improve IUCN Red List assessments (B Schröder, Ed.). - *Divers. Distrib.* 23: 484–495.

Broennimann, O. and Guisan, A. 2008. Predicting current and future biological invasions: both native and invaded ranges matter. - *Biol. Lett.* 4: 585–9.

Broennimann, O. et al. 2006. Do geographic distribution, niche property and life form explain plants’ vulnerability to global change? - *Glob. Chang. Biol.* 12: 1079–1093.

Broennimann, O. et al. 2012. Measuring ecological niche overlap from occurrence and spatial environmental data. - *Glob. Ecol. Biogeogr.* 21: 481–497.

Brown, J. H. 1984. On the Relationship between Abundance and Distribution of Species. - *Am. Nat.* 124: 255–279.

- Cáceres, M. De et al. 2015. Coupling a water balance model with forest inventory data to predict drought stress: the role of forest structural changes vs. climate changes. - *Agric. For. Meteorol.* 213: 77–90.
- Cadotte, M. W. and Tucker, C. M. 2017. Should Environmental Filtering be Abandoned? - *Trends Ecol. Evol.* 32: 429–437.
- Carnicer, J. et al. 2011. Widespread crown condition decline, food web disruption, and amplified tree mortality with increased climate change-type drought. - *Proc. Natl. Acad. Sci. U. S. A.* 108: 1474–8.
- Cassel, D. K. and Nielsen, D. R. 1986. Field capacity and available water capacity. - In: Klute, A. (ed), *Methods of Soil Analysis: Part 1—Physical and Mineralogical Methods*. Agronomy m. Soil Science Society of America, pp. 901–926.
- Clark, J. D. et al. 1993. A Multivariate Model of Female Black Bear Habitat Use for a Geographic Information System. - *J. Wildl. Manage.* 57: 519.
-
- Colwell, R. K. and Rangel, T. F. 2009. Hutchinson’s duality: the once and future niche. - *Proc. Natl. Acad. Sci. U. S. A.* 106 Suppl 2: 19651–8.
- Colwell, R. K. et al. 2008. Global Warming, Elevational Range Shifts, and Lowland Biotic Attrition in the Wet Tropics. *Science.* 322: 258–261.
- Cornwell, W. K. and Ackerly, D. D. 2009. Community Assembly and Shifts in Plant Trait Distributions across an Environmental Gradient in Coastal California. - *Source Ecol. Monogr.* 79.
- Coumou, D. and Rahmstorf, S. 2012. A decade of weather extremes. - *Nat. Clim. Chang.* 2: 491–496.
- Csergő, A. M. et al. 2017. Less favourable climates constrain demographic strategies in plants (J Gurevitch, Ed.). - *Ecol. Lett.* 20: 969–980.
- D’Amen, M. et al. 2017. Spatial predictions at the community level: From current approaches to future frameworks. - *Biol. Rev.* 92: 169–187.
- Dallas, T. A. and Hastings, A. 2018. Habitat suitability estimated by niche

1043. Climate and functional traits jointly mediate tree water use strategies

models is largely unrelated to species abundance. - *Glob. Ecol. Biogeogr.* 27: 1448–1456.

Dallas, T. et al. 2017. Species are not most abundant in the centre of their geographic range or climatic niche. - *Ecol. Lett.* 20: 1526–1533.

Davis, M. B. 1986. Climatic Instability, Time, Lags, and Community Disequilibrium.: 269–284.

Davis, M. B. and Shaw, R. G. 2001. Range shifts and adaptive responses to quaternary climate change. *Science.* 292: 673–679.

Davis, K. T. et al. 2019. Microclimatic buffering in forests of the future: the role of local water balance. - *Ecography (Cop.).* 42: 1–11.

De Frenne, P. et al. 2013. Microclimate moderates plant responses to macroclimate warming. - *Proc. Natl. Acad. Sci. U. S. A.* 110: 18561–5. de la Riva, E. G. et al. 2016a. Leaf Mass per Area (LMA) and Its Relationship with Leaf Structure and Anatomy in 34 Mediterranean Woody Species along a Water Availability Gradient. - *PLoS One* 11: e0148788.

de la Riva, E. G. et al. 2016. Disentangling the relative importance of species occurrence, abundance and intraspecific variability in community assembly: a trait-based approach at the whole-plant level in Mediterranean forests. - *Oikos* 125: 354–363.

de la Riva, E. G. et al. 2017. A Multidimensional Functional Trait Approach Reveals the Imprint of Environmental Stress in Mediterranean Woody Communities. - *Ecosystems* 21: 248–262.

del Cacho, M. and Lloret, F. 2012. Resilience of Mediterranean shrubland to a severe drought episode: The role of seed bank and seedling emergence. - *Plant Biol.* 14: 458–466.

Devictor, V. et al. 2012. Differences in the climatic debts of birds and butterflies at a continental scale. - *Nat. Clim. Chang.* 2: 121–124.

Diaz, S. et al. 1998. Plant functional traits and environmental filters at a

- regional scale. - *J. Veg. Sci.* 9: 113–122.
- Dormann, C. F. 2007. Promising the future? Global change projections of species distributions. - *Basic Appl. Ecol.* 8: 387–397.
- Duchaufour, P. 1970. *Pédologie* (M& Paris, Ed.).
- Duong, T. 2018. Package “ks”. *ks: Kernel Smoothing*. in press.
- Duong, T. and Hazelton, M. L. 2005. Cross-validation bandwidth matrices for multivariate kernel density estimation. - *Scand. J. Stat.* 32: 485–506.
- Easterling, D. R. et al. 2000. Climate Extremes: Observations, Modeling, and Impacts. *Science*. 289: 2068–2074.
- Elith, J. 2006. Novel methods improve prediction of species’ distributions from occurrence data: Supplement. - *Ecography* (Cop.). 29: 129–151.
- Elith, J. and Leathwick, J. R. 2009. Species Distribution Models: Ecological Explanation and Prediction Across Space and Time. - *Annu. Rev. Ecol. Evol. Syst.* 40: 677–697.
- Elith, J. and Graham, C. H. 2009. Do they? How do they? WHY do they differ? on finding reasons for differing performances of species distribution models. - *Ecography* (Cop.). 32: 66–77.
- Elith, J. et al. 2002. Mapping epistemic uncertainties and vague concepts in predictions of species distribution. - *Ecol. Modell.* 157: 313–329.
- Elith, J. et al. 2008. A working guide to boosted regression trees. - *J. Anim. Ecol.* 77: 802–813.
- Elith, J. et al. 2010. The art of modelling range-shifting species. - *Methods Ecol. Evol.* 1: 330–342.
- Elton, C. S. 1927. *Animal ecology*. - University of Chicago Press.
- Esteve-Selma, M. A. et al. 2010. Effects of climatic change on the distribution and conservation of Mediterranean forests: The case of *Tetraclinis articulata* in the Iberian Peninsula. - *Biodivers. Conserv.* 19: 3809–3825.

1063. Climate and functional traits jointly mediate tree water use strategies

Esteve-Selma, M. A. et al. 2015. Cambio climático y biodiversidad en el contexto de la Región de Murcia. - In: Consejería de Agua Agricultura y Medio Ambiente (ed), Cambio climático en la Región de Murcia. Evaluación basada en indicadores. pp. 105–132.

Fick, S. E. and Hijmans, R. J. 2017. WorldClim 2: new 1-km spatial resolution climate surfaces for global land areas. - Int. J. Climatol. 37: 4302–4315.

Fielding, A. H. and Bell, J. F. 1997. A review of methods for the assessment of prediction errors in conservation presence/absence models. - Environ. Conserv. 24: 38–49.

Franklin, J. 2010. Mapping species distributions. Spatial inference and prediction. - Cambridge University Press.

Franklin, J. et al. 2013. Modeling plant species distributions under future climates: how fine scale do climate projections need to be? - Glob. Chang. Biol. 19: 473–483.

Franklin, J. et al. 2016. Global change and terrestrial plant community dynamics. - Proc. Natl. Acad. Sci. 113: 3725–3734.

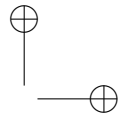
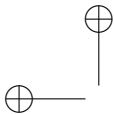
Franks, S. J. et al. 2014. Evolutionary and plastic responses to climate change in terrestrial plant populations. - Evol. Appl. 7: 123–139.

Freckleton, R. P. et al. 2002. Phylogenetic Analysis and Comparative Data: 160: 712–726.

Fridley, J. 2009. Downscaling Climate over Complex Terrain: High Finescale (<1000 m) Spatial Variation of Near-Ground Temperatures in a Montane Forested Landscape (Great Smoky Mountains)*. - J. Appl. Meteorol. Climatol. 48: 1033–1049.

Fridley, J. D. et al. 2011. Soil heterogeneity buffers community response to climate change in species-rich grassland. - Glob. Chang. Biol. 17: 2002–2011.

Galiano, L. et al. 2010. Drought-Induced Multifactor Decline of Scots Pine



- in the Pyrenees and Potential Vegetation Change by the Expansion of Co-occurring Oak Species. - *Ecosystems* 13: 978–991.
- Gause, G. F. 1934. The struggle for existence (Williams & Wilkin, Ed..
- Gaüzère, P. et al. 2018. Empirical Predictability of Community Responses to Climate Change. - *Front. Ecol. Evol.* 6: 186.
- GBIF.org (18 January 2019), GBIF Occurrence Download <https://doi.org/10.15468/dl.er7c3e>
- Gee, G. W. and Bauder, J. W. 1986. Particle size analysis. - In: Klute, A. (ed), *Methods of Soil Analysis: Part 1—Physical and Mineralogical Methods*. Soil Science Society of America, pp. 383–411.
- Geiger, R. et al. 1995. *The Climate Near the Ground*. - Vieweg+Teubner Verlag.
- Giorgi, F. and Lionello, P. 2008. Climate change projections for the Mediterranean region. - *Glob. Planet. Change* 63: 90–104.
- Gotelli, N. J. et al. 2010. Macroecological signals of species interactions in the Danish avifauna. - *Proc. Natl. Acad. Sci. U. S. A.* 107: 5030–5.
- Graae, B. J. et al. 2018. Stay or go – how topographic complexity influences alpine plant population and community responses to climate change. - *Perspect. Plant Ecol. Evol. Syst.* 30: 41–50.
- Graham, C. H. et al. 2004. Integrating phylogenetics and environmental niche models to explore speciation mechanisms in dendrobatid frogs. - *Evolution* 58: 1781–93.
- Grant, P. R. et al. 2016. Evolution caused by extreme events. - *Philos. Trans. R. Soc. Lond. B. Biol. Sci.* 372: 20160146.
- Greenwood, S. et al. 2017. Tree mortality across biomes is promoted by drought intensity, lower wood density and higher specific leaf area. - *Ecol. Lett.* 20: 539–553.



1083. Climate and functional traits jointly mediate tree water use strategies

- Grinnell, J. 1917. The Niche-Relationships of the California Thrasher. - *Auk* 34: 427–433.
- Guiot, J. and Cramer, W. 2016. Climate change: The 2015 Paris Agreement thresholds and Mediterranean basin ecosystems. *Science*. 354: 4528–4532.
- Guisan, A. and Zimmermann, N. E. 2000. Predictive habitat distribution models in ecology. - *Ecol. Modell.* 135: 147–186.
- Guisan, A. and Thuiller, W. 2005. Predicting species distribution: Offering more than simple habitat models. - *Ecol. Lett.* 8: 993–1009.
- Guisan, A. et al. 2013. Predicting species distributions for conservation decisions (H Arita, Ed.). - *Ecol. Lett.* 16: 1424–1435.
- Guisan, A. et al. 2014. Unifying niche shift studies: insights from biological invasions. - *Trends Ecol. Evol.* 29: 260–269.
- Guisan, A. et al. 2017. Habitat Suitability and Distribution Models (Cambridge University Press, Ed.). - Cambridge University Press.
- Guisan, A. et al. 2019. Scaling the linkage between environmental niches and functional traits for improved spatial predictions of biological communities (A Hampe, Ed.). - *Glob. Ecol. Biogeogr.*: geb.12967.
- Hamerlynck, E. P. and McAuliffe, J. R. 2008. Soil-dependent canopy die-back and plant mortality in two Mojave Desert shrubs. - *J. Arid Environ.* 72: 1793–1802.
- Hampe, A. and Petit, R. J. 2005. Conserving biodiversity under climate change: the rear edge matters. - *Ecol. Lett.* 8: 461–467.
- Hanley, A. J. and McNeil, J. B. 1982. The Meaning and Use of the Area under a Receiver Operating Characteristic (ROC) Curve. - *Radiology* 143: 29–36.
- Hannah, L. et al. 2007. Protected area needs in a changing climate. - *Front. Ecol. Environ.* 5: 131–138.

- Hanski, I. 1999. Metapopulation ecology. - Oxford University Press.
- Hewitt, G. 2000. The genetic legacy of the Quaternary ice ages. - *Nature* 405:
- Hijmans, R. J. et al. 2005. Very high resolution interpolated climate surfaces for global land areas. - *Int. J. Climatol.* 25: 1965–1978.
- Hijmans, R. J. et al. 2011. Package ‘dismo’ - October: 55.
- Hijmans, A. R. J. et al. 2016. Package ‘dismo’ Species Distribution Modeling. - <https://cran.r-project.org/web/packages/dismo/dismo.pdf>: (accesed 11.01.2016).
- HilleRisLambers, J. et al. 2012. Rethinking Community Assembly through the Lens of Coexistence Theory. - *Annu. Rev. Ecol. Evol. Syst.* 43: 227–248.
- Hirzel, A. H. et al. 2006. Evaluating the ability of habitat suitability models to predict species presences. - *Ecol. Modell.* 199: 142–152.
-
- Holt, R. D. 2009. Bringing the Hutchinsonian niche into the 21st century: Ecological and evolutionary perspectives. - *Proc. Natl. Acad. Sci. U. S. A.* 106: 19659–19665.
- Holt, R. D. et al. 2005. Theoretical models of species’ borders: single species approaches. - *Oikos* 108: 18–27.
- Hubbell, S. P. 2001. The unified neutral theory of biodiversity and biogeography. - Princeton University Press.
- Huberty, C. J. 1994. Applied discriminant analysis. - Wiley.
- Huntley, B. and Webb, T. 1989. Migration: Species’ Response to Climatic Variations Caused by Changes in the Earth’s Orbit. - *J. Biogeogr.* 16: 5.
- Hutchinson, G. E. 1957. Concluding Remarks - The Demographic Symposium as a Heterogeneous Unstable Population. 53: 415–427.
- Hutchinson, G. E. 1978. An introduction to population ecology. - Yale University Press.

1103. Climate and functional traits jointly mediate tree water use strategies

IPCC Working Group 1 2014. IPCC Fifth Assessment Report (AR5) - The physical science basis (VB and PMM (eds. . Stocker, T.F., D. Qin, G.-K. Plattner, M. Tignor, S.K. Allen, J. Boschung, A. Nauels, Y. Xia, Ed.).

IUSS Working Group WRB 2015. World Reference Base for Soil Resources 2014, update 2015. International soil classification system for naming soils and creating legends for soil maps. - World Soil Resour. Reports No. 106.

Jackson, S. T. 2009. Introduction. - In: (editor), S. T. J. (ed), *Essay on the Geography of Plants*. The University of Chicago Press, pp. 1–52.

Jackson, S. T. and Sax, D. F. 2010. Balancing biodiversity in a changing environment: extinction debt, immigration credit and species turnover. - Trends Ecol. Evol. 25: 153–160.

Jaime, L. et al. 2019. Scots pine (*Pinus sylvestris* L.) mortality is explained by the climatic suitability of both host tree and bark beetle populations. - For. Ecol. Manage. 448: 119–129.

—
Jentsch, A. et al. 2007. A new generation of events , not trends experiments. - Front. Ecol. Environ. 5: 365–374.

Joppa, L. N. et al. 2013. Troubling trends in scientific software use. - Science (80-.). 340: 814–815.

Jump, A. S. and Woodward, F. I. 2003. Seed production and population density decline approaching the range-edge of *Cirsium* species. - New Phytol. 160: 349–358.

Jump, A. S. et al. 2006. Rapid climate change-related growth decline at the southern range edge of *Fagus sylvatica*. - Glob. Chang. Biol. 12: 2163–2174.

Jump, A. S. et al. 2009. The altitude-for-latitude disparity in the range retractions of woody species. - Trends Ecol. Evol. 24: 694–701.

Karger, D. N. et al. 2017. Climatologies at high resolution for the earth’s land surface areas. - Sci. Data 4: 170122.

3.4. Discussion

111

- Kearney, M. 2006. Habitat , environment and niche: what are we modelling? - Oikos 115: 186–191.
- Kearney, M. and Porter, W. 2009. Mechanistic niche modelling: Combining physiological and spatial data to predict species’ ranges. - Ecol. Lett. 12: 334–350.
- Keddy, P. A. 1992. Assembly and response rules: two goals for predictive community ecology. - J. Veg. Sci. 3: 157–164.
- Kramer, P. J. and Boyer, J. S. 1995. Water relations of plants and soils. - Academic Press.
- Kreuzwieser, J. and Gessler, A. 2010. Global climate change and tree nutrition: Influence of water availability. - Tree Physiol. 30: 1221–1234.
- Kreyling, J. et al. 2011. Stochastic trajectories of succession initiated by extreme climatic events. - Ecol. Lett. 14: 758–764.
- Kruckeberg, A. R. 2002. Geology and plant life: the effects of landforms and rock types on plants. - University of Washington Press.
- Kuussaari, M. et al. 2009. Extinction debt: a challenge for biodiversity conservation. - Trends Ecol. Evol. 24: 564–571.
- Kuznetsova, A. et al. 2017. lmerTest Package: Tests in Linear Mixed Effects Models. - J. Stat. Softw. 82: 1–26.
- Lázaro, R. et al. 2001. Analysis of a 30-year rainfall record (1967–1997) in semi-arid SE Spain for implications on vegetation. - J. Arid Environ. 48: 373–395.
- Leathwick, J. R. 1998. Are New Zealand’s Nothofagus species in equilibrium with their environment? - J. Veg. Sci. 9: 719–732.
- Lembrechts, J. J. et al. 2019a. Comparing temperature data sources for use in species distribution models: From in-situ logging to remote sensing. - Glob. Ecol. Biogeogr.: geb.12974.

1123. Climate and functional traits jointly mediate tree water use strategies

- Lembrechts, J. J. et al. 2019b. Incorporating microclimate into species distribution models. - *Ecography* (Cop.). 42: 1267–1279.
- Lenoir, J. and Svenning, J.-C. 2015. Climate-related range shifts - a global multidimensional synthesis and new research directions. - *Ecography* (Cop.). 38: 15–28.
- Lenoir, J. et al. 2008. A Significant Upward Shift in Plant Species Optimum Elevation During the 20th Century. *Science*. 320: 1768–1771.
- Lenoir, J. et al. 2013. Local temperatures inferred from plant communities suggest strong spatial buffering of climate warming across Northern Europe. - *Glob. Chang. Biol.* 19: 1470–1481.
- Lenth, R. V. 2016. Least-Squares Means: The R Package *lsmeans*. - *J. Stat. Softw.* 69: 1–33.
- Lesica, P. and Crone, E. E. 2016. Arctic and boreal plant species decline at their southern range limits in the Rocky Mountains. - *Ecol. Lett.*: 166–174.
- Lévesque, M. et al. 2016. Soil nutrients influence growth response of temperate tree species to drought (R Jones, Ed.). - *J. Ecol.* 104: 377–387.
- Li, Y. and Shipley, B. 2018. Community divergence and convergence along experimental gradients of stress and disturbance. - *Ecology* 99: 775–781.
- Li, Y. et al. 2018. Habitat filtering determines the functional niche occupancy of plant communities worldwide. - *J. Ecol.* 106: 1001–1009.
- Lloret, F. and Granzow-de la Cerda, I. 2013. Plant competition and facilitation after extreme drought episodes in Mediterranean shrubland: Does damage to vegetation cover trigger replacement by juniper woodland? - *J. Veg. Sci.* 24: 1020–1032.
- Lloret, F. and García, C. 2016. Inbreeding and neighbouring vegetation drive drought-induced die-off within juniper populations. - *Funct. Ecol.* 30: 1696–1704.

- Lloret, F. and Kitzberger, T. 2018. Historical and event-based bioclimatic suitability predicts regional forest vulnerability to compound effects of severe drought and bark beetle infestation. - *Glob. Chang. Biol.* in press.
- Lloret, F. et al. 2012. Extreme climatic events and vegetation: The role of stabilizing processes. - *Glob. Chang. Biol.* 18: 797–805.
- Lloret, F. et al. 2016. Climatic events inducing die-off in Mediterranean shrublands: are species responses related to their functional traits? - *Oecologia* 180: 961–973.
- Lomolino, M. V. et al. 2004. Foundations of biogeography: classic papers with commentaries. - University of Chicago Press.
- MacArthur, R. and Levins, R. 1967. The Limiting Similarity, Convergence, and Divergence of Coexisting Species. - *Am. Nat.* 101: 377–385.
- Maestre, F. T. and Cortina, J. 2002. Spatial patterns of surface soil properties and vegetation in a Mediterranean semi-arid steppe. - *Plant Soil* 241: 279–291.
- Maggini, R. et al. 2011. Are Swiss birds tracking climate change?: Detecting elevational shifts using response curve shapes. - *Ecol. Modell.* 222: 21–32.
- Maguire, B. 1973. Niche Response Structure and the Analytical Potentials of Its Relationship to the Habitat. - *Am. Nat.* 107: 213–246.
- Martinez-Meyer, E. et al. 2013. Ecological niche structure and rangewide abundance patterns of species. - *Biol. Lett.* 9: 20120637–20120637.
- Martínez-Vilalta, J. and Lloret, F. 2016. Drought-induced vegetation shifts in terrestrial ecosystems: The key role of regeneration dynamics. - *Glob. Planet. Change* 144: 94–108.
- Mauri, A. et al. 2016. *Pinus halepensis* and *Pinus brutia* in Europe: distribution, habitat, usage and threats. - In: European Atlas of Forest Tree Species. in press.
- Mauri, A. et al. 2017. EU-Forest, a high-resolution tree occurrence dataset

1143. Climate and functional traits jointly mediate tree water use strategies

for Europe. - Sci. Data in press.

McDowell, N. et al. 2008. Mechanisms of Plant Survival and Mortality during Drought: Why Do Some Plants Survive while Others Succumb to Drought? - *New Phytol.* 178: 719–739.

McDowell, N. et al. 2019. Mechanisms of a coniferous woodland persistence under drought and heat. - *Environ. Res. Lett.* in press.

Mellert, K. H. et al. 2011. Hypothesis-driven species distribution models for tree species in the Bavarian Alps. - *J. Veg. Sci.* 22: 635–646.

Merow, C. et al. 2013. A practical guide to MaxEnt for modeling species' distributions: what it does, and why inputs and settings matter. - *Ecography* (Cop.). 36: 1058–1069.

Merow, C. et al. 2014. What do we gain from simplicity versus complexity in species distribution models? - *Ecography* (Cop.). 37: 1267–1281.

— Miriti, M. N. et al. 2007. Episodic death across species of desert shrubs. - *Ecology* 88: 32–36. —

Morueta-Holme, N. and Svenning, J.-C. 2018. Geography of Plants in the New World: Humboldt's Relevance in the Age of Big Data. - *Ann. Missouri Bot. Gard.* 103: 315–329.

Mouillot, F. et al. 2002. Simulating climate change impacts on fire frequency and vegetation dynamics in a Mediterranean ecosystem. - *Glob. Chang. Biol.* 8: 423–437.

Murphy, H. T. et al. 2006. Distribution of abundance across the range in eastern North American trees. - *Glob. Ecol. Biogeogr.* 15: 63–71.

Niehaus, A. C. et al. 2012. Predicting the physiological performance of ectotherms in fluctuating thermal environments. - *J. Exp. Biol.* 215: 694–701.

Ninyerola, M. et al. 2000. A methodological approach of climatological modelling of air temperature and precipitation through GIS techniques. - *Int.*

3.4. Discussion

115

- J. Climatol. 20: 1823–1841.
- Ninyerola, M. et al. 2007. Monthly precipitation mapping of the Iberian Peninsula using spatial interpolation tools implemented in a Geographic Information System. - Theor. Appl. Climatol. 89: 195–209.
- Osorio-Olvera, L. et al. 2019. On population abundance and niche structure. - Ecography (Cop.). 42: 1415–1425.
- Parmesan, C. 2006. Ecological and Evolutionary Responses to Recent Climate Change. - Annu. Rev. Ecol. Evol. Syst. 37: 637–669.
- Parmesan, C. and Yohe, G. 2003. A globally coherent fingerprint of climate change impacts across natural systems. - Nature 421: 37–42.
- Pausas, J. G. and Bond, W. J. 2018. Humboldt and the reinvention of nature. - J. Ecol. in press.
- Pearman, P. B. et al. 2008. Niche dynamics in space and time. - Trends Ecol. Evol. 23: 149–158.
- Pearson, R. G. and Dawson, T. P. 2003. Predicting the Impacts of Climate Change on the Distribution of Species: Are Bioclimate Envelope Models Useful? - Glob. Ecol. Biogeogr. 12: 361–371.
- Pearson, R. G. et al. 2006. Model-based uncertainty in species range prediction. - J. Biogeogr. 33: 1704–1711.
- Pearson, D. E. et al. 2018. Community Assembly Theory as a Framework for Biological Invasions. - Trends Ecol. Evol. 33: 313–325.
- Peñuelas, J. et al. 2001. Severe drought effects on mediterranean woody flora in Spain. - For. Sci. 47: 214–218.
- Pérez-Ramos, I. M. et al. 2017. Climate variability and community stability in Mediterranean shrublands: the role of functional diversity and soil environment. - J. Ecol. 105: 1335–1346.
- Pérez Navarro, M. Á. et al. 2018. Climatic Suitability Derived from Species

1163. Climate and functional traits jointly mediate tree water use strategies

Distribution Models Captures Community Responses to an Extreme Drought Episode. - *Ecosystems*: 1–14.

Peterson, A. T. 2011. Ecological Niches and Geographic Distributions (Princeton University Press, Ed.).

Peterson, A. T. and Vieglais, D. A. 2001. Predicting Species Invasions Using Ecological Niche Modeling: New Approaches from Bioinformatics Attack a Pressing Problem. - *Bioscience* 51: 363–371.

Petitpierre, B. et al. 2012. Climatic Niche Shifts Are Rare Among Terrestrial Plant Invaders. *Science*. 335: 1344–1348.

Phillips, S. J. and Dudík, M. 2008a. Modeling of species distribution with Maxent: new extensions and a comprehensive evalutation. - *Ecography* (Cop.). 31: 161–175.

Phillips, S. J. and Dudík, M. 2008b. Modeling of species distributions with Maxent: new extensions and a comprehensive evaluation. - *Ecography* (Cop.). 31: 161–175.

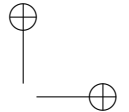
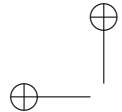
Piedallu, C. et al. 2013. Soil water balance performs better than climatic wa- ter variables in tree species distribution modelling. - *Glob. Ecol. Biogeogr.* 22: 470–482.

Pironon, S. et al. 2015. Do geographic, climatic or historical ranges differ- entiate the performance of central versus peripheral populations? - *Glob. Ecol. Biogeogr.* 24: 611–620.

Pironon, S. et al. 2016. Geographic variation in genetic and demographic performance: new insights from an old biogeographical paradigm. - *Biol. Rev.*: 000–000.

Pironon, S. et al. 2017. The ‘Hutchinsonian niche’ as an assemblage of de- mographic niches: implications for species geographic ranges. - *Ecography* (Cop.). in press.

Porporato, A. et al. 2004. Soil Water Balance and Ecosystem Response to



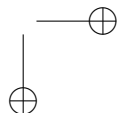
3.4. Discussion

117

- Climate Change. - Am. Nat. 164: 625–632.
- Prentice, I. C. et al. 1992. A Global Biome Model Based on Plant Physiology and Dominance, Soil Properties and Climate. - J. Biogeogr. 19: 117.
- Pulliam, H. R. 1988. Sources, Sinks, and Population Regulation. - Am. Nat. 132: 652–661.
- Pulliam, H. R. 2000. On the relationship between niche and distribution. - Ecol. Lett. 3: 349–361.
- Randin, C. F. et al. 2009. Climate change and plant distribution: local models predict high-elevation persistence. - Glob. Chang. Biol. 15: 1557–1569.
- Ricklefs, R. E. 2008. Disintegration of the ecological community. - Am. Nat. 172: 741–750.
- Rivas-Martínez, S. et al. 2011. Worldwide bioclimatic classification system. - Glob. Geobot. 1: 1–638.
-
- Rivas-Martínez, S. et al. 2017. Bioclimatology of the Iberian Peninsula and the Balearic Islands. - In: Springer, Cham, pp. 29–80.
- Sangüesa-Barreda, G. et al. 2018. Delineating limits: Confronting predicted climatic suitability to field performance in mistletoe populations. - J. Ecol. 106: 2218–2229.
- Sapes, G. et al. 2017. Species climatic niche explains drought-induced die-off in a Mediterranean woody community. - Ecosphere 8: e01833.
- Schurr, F. M. et al. 2012. How to understand species' niches and range dynamics: A demographic research agenda for biogeography. - J. Biogeogr. 39: 2146–2162.
- Segurado, P. and Araújo, M. B. 2004. An evaluation of methods for modelling species distributions. - J. Biogeogr. 31: 1555–1568.
- Serra-Díaz, J. M. et al. 2013. Geographical patterns of congruence and incongruence between correlative species distribution models and a process-

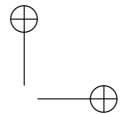


|



1183. Climate and functional traits jointly mediate tree water use strategies

- based ecophysiological growth model. - *J. Biogeogr.* 40: 1928–19338.
- Sexton, J. P. et al. 2009. Evolution and Ecology of Species Range Limits. - *Annu. Rev. Ecol. Evol. Syst.* 40: 415–36.
- Sexton, J. P. et al. 2014. Genetic isolation by environment or distance: which pattern of gene flow is most common? - *Evolution*. 68: 1–15.
- Shantz, H. L. 1927. Drought Resistance and Soil Moisture. - *Ecology* 8: 145–157.
- Sheffield, J. and Wood, E. F. 2008. Projected changes in drought occurrence under future global warming from multi-model , multi-scenario , IPCC AR4 simulations. - *Clim. Dyn.* 31: 79–105.
- Simpson, A. H. et al. 2016. Soil–climate interactions explain variation in foliar, stem, root and reproductive traits across temperate forests. - *Glob. Ecol. Biogeogr.* 25: 964–978.
- Soberón, J. 2007. Grinnellian and Eltonian niches and geographic distributions of species. - *Ecol. Lett.* 10: 1115–1123.
- Soberón, J. and Nakamura, M. 2009. Niches and distributional areas: Concepts, methods, and assumptions. - *Proc. Natl. Acad. Sci.* 106: 19645–19650.
- Solarik, K. A. et al. 2018. Local adaptation of trees at the range margins impacts range shifts in the face of climate change. - *Glob. Ecol. Biogeogr.* 27: 1507–1519.
- Suggitt, A. J. et al. 2011. Habitat microclimates drive fine-scale variation in extreme temperatures. - *Oikos* 120: 1–8.
- Svenning, J.-C. and Skov, F. 2004. Limited filling of the potential range in European tree species. - *Ecol. Lett.* 7: 565–573.
- Svenning, J.-C. and Skov, F. 2007. Could the tree diversity pattern in Europe be generated by postglacial dispersal limitation? - *Ecol. Lett.* 10: 453–460.



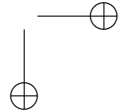
3.4. Discussion

119

- Svenning, J. C. and Sandel, B. 2013. Disequilibrium vegetation dynamics under future climate change. - *Am. J. Bot.* 100: 1266–1286.
- Takahashi, K. and Tanaka, S. 2016. Relative importance of habitat filtering and limiting similarity on species assemblages of alpine and subalpine plant communities. - *J. Plant Res.* 129: 1041–1049.
- Thibault, K. M. and Brown, J. H. 2008. Impact of an extreme climatic event on community assembly. - *Proc. Natl. Acad. Sci.* 105: 3410–3415.
- Thomas, C. D. et al. 2004. Extinction risk from climate change. - *Nature* 427: 145–148.
- Thorntwaite, C. W. and Mather, J. R. 1957. Instructions and tables for computing potential evapotranspiration and the water balance,. - *Publ. Climatol.* 10: 185–311.
- Thuiller, W. 2004. Patterns and uncertainties of species' range shifts under climate change. - *Glob. Chang. Biol.* 10: 2020–2027.
- Thuiller, W. 2013. On the importance of edaphic variables to predict plant species distributions - limits and prospects. - *J. Veg. Sci.* 24: 591–592.
- Thuiller, W. et al. 2005a. Niche properties and geographical extent as predictors of species sensitivity to climate change. - *Glob. Ecol. Biogeogr.* 14: 347–357.
- Thuiller, W. et al. 2005b. Climate change threats to plant diversity in Europe. - *Proc. Natl. Acad. Sci. U. S. A.* 102 (23): 8245–8250.
- Thuiller, W. et al. 2010. Variation in habitat suitability does not always relate to variation in species' plant functional traits. - *Biol. Lett.* 6: 120–123.
- Thuiller, W. et al. 2014. Does probability of occurrence relate to population dynamics? - *Ecography (Cop.)*. 37: 1155–1166.
- Tulloch, A. I. T. et al. 2016. Conservation planners tend to ignore improved accuracy of modelled species distributions to focus on multiple threats and



|



1203. Climate and functional traits jointly mediate tree water use strategies

- ecological processes. - Biol. Conserv. 199: 157–171.
- Ulrich, W. et al. 2014. Climate and soil attributes determine plant species turnover in global drylands. - J. Biogeogr. 41: 2307–2319.
- Valladares, F. et al. 2004. CAPÍTULO 6 Estrés hídrico: ecofisiología y escalas de la sequía. - In: Valladares, F. (ed), Ecología del bosque mediterráneo en un mundo cambiante. Ministerio. pp. 163–190.
- Valladares, F. et al. 2008. Functional traits and phylogeny: What is the main ecological process determining species assemblage in roadside plant communities? - J. Veg. Sci. 19: 381–392.
- Valladares, F. et al. 2014a. Global change and Mediterranean forests: current impacts and potential responses. - In: Forests and Global Change. pp. 47–75.
- Valladares, F. et al. 2014b. The effects of phenotypic plasticity and local adaptation on forecasts of species range shifts under climate change. - Ecol. Lett. 17: 1351–1364.
- van der Maaten, E. et al. 2017. Species distribution models predict temporal but not spatial variation in forest growth. - Ecol. Evol. 7: 2585–2594.
- van Mantgem, P. J. et al. 2009. Widespread Increase of Tree Mortality Rates in the Western United States. Science. 323: 521–524.
- VanDerWal, J. et al. 2009. Abundance and the environmental niche: environmental suitability estimated from niche models predicts the upper limit of local abundance. - Am. Nat. 174: 282–91.
- Vellend, M. 2010. Conceptual synthesis in community ecology. - Q. Rev. Biol. 85: 183–206.
- Vicente-Serrano, S. M. et al. 2013. Response of vegetation to drought time-scales across global land biomes. - Proc. Natl. Acad. Sci. U. S. A. 110: 52–57.
- Volterra, V. 1926. Fluctuations in the Abundance of a Species considered

- Mathematically1. - *Nature* 118: 558–560.
- von Humboldt, A. and Bonpland, A. 1807 (2009). *Essay on the geography of plants*. Reprint, translated by Sylvie Romanowski, edited with an introduction by S. T. Jackson. The University of Chicago Press.
- Walther, G.-R. et al. 2009. Alien species in a warmer world: risks and opportunities. - *Trends Ecol. Evol.* 24: 686–693.
- Wan, Z. 2008. New refinements and validation of the MODIS Land-Surface Temperature/Emissivity products. - *Remote Sens. Environ.* 112: 59–74.
- Wan, Z. et al. 2015. MOD11C2 MODIS/Terra Land Surface Temperature/Emissivity 8-Day L3 Global 0.05° CMG V006 [Data set]. In NASA EOSDIS LP DAAC.
- Wang, J. and Maintainer, L. S. C. 2016. Package “MixRF.” in press.
- Webb, T. 1986. Is vegetation in equilibrium with climate? How to interpret late-Quaternary pollen data. - *Vegetatio* 67: 75–91.
- Webb, C. O. and Donoghue, M. J. 2005. Phyloomatic: Tree assembly for applied phylogenetics. - *Mol. Ecol. Notes* 5: 181–183.
- Webb III, T. 1992. Global Changes During the Last 3 Million Years: Climatic Controls and Biotic Responses. - *Annu. Rev. ecology Syst.* 23: 141–173.
- Weber, M. M. et al. 2016. Is there a correlation between abundance and environmental suitability derived from ecological niche modelling? A meta-analysis. - *Ecography (Cop.)*. 40: 817–828.
- Weiher, E. et al. 2011. Advances, challenges and a developing synthesis of ecological community assembly theory. - *Philos. Trans. R. Soc. B Biol. Sci.* 366: 2403–2413.
- Wessels, K. J. et al. 1998. An evaluation of the gradsect biological survey method. - *Biodivers. Conserv.* 7: 1093–1121.
- Wiens, J. J. and Graham, C. H. 2005. Niche Conservatism: Integrating

1223. Climate and functional traits jointly mediate tree water use strategies

Evolution, Ecology, and Conservation Biology. - Annu. Rev. Ecol. Evol. Syst. 36: 519–539.

Wiens, J. A. et al. 2009. Niches, models, and climate change: Assessing the assumptions and uncertainties. - Proc. Natl. Acad. Sci. 106: 19729–19736.

Woodward, F. I. 1987. Climate and plant distribution. - Cambridge University Press.

Wright, J. W. et al. 2006. Experimental verification of ecological niche modeling in a heterogeneous environment. - Ecology 87: 2433–2439.

Zavaleta, E. S. et al. 2003. Grassland Responses To Three Years of Elevated Temperature, Co₂, Precipitation, and N Deposition. - Ecol. Monogr. 73: 585–604.

Zimmermann, N. E. et al. 2009. Climatic extremes improve predictions of spatial patterns of tree species. - Proc. Natl. Acad. Sci. U. S. A. 106 Suppl: 19723–8.

Zunzunegui, M. et al. 2005. To live or to survive in Doñana dunes: Adaptive responses of woody species under a Mediterranean climate. - Plant Soil 273: 77–89.

Allen, C. D., Breshears, D. D., & McDowell, N. G. (2015). On underestimation of global vulnerability to tree mortality and forest die-off from hotter drought in the Anthropocene. *Ecosphere*, 6(8), 1–55. <http://doi.org/10.1890/ES15-00203.1>

Barrett, D. J., Hatton, T. J., Ash, J. E., & Ball, M. C. (1995). Evaluation of the heat pulse velocity technique for measurement of sap flow In rainforest and eucalypt forest species of south-eastern Australia, (1), 463–469.

Barton, K. (2017). *MuMIn: Multi-Model Inference*. Retrieved from <https://cran.r-project.org/package=MuMIn>

Bates, D., Mächler, M., Bolker, B., & Walker, S. (2015). Fitting Linear

- Mixed-Effects Models Using {lme4}. *Journal of Statistical Software*, 67(1), 1–48. <http://doi.org/10.18637/jss.v067.i01>
- Becker, P. (1998). Limitations of a compensation heat pulse velocity system at low sap flow: implications for measurements at night and in shaded trees. *Tree Physiology*, 18(3), 177–184. <http://doi.org/10.1093/treephys/18.3.177>
- Bleby, T. M., Burgess, S. S. O., & Adams, M. A. (2004). A validation, comparison and error analysis of two heat-pulse methods for measuring sap flow in *Eucalyptus marginata* saplings. *Functional Plant Biology*, 31(6), 645–658. <http://doi.org/10.1071/FP04013>
- Bleby, T., McElrone, A., & Burgess, S. (2008). Limitations of the HRM: great at low flow rates, but not yet up to speed? In *7th sap flow workshop*. Seville.
- Braun, P., & Schmid, J. (1999). Sap flow measurements in grapevines (*Vitis vinifera L.*) 2. Granier measurements. *Plant and Soil*, 215, 47–55.
- Burgess, S. S., Adams, M. a, Turner, N. C., Beverly, C. R., Ong, C. K., Khan, a a, & Bleby, T. M. (2001). An improved heat pulse method to measure low and reverse rates of sap flow in woody plants. *Tree Physiology*, 21(9), 589–598. <http://doi.org/10.1093/treephys/21.9.589>
- Bush, S. E., Hultine, K. R., Sperry, J. S., Ehleringer, J. R., & Phillips, N. (2010). Calibration of thermal dissipation sap flow probes for ring- and diffuse-porous trees. *Tree Physiology*, 30(12), 1545–1554. <http://doi.org/10.1093/treephys/tpq096>
- Cabibel, B., & F, D. (1991). Mesures thermiques des flux de sève dans les troncs et les racines et fonctionnement hydriques des arbres. I. I., (fig 4).
- Cain, R. (2009). *The climatic significance of tropical forest edges and their representation in global climate models* (PhD thesis). Durham University. Retrieved from <http://etheses.dur.ac.uk/302/>
- Castelan-Estrada, M., Vivin, P., & Gaudillière, J. P. (2002). Allometric rela-

1243. Climate and functional traits jointly mediate tree water use strategies

tionships to estimate seasonal above-ground vegetative and reproductive biomass of *Vitis vinifera* L. *Annals of Botany*, 89(4), 401–408. <http://doi.org/10.1093/aob/mcf059>

Caterina, G. L., Will, R. E., Turton, D. J., Wilson, D. S., & Zou, C. B. (2014). Water use of *Juniperus virginiana* trees encroached into mesic prairies in Oklahoma, USA. *Ecohydrology*, 7(4), 1124–1134. <http://doi.org/10.1002/eco.1444>

Chen, X., Miller, G. R., Rubin, Y., & Baldocchi, D. D. (2012). A statistical method for estimating wood thermal diffusivity and probe geometry using in situ heat response curves from sap flow measurements. *Tree Physiology*, 32(12), 1458–1470. <http://doi.org/10.1093/treephys/tps100>

Clearwater, M. J., Luo, Z., Mazzeo, M., & Dichio, B. (2009). An external heat pulse method for measurement of sap flow through fruit pedicels, leaf petioles and other small-diameter stems. *Plant, Cell and Environment*, 32(12), 1652–1663. <http://doi.org/10.1111/j.1365-3040.2009.02026.x>

Clearwater, M. J., Meinzer, F. C., Andrade, J. L., Goldstein, G., & Holbrook, N. M. (1999). Potential errors in measurement of nonuniform sap flow using heat dissipation probes. *Tree Physiology*, 19(Equation 4), 681–687. <http://doi.org/10.1093/treephys/19.10.681>

Cohen, Y., Fuchs, M., & Green, G. C. (1981). Improvement of the heat pulse method for determining sap flow in trees. *Plant, Cell and Environment*, 4, 391–397. <http://doi.org/10.1111/j.1365-3040.1981.tb02117.x>

Čermák, J., Kučera, J., & Nadezhdina, N. (2004). Sap flow measurements with some thermodynamic methods, flow integration within trees and scaling up from sample trees to entire forest stands. *Trees - Structure and Function*, 18(5), 529–546. <http://doi.org/10.1007/s00468-004-0339-6>

de Oliveira Reis, F., Campostrini, E., Sousa, E. F. de, & Silva, M. G. e. (2006). Sap flow in papaya plants: Laboratory calibrations and relationships with gas exchanges under field conditions. *Scientia Horticulturae*,

110(3), 254–259. <http://doi.org/10.1016/j.scienta.2006.07.010>

Diawara, a., Loustau, D., & Berbigier, P. (1991). Comparison of 2 Methods for Estimating the Evaporation of A Pinus-Pinaster (Ait) Stand - Sap Flow and Energy-Balance with Sensible Heat-Flux Measurements by An Eddy Covariance Method. *Agricultural and Forest Meteorology*, 54(1), 49–66. [http://doi.org/10.1016/0168-1923\(91\)90040-W](http://doi.org/10.1016/0168-1923(91)90040-W)

Do, F., & Rocheteau, a. (2002). Influence of natural temperature gradients on measurements of xylem sap flow with thermal dissipation probes. 2. Advantages and calibration of a noncontinuous heating system. *Tree Physiology*, 22(9), 649–654. <http://doi.org/10.1093/treephys/22.9.649>

Fan, J., Guyot, A., Ostergaard, K. T., & Lockington, D. A. (2018). Effects of earlywood and latewood on sap flux density-based transpiration estimates in conifers. *Agricultural and Forest Meteorology*, 249(November 2017), 264–274. <http://doi.org/10.1016/j.agrformet.2017.11.006>

— Fathi, L. (2014). *Structural and mechanical properties of the wood from coconut palms, oil palms and date palms* (PhD thesis). Hamburg.

Frank, D. C., Poulter, B., Saurer, M., Esper, J., Huntingford, C., Helle, G., ... Weigl, M. (2015). Water-use efficiency and transpiration across European forests during the Anthropocene. *Nature Climate Change*, 5(6), 579–583. <http://doi.org/10.1038/nclimate2614>

Fuchs, S., Leuschner, C., Link, R., Coners, H., & Schuldt, B. (2017). Calibration and comparison of thermal dissipation, heat ratio and heat field deformation sap flow probes for diffuse-porous trees. *Agricultural and Forest Meteorology*, 244-245(June), 151–161. <http://doi.org/10.1016/j.agrformet.2017.04.003>

Granier, A., & Une, A. G. (1985). Une nouvelle m ‘ ethode pour la mesure du flux de s ‘ eve brute dans le tronc des arbres.

Green, S. R., & Clothier, B. E. (1988). Water use of kiwifruit vines and apple trees by the heat pulse technique. *Journal of Experimental Botany*,

1263. Climate and functional traits jointly mediate tree water use strategies

39(198), 115–123.

Green, S., Clothier, B., & Jardine, B. (2003). Theory and Practical Application of Heat Pulse to Measure Sap Flow. *Agriculture*.

Green, S., Clothier, B., & Perie, E. (2009). A re-analysis of heat pulse theory across a wide range of sap flows. *Acta Horticulturae*, 846, 95–104.

Hanssens, J., De Swaef, T., Nadezhina, N., & Steppe, K. (2013). Measurement of sap flow dynamics through the tomato peduncle using a non-invasive sensor based on the heat field deformation method. *Acta Horticulturae*, 991, 409–416. <http://doi.org/10.17660/ActaHortic.2013.991.50>

Hatton, T. (1990). Integration of sapflow velocity to estimate plant water use. *Tree Physiology*, 6(v), 201–209. <http://doi.org/10.1093/treephys/6.2.201>

—
Hatton, T. J., Moore, S. J., & Reece, P. H. (1995). Estimating stand transpiration in a Eucalyptus populnea woodland with the heat pulse method: measurement errors and sampling strategies. *Tree Physiology*, 15(4), 219–227. <http://doi.org/10.1093/treephys/15.4.219>

Hernandez-Santana, V., Hernandez-Hernandez, A., Vadeboncoeur, M. A., & Asbjornsen, H. (2015). Scaling from single-point sap velocity measurements to stand transpiration in a multispecies deciduous forest: uncertainty sources, stand structure effect, and future scenarios. *Canadian Journal of Forest Research*, 45(11), 1489–1497. <http://doi.org/10.1139/cjfr-2015-0009>

Hogg, E. H., Black, T. A., Hartog, G. den, Neumann, H. H., Zimmermann, R., Hurdle, P. A., ... Oren, R. (1997). A comparison of sap flow and eddy fluxes of water vapor from a boreal deciduous forest. *Journal of Geophysical Research*, 102(D24), 28929. <http://doi.org/10.1029/96JD03881>

Hölttä, T., Linkosalo, T., Riikonen, A., Sevanto, S., & Nikinmaa, E. (2015). An analysis of Granier sap flow method, its sensitivity to heat storage and

a new approach to improve its time dynamics. *Agricultural and Forest Meteorology*, 211–212, 2–12. <http://doi.org/10.1016/j.agrformet.2015.05.005>

Hultine, K. R., Nagler, P. L., Morino, K., Bush, S. E., Burtch, K. G., Dennison, P. E., ... Ehleringer, J. R. (2010). Sap flux-scaled transpiration by tamarisk (*Tamarix* spp.) before, during and after episodic defoliation by the saltcedar leaf beetle (*Diorhabda carinulata*). *Agricultural and Forest Meteorology*, 150(11), 1467–1475. <http://doi.org/10.1016/j.agrformet.2010.07.009>

Jasechko, S., Sharp, Z. D., Gibson, J. J., Birks, S. J., Yi, Y., & Fawcett, P. J. (2013). Terrestrial water fluxes dominated by transpiration. *Nature*, 496(7445), 347–350. <http://doi.org/10.1038/nature11983>

Kempe, A., Lautenschlager, T., Lange, A., & Neinhuis, C. (2014). How to become a tree without wood - biomechanical analysis of the stem of *Carica papaya* L. *Plant Biology*, 16(1), 264–271. <http://doi.org/10.1111/plb.12035>

Konings, A. G., Williams, A. P., & Gentine, P. (2017). Sensitivity of grassland productivity to aridity controlled by stomatal and xylem regulation. *Nature Geoscience*, 10(4), 284–288. <http://doi.org/10.1038/NGEO2903>

Kool, D., Agam, N., Lazarovitch, N., Heitman, J. L., Sauer, T. J., & Bengal, a. (2014). A review of approaches for evapotranspiration partitioning Author ’ s personal copy. *Agricultural and Forest Meteorology*, 184, 56–70. <http://doi.org/10.1016/j.agrformet.2013.09.003>

Lenth, R. V. (2016). Least-Squares Means: The {R} Package *{lsmeans}*. *Journal of Statistical Software*, 69(1), 1–33. <http://doi.org/10.18637/jss.v069.i01>

Looker, N., Martin, J., Jencso, K., & Hu, J. (2016). Contribution of sapwood traits to uncertainty in conifer sap flow as estimated with the heat-ratio method. *Agricultural and Forest Meteorology*, 223, 60–71. <http://doi.org/10.1016/j.agrformet.2016.02.001>

1283. Climate and functional traits jointly mediate tree water use strategies

[org/10.1016/j.agrformet.2016.03.014](https://doi.org/10.1016/j.agrformet.2016.03.014)

Lu, P. (2002). Whole-plant water use of some tropical and subtropical tree crops and its application in irrigation management., (575(Vol. 2)), 781–789.

Lu, P., & Chacko, E. (1998). Evaluation of Granier’s sap flux in young mango trees sensor. *Agronomie*, 18(August 1997), 461–471.

Lu, P., Urban, L., & Zhao, P. (2004). Granier’s thermal dissipation probe (TDP) method for measuring sap flow in trees: theory and practice. *Acta Botanica Sinica*, 46(6), 631–646.

MacLean, J. (1941). Thermal Conductivity of wood. *Heating, Piping & Air Conditioning*, 13(6), 380–391.

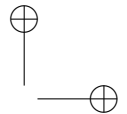
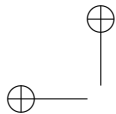
Marañón-Jiménez, S., Bulcke, J. den, Piayda, A., Van Acker, J., Cuntz, M., Rebmann, C., & Steppe, K. (2018). X-ray computed microtomography characterizes the wound effect that causes sap flow underestimation by thermal dissipation sensors. *Tree Physiology*, 38(2), 287–301. <http://doi.org/10.1093/treephys/tpx103>

Martínez-Vilalta, J., Korakaki, E., Vanderklein, D., & Mencuccini, M. (2007). Below-ground hydraulic conductance is a function of environmental conditions and tree size in Scots pine. *Functional Ecology*, 21(6), 1072–1083. <http://doi.org/10.1111/j.1365-2435.2007.01332.x>

McCulloh, K. a, Winter, K., Meinzer, F. C., Garcia, M., Aranda, J., & Lachenbruch, B. (2007). A comparison of daily water use estimates derived from constant-heat sap-flow probe values and gravimetric measurements in pot-grown saplings. *Tree Physiology*, 27(9), 1355–1360. <http://doi.org/10.1093/treephys/27.9.1355>

Mitchell, R. J., Irwin, R. E., Flanagan, R. J., & Karron, J. D. (2009). Ecology and evolution of plant-pollinator interactions. *Annals of Botany*, 103(9), 1355–1363. <http://doi.org/10.1093/aob/mcp122>

Montague, T., & Kjelgren, R. (2006). Use of Thermal Dissipation Probes



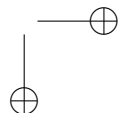
3.4. Discussion

129

- to Estimate Water Loss of Containerized Landscape Trees. *Journal of Environmental Horticulture*, 24(2), 95–104.
- Nadezhina, N. (2018). Revisiting the heat field deformation (HFD) method for measuring sap flow. *IForest*, 11(1), 118–130. <http://doi.org/10.3832/ifor2381-011>
- Nadezhina, N., Cermák, J., & Nadezhdin, V. (1998). Heat field deformation method for sap flow measurements. Zidlochovice, Czech Republic: IUFRO Publications.
- Nakagawa, S., & Schielzeth, H. (2013). A general and simple method for obtaining R² from generalized linear mixed-effects models. *Methods in Ecology and Evolution*, 4(2), 133–142. <http://doi.org/10.1111/j.2041-210x.2012.00261.x>
- Novick, K. A., Ficklin, D. L., Stoy, P. C., Williams, C. A., Bohrer, G., Oishi, A. C. C., ... Phillips, R. P. (2016). The increasing importance of atmospheric demand for ecosystem water and carbon fluxes. *Nature Climate Change*, 1(September), 1–5. <http://doi.org/10.1038/nclimate3114>
- Oishi, A. C., Hawthorne, D. A., & Oren, R. (2016). Baseline: An open-source, interactive tool for processing sap flux data from thermal dissipation probes. *SoftwareX*, 5, 139–143. <http://doi.org/10.1016/j.softx.2016.07.003>
- Oishi, A. C., Oren, R., & Stoy, P. C. (2008). Estimating components of forest evapotranspiration: A footprint approach for scaling sap flux measurements. *Agricultural and Forest Meteorology*, 148(11), 1719–1732. <http://doi.org/10.1016/j.agrformet.2008.06.013>
- Oliveras, I., & Llorens, P. (2001). Medium-term sap flux monitoring in a Scots pine stand: analysis of the operability of the heat dissipation method for hydrological purposes. *Tree Physiology*, 21(7), 473–480. <http://doi.org/10.1093/treephys/21.7.473>
- Paudel, I., Kanety, T., & Cohen, S. (2013). Inactive xylem can explain dif-



|



1303. Climate and functional traits jointly mediate tree water use strategies

ferences in calibration factors for thermal dissipation probe sap flow measurements. *Tree Physiology*, 33(9), 986–1001. <http://doi.org/10.1093/treephys/tpt070>

Pearsall, K. R., Williams, L. E., Castorani, S., Bleby, T. M., & McElrone, A. J. (2014). Evaluating the potential of a novel dual heat-pulse sensor to measure volumetric water use in grapevines under a range of flow conditions. *Functional Plant Biology*, 41(8), 874–883. <http://doi.org/10.1071/FP13156>

Peters, R. L., Fonti, P., Frank, D. C., Poyatos, R., Pappas, C., Kahmen, A., ... Steppe, K. (2018). Quantification of uncertainties in tree sap flow measured with the thermal dissipation method. *Under Review*. <http://doi.org/10.1111/nph.15241>

Poyatos, R., Granda, V., Molowny-Horas, R., Mencuccini, M., Steppe, K., & Martínez-Vilalta, J. (2016). SAPFLUXNET: Towards a global database of sap flow measurements. *Tree Physiology*, 36(12), 1449–1455. <http://doi.org/10.1093/treephys/tpw110>

R Core Team. (2017). *R: A Language and Environment for Statistical Computing*. Vienna, Austria: R Foundation for Statistical Computing. Retrieved from <https://www.r-project.org/>

Ren, R., Liu, G., Wen, M., Horton, R., Li, B., & Si, B. (2017). The effects of probe misalignment on sap flux density measurements and in situ probe spacing correction methods. *Agricultural and Forest Meteorology*, 232, 176–185. <http://doi.org/10.1016/j.agrformet.2016.08.009>

Reyes-Acosta, J. L., Vandegheuchte, M. W., Steppe, K., & Lubczynski, M. W. (2012). Novel, cyclic heat dissipation method for the correction of natural temperature gradients in sap flow measurements. Part 2. Laboratory validation. *Tree Physiology*, 32(7), 913–929. <http://doi.org/10.1093/treephys/tps042>

Rubilar, R. A., Hubbard, R. M., Yañez, M. A., Medina, A. M., & Valenzuela, H. E. (2017). Quantifying differences in thermal dissipation probe cali-

- brations for *Eucalyptus globulus* species and *E. nitens* × *globulus* hybrid. *Trees - Structure and Function*, 31(4), 1263–1270. <http://doi.org/10.1007/s00468-017-1545-3>
- Sakuratani, T. (1981). A Heat Balance Method for Measuring Water Flux in the Stem of Intact Plants. *J. Agr. Met.*, 37(1964), 9–17. <http://doi.org/10.2480/agrmet.37.9>
- Schielzeth, H., & Nakagawa, S. (2013). Nested by design: Model fitting and interpretation in a mixed model era. *Methods in Ecology and Evolution*, 4(1), 14–24. <http://doi.org/10.1111/j.2041-210x.2012.00251.x>
- Schlesinger, W. H., & Jasechko, S. (2014). Transpiration in the global water cycle. *Agricultural and Forest Meteorology*, 189–190, 115–117. <http://doi.org/10.1016/j.agrformet.2014.01.011>
- Schreel, J. D. M., & Steppe, K. (2018). Analysis of sap flow dynamics in saplings with mini-HFD (heat field deformation) sensors. In *Acta horticulturae* (pp. 161–166). International Society for Horticultural Science (ISHS), Leuven, Belgium. <http://doi.org/10.17660/ActaHortic.2018.1222.33>
- Shimizu, T., Kumagai, T., Kobayashi, M., Tamai, K., Iida, S., Kabeya, N., ... Shimizu, A. (2015). Estimation of annual forest evapotranspiration from a coniferous plantation watershed in Japan (2): Comparison of eddy covariance, water budget and sap-flow plus interception loss. *Journal of Hydrology*, 522, 250–264. <http://doi.org/10.1016/j.jhydrol.2014.12.021>
- Simpson, W. T. (1993). Specific Gravity , Moisture Content , and Density Relationship for Wood. *Gen Tech Rep Fplgr76 Madison WI US Department of Agriculture Forest Service Forest Products Laboratory 13 P, Gen. Tech.*, 13. Retrieved from <http://citeseerx.ist.psu.edu/viewdoc/download?doi=10.1.1.155.4926{\&}rep>
- Smith, D. M. (1995). *Water Use by Windbreak Trees in the Sahel* (PhD

1323. Climate and functional traits jointly mediate tree water use strategies

thesis). University of Edinburgh.

Smith, D., & Allen, S. (1996). Measurement of sap flow in plant.pdf.

Sperling, O., Shapira, O., Cohen, S., Tripler, E., Schwartz, A., & Lazarovitch, N. (2012). Estimating sap flux densities in date palm trees using the heat dissipation method and weighing lysimeters. *Tree Physiology*, 32(9), 1171–1178. <http://doi.org/10.1093/treephys/tps070>

Steppe, K., De Pauw, D. J. W., Doody, T. M., & Teskey, R. O. (2010). A comparison of sap flux density using thermal dissipation, heat pulse velocity and heat field deformation methods. *Agricultural and Forest Meteorology*, 150(7-8), 1046–1056. <http://doi.org/10.1016/j.agrformet.2010.04.004>

Steppe, K., Vandegehuchte, M. W., Tognetti, R., & Mencuccini, M. (2015). Sap flow as a key trait in the understanding of plant hydraulic functioning. *Tree Physiology*, 35(4), 341–345. <http://doi.org/10.1093/treephys/tpv033>

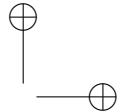
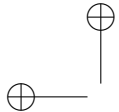
Suleiman, B. M., Larfeldt, J., Leckner, B., & Gustavsson, M. (1999). Thermal conductivity and diffusivity of wood. *Wood Science and Technology*, 33(6), 465–473. <http://doi.org/10.1007/s002260050130>

Sun, H., Aubrey, D. P., & Teskey, R. O. (2012). A simple calibration improved the accuracy of the thermal dissipation technique for sap flow measurements in juvenile trees of six species. *Trees - Structure and Function*, 26(2), 631–640. <http://doi.org/10.1007/s00468-011-0631-1>

Swanson, R. (1983). *Numerical and experimental analyses of implanted probe heat pulse velocity theory* (PhD thesis). Univ. Alberta, Edmonton, Canada.

Swanson, R., & Whitfield, W. (1981). A numerical analysis of heat pulse velocity theor. *Journal of Experimental Botany*, 32(126), 221–239.

Taneda, H., & Sperry, J. S. (2008). A case-study of water transport in co-occurring ring- versus diffuse-porous trees: Contrasts in water-status, con-



3.4. Discussion

133

- ducting capacity, cavitation and vessel refilling. *Tree Physiology*, 28(11), 1641–1651. <http://doi.org/10.1093/treephys/28.11.1641>
- Testi, L., & Villalobos, F. J. (2009). New approach for measuring low sap velocities in trees. *Agricultural and Forest Meteorology*, 149(3-4), 730–734. <http://doi.org/10.1016/j.agrformet.2008.10.015>
- Uddling, J., Teclaw, R. M., Pregitzer, K. S., & Ellsworth, D. S. (2009). Leaf and canopy conductance in aspen and aspen-birch forests under free-air enrichment of carbon dioxide and ozone. *Tree Physiology*, 29(11), 1367–1380. <http://doi.org/10.1093/treephys/tpp070>
- Vandegehuchte, M. W., & Steppe, K. (2012a). A triple-probe heat-pulse method for measurement of thermal diffusivity in trees. *Agricultural and Forest Meteorology*, 160, 90–99. <http://doi.org/10.1016/j.agrformet.2012.03.006>
- Vandegehuchte, M. W., & Steppe, K. (2012b). Interpreting the Heat Field Deformation method: Erroneous use of thermal diffusivity and improved correlation between temperature ratio and sap flux density. *Agricultural and Forest Meteorology*, 162-163, 91–97. <http://doi.org/10.1016/j.agrformet.2012.04.013>
- Vandegehuchte, M. W., & Steppe, K. (2012c). Sapflow+: A four-needle heat-pulse sap flow sensor enabling nonempirical sap flux density and water content measurements. *New Phytologist*, 196(1), 306–317. <http://doi.org/10.1111/j.1469-8137.2012.04237.x>
- Vandegehuchte, M. W., & Steppe, K. (2013). Sap- flux density measurement methods : working principles and applicability. *Fumctional Plant Biology*, 213–223. <http://doi.org/http://dx.doi.org/10.1071/FP12233>
- Vandegehuchte, M. W., Burgess, S. S., Downey, A., & Steppe, K. (2015). Influence of stem temperature changes on heat pulse sap flux density measurements. *Tree Physiology*, 35(4), 346–353. <http://doi.org/10.1093/>



|



1343. Climate and functional traits jointly mediate tree water use strategies

treephys/tpu068

Vandegehuchte, M. W., Steppe, K., & Phillips, N. (2012). Improving sap flux density measurements by correctly determining thermal diffusivity, differentiating between bound and unbound water. *Tree Physiology*, 32(7), 930–942. <http://doi.org/10.1093/treephys/tps034>

Vergeynst, L. L., Vandegehuchte, M. W., McGuire, M. A., Teskey, R. O., & Steppe, K. (2014). Changes in stem water content influence sap flux density measurements with thermal dissipation probes. *Trees - Structure and Function*, 28(3), 949–955. <http://doi.org/10.1007/s00468-014-0989-y>

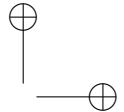
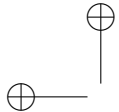
Wei, Z., Yoshimura, K., Wang, L., Miralles, D. G., Jasechko, S., & Lee, X. (2017). Revisiting the contribution of transpiration to global terrestrial evapotranspiration. *Geophysical Research Letters*, 44(6), 2792–2801. <http://doi.org/10.1002/2016GL072235>

— Wheeler, E. A. (2011). Inside Wood – A Web resource for hardwood anatomy. *IAWA Journal*, 32(2), 199–211. <https://doi.org/10.1163/22941932-90000051> —

Wiedemann, A., Jiménez, S. M., Rebman, C., Cuntz, M., & Herbst, M. (2013). Empirical study of wound response dynamics on sap flow measured with thermal dissipation probes. International Society for Horticultural Science.

Wiedemann, A., Marañón-Jiménez, S., Rebmann, C., Herbst, M., Cuntz, M., Walther, B. A., ... Rahbek, C. (2016). An empirical study of the wound effect on sap flux density measured with thermal dissipation probes. *Tree Physiology*, 36(12), 1471–1484. <http://doi.org/10.1093/treephys/tpw071>

Wilson, K. B., Hanson, P. J., Mulholland, P. J., Baldocchi, D. D., & Wullschleger, S. D. (2001). A comparison of methods for determining forest evapotranspiration and its components: Sapflow, soil water budget, eddy covariance and catchment water



3.4. Discussion

135

balance. *Agricultural and Forest Meteorology*, 106(2), 153–168.
[http://doi.org/10.1016/S0168-1923\(00\)00199-4](http://doi.org/10.1016/S0168-1923(00)00199-4)

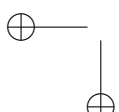
Wullschleger, S. D., Childs, K. W., King, A. W., & Hanson, P. J. (2011). A model of heat transfer in sapwood and implications for sap flux density measurements using thermal dissipation probes. *Tree Physiology*, 31(6), 669–679. <http://doi.org/10.1093/treephys/tpr051>

Wullschleger, S. D., Meinzer, F. C., & Vertessy, R. A. (1998). A review of whole-plant water use studies in tree. *Tree Physiology*, 18(8-9), 499–512.
<http://doi.org/10.1093/treephys/18.8-9.499>

Xie, J., & Wan, X. (2018). The accuracy of the thermal dissipation technique for estimating sap flow is affected by the radial distribution of conduit diameter and density. *Acta Physiologiae Plantarum*. <http://doi.org/10.1007/s11738-018-2659-y>

—
Zanne, A. E., Westoby, M., Falster, D. S., Ackerly, D. D., Loarie, S. R., Arnold, S. E., & Coomes, D. A. (2010). Angiosperm wood structure: Global patterns in vessel anatomy and their relation to wood density and potential conductivity. *American Journal of Botany*, 97(2), 207–215.
<http://doi.org/10.3732/ajb.0900178>

Zhang, Q., Manzoni, S., Katul, G., Porporato, A., & Yang, D. (2014). The hysteretic evapotranspiration—Vapor pressure deficit relation. *Journal of Geophysical Research: Biogeosciences*, 119, 125–140. <http://doi.org/10.1002/2013JG002484>. Received



|

